CORA Cork Open Research Archive
Cartlann Taighde Oscailte Chorcaí

Title	Direct air capture (DAC): capturing CO2 from the air – design of a lab-scale PVSA system and the development of a carbon-based adsorbent material for atmospheric CO2 capture
Authors	Dineen, Cormac P.J.
Publication date	2020-05-06
Original Citation	Dineen, C. P. J. 2020. Direct air capture (DAC): capturing CO2 from the air – design of a lab-scale PVSA system and the development of a carbon-based adsorbent material for atmospheric CO2 capture. MRes Thesis, University College Cork.
Type of publication	Masters thesis (Research)
Rights	© 2020, Cormac P.J. Dineen. - https://creativecommons.org/licenses/by-nc-nd/4.0/
Download date	2026-11-10 17:16:13
Item downloaded from	https://hdl.handle.net/10468/10012

UCC
University College Cork, Ireland
Coláiste na hOllscoile Corcaigh



ucc

Coláiste na hOllscoile Corcaigh, Éire
University College Cork, Ireland



THESIS:

"Direct Air Capture (DAC): Capturing CO_2 from the air – Design of a lab-scale PVSA system and the development of a carbon-based adsorbent material for atmospheric CO_2 capture"

FOR THE DEGREE OF MENGSC BY RESEARCH

MAY 6TH 2020

CORMAC DINEEN, 114338076
SCHOOL OF ENGINEERING, PROCESS & CHEMICAL ENGINEERING DEPT.
SUPERVISORS: DR ELENA TSALAPORTA & DR EOIN FLYNN
HEAD OF SCHOOL: PROF. LIAM MARNANE
HEAD OF DEPTARTMENT: PROF. EDMUND BYRNE

Abstract

Mankind faces huge economic, technological and societal challenges if we are to meet the climate targets set out in the Paris Climate Agreement of limiting global warming to 2°C and avoid the most devastating effects of climate change. Research carried out by the IPCC in 2018 on emissions mitigations pathways compatible with our climate targets shows that commercial-scale deployment of Carbon Dioxide Removal (CDR) technologies will be almost certainly be required if we are to limit warming to 2°C.

This research focuses on Direct Air Capture (DAC), an emerging CDR technology designed to remove CO_2 directly from the atmosphere using sorbent materials. Building on a rapidly expanding body of work, this research has two primary goals. Firstly, it aims to create a laboratory scale, Pressure Vacuum Swing Adsorption (PVSA) system, designed for the testing of the CO_2 adsorption isotherms of new adsorbent materials. The second goal is the development and testing of a new adsorbent material for CO_2 capture.

Having reviewed the relevant literature, a dual-column PVSA system was designed to operate a Skarstrom cycle for atmospheric CO_2 adsorption. The cycle was modified to include a vacuum pump, which provides further testing capabilities in the system. The designed system can assess adsorption-desorption isotherms at sub-atmospheric conditions of pressure, as well as atmospheric conditions of pressure. Following the build phase, the system was tested at a variety of different inlet pressures and it was found that the PVSA Skarstrom cycle operated successfully and as designed.

A biopolymer adsorbent material was developed by expanding the surface area of a native Irish seaweed, Ascophyllum Nodosum. The adsorbent powder product was shown, using SEM and BET analysis, to have a vastly expanded surface area when compared with that of the initial biopolymer material. The adsorbent powder was then pelletized using different techniques, and the structural properties of the pellets, which are key performance parameters for PVSA systems, were analysed and described.

On the basis of the work carried out in this research, and the current global GHG emissions profile, further opportunities for research exist, and are necessary, in the development of new adsorbent materials for atmospheric CO_2 capture. As a result of this research, it is recommended that research be carried out in the development of new, carbon-based adsorbents, which exhibit good structural and chemical properties for CO_2 adsorption but have not yet been widely analysed for suitability within DAC systems.

Acknowledgements:

I would like to take this opportunity to acknowledge all those who have aided me in the completion of this research.

Firstly, I am grateful to my family for their unwavering support throughout my entire educational journey, from the very first time I misplaced, a comma, to the last.

I would like to give my sincere thanks to my academic supervisor, Dr Elena Tsalaporta, for her help and guidance throughout the course of this research, and the education she has helped me receive over the last two years in the field of CO_2 capture. I would like to thank the technical officers Paul Conway and John Barrett, who both readily and generously provided their invaluable assistance in the design and commissioning of the lab rig.

I give my sincerest thanks to my secondary supervisor, Dr Eoin Flynn, and the rest of his Materials Science Group in ERI, including Ricky Hurley and Russell Banta. Eoin readily gave his time to assist my project and became a secondary supervisor without having any responsibility to do so. I am very grateful for all he did to help me.

I am also grateful to all of the rest of the UCC Process & Chemical Engineering department, and my colleagues in the post-graduate office, who offered their assistance on each and every occasion it was requested, without expecting anything in return.

My gratitude must be extended to my favourite music artists, particularly Snoop Dogg, whose flavour-filled rhymes boosted my ebbing morale on numerous occasions throughout the course of this research.

Finally, I would like to thank all of the researchers, engineers, scientists, companies, and activists, who have contributed to the emergence of DAC as a possible means of mitigating climate change or have contributed at all in our fight to halt the march of climate change. 2019 has seen the most marked increase in climate awareness and activism I have seen over the course of my life, and through the work of Greta Thunberg and fellow activists, there is now hope for the future of our planet and our species. It is these people, who dedicate their lives to creating a sustainable and accommodating planet for future generations to inhabit, who are worthy of the greatest thanks.

Declaration

I hereby certify that the work contained in this thesis is my own and will not be submitted for any other degree, either at University College Cork or elsewhere. Any external references and sources used for the purposes of this research are clearly acknowledged and identified at the point of reference within the contents of this thesis. I have read and understood the regulations of University College Cork concerning plagiarism.

Cormac Dineen Date

Table of Contents

Abstract ..... **i**

Acknowledgements: ..... **ii**

Declaration ..... **iii**

List of Figures ..... **iv**

List of Tables ..... **vi**

Acronyms ..... **vii**

Scientific Notation ..... **viii**

1. Introduction **1**

1.1 Rationale 1

1.2 Origin and Development of atmospheric CO_2 capture systems 3

1.3 Industrial Projects and Developments in DAC Technology 4

1.3.1 Carbon Engineering (CE) 4

1.3.2 Climeworks 5

2. Materials & Methods: **8**

3. PVSA System Design: **10**

3.1 Overview 10

3.2 Potential Designs and Sorbent Regeneration Techniques: 11

3.2.1 Pressure/Vacuum Swing Adsorption 11

3.2.2 Temperature Swing Adsorption 12

3.2.3 Moisture Swing Absorption 13

3.2.4 Kraft Process 14

3.3 Preliminary Design: 15

3.3.1 Skarstrom cycle overview: 15

3.4 Alternate Design Schemes: 18

3.4.1 Single Bed PSA System 18

3.4.2 Single Bed PVSA System 18

3.5 Detailed Design: 19

3.5.1 Piping and Instrumentation Diagram (PID) 19

3.5.2 Feed Sources 20

3.5.3 Flow Control 20

3.5.4 Pressure Control 20

3.5.5 Temperature Control 20
3.5.6 Humidity Control 21
3.5.7 Gas Analysis 21
3.6 Equipment Selection & Sourcing 23
3.6.1 Sample Columns: 23
3.6.2 Piping: 24
3.6.3 Fittings 24
3.6.4 Valves 28
3.6.5 Vacuum Pump 32
3.6.6 Pressure Gauges 33
3.6.7 CO_2 Sensors 34
3.7 PVSA System Control Scheme 35
3.7.1 Start-up 36
3.7.2 Operation 1 (OP1) 37
3.7.3 Operation 2 (OP2) 38
3.7.4 Operation 3 (OP3) 39
3.7.5 Operation 4 (OP4) 40
3.7.6 Shut-down 41
3.8 PVSA System Safety Analysis 42
3.8.1 HAZOP 42
3.9 PVSA System Operation Manual 51
3.9.1 Start-up (C-1 Adsorption) 51
3.9.2 Operation 1 (OP1) – C2 Adsorption/C1 Blowdown 51
3.9.3 Operation 2 (OP2) – C2 Adsorption/C1 Purge 52
3.9.4 Operation 3 (OP3) – C1 Adsorption/C2 Blowdown 52
3.9.5 Operation 2 (OP2) – C1 Adsorption/C2 Purge 52
3.9.6 Shutdown 53
4. Development of a Carbon-Based Adsorbent for DAC 54
4.1 Overview 54
4.2 Sorbent Families used in DAC Technologies 55
4.2.1 Chemisorbents 55
4.2.2 Physisorbents 57

4.3 Experimental Method for Development of a Biopolymer Adsorbent Material 60
4.3.1 Material Selection 60
4.3.2 Material Sourcing, Primary Processing and Size Reduction 61
4.3.3 Surface area expansion 62
4.3.4 Vacuum Drying 63
4.4 Experimental observations 67
4.4.1 Size Reduction Observations 67
4.4.2 Surface Area Expansion Observations 67
4.4.3 Vacuum Drying Observations 68
4.5 Product Analysis 69
4.5.1 Scanning Electron Microscopy (SEM) 69
4.5.2 Energy Dispersive X-rays (EDX) in conjunction with SEM 70
4.5.3 Brunauer-Emmett-Teller Analysis (BET) 71
4.6 Pelletisation and Shaping of Adsorbent Material 72
4.6.1 Typical PSA adsorbent structures 73
4.6.2 Powder Shaping Methods 77
5. Results 79
5.1 Rig Design Results 79
5.2.1 Mechanical Assembly 79
5.2.2 Electrical Assembly 79
5.2 Development of Biopolymer Adsorbent Results: 84
5.2.1 SEM Results: 84
5.2.2 BET Results: 84
5.2.3 Discussion on adsorbent characteristics 88
5.2.4 Pelletisation & Agglomeration 91
5.2.4.3 Analysis of results of mechanical stress testing 104
5.2.4.4 Results in the context of a PSA system 105
6. Conclusions & Future Perspectives 107
6.1 Conclusion 107
6.2 Discussion & Suggestions for Future Work 108
6.1.1 Chemical and Material Sciences 108
6.1.2 Engineering and Process Design: 111

6.1.3 Final Remarks 114

7. Bibliography 115

List of Figures

Figure 1 IPCC Visual representation of impacts and risks for selected natural, managed and human systems [1] 1
Figure 2 Carbon Dioxide Removal technologies currently being funded by US agencies [5] 2
Figure 3 Simplified schematic of the Carbon Engineering capture process (CE) 5
Figure 4 Graphical representation of Climeworks DAC module 6
Figure 5 Type I adsorption isotherm showing the ratio of adsorbate(x) to adsorbent(m) as it varies with pressure 11
Figure 6 Schematic diagrams of TSA, PSA and VSA processes for regenerating solid adsorbents in fixed-bed columns [29] 12
Figure 7 Visual representation of an MSA system for capture of atmospheric CO2 [36] 13
Figure 8 Process Flow diagram of a modified Kraft process for capturing CO_2 from the atmosphere[12] 14
Figure 9 Process patented by Charles Skarstrom [26] 15
Figure 10 PSA Column operational schematic[38] 16
Figure 11 Typical Pressure vs Time graph during PSA cycling[41] 17
Figure 12 Lab PVSA System PID 22
Figure 13 Union T-Fitting 24
Figure 14 Swagelok 90° Union 25
Figure 15 Swagelok Reducer 25
Figure 16 Swagelok Parallel Thread Female Connector 26
Figure 17 Swagelok NPT Female Connector 26
Figure 18 Swagelok Nut and Ferrule Set 27
Figure 19 Swagelok poppet check valve 29
Figure 20 Swagelok bleed valve 30
Figure 21 Swagelok Needle Valve 31
Figure 22 Swagelok Pressure Gauges 33
Figure 23 K30 FR 10000 ppm CO2 sensor 34
Figure 24 Start-up Control Scheme 36
Figure 25 Operation 1 Valve Control Scheme 37
Figure 26 Operation 2 Valve Control Scheme 38
Figure 27 Operation 3 Valve Control Scheme 39
Figure 28 Operation 4 Valve control scheme 40
Figure 29 Shut down Valve Control Scheme 41
Figure 30 HAZOP Node 1 - Adsorption 43
Figure 31 HAZOP Node 2 - Desorption 44
Figure 32 PFD of a DAC process using an aqueous hydroxide solution (NaOH)[11] 56
Figure 33 Graphical representation of structures of three common MOFs [54] 59
Figure 34 Graphical representation of typical zeolite structures, zeolite A and faujasite [62] 59
Figure 35 Graphical representation of typical carbon-based structures 59

Figure 36 Wet (left) and Dried (right) sample of A. nodosum 60
Figure 37 A.nodosum particles 75-150 64
Figure 38 A. nodosum & Ethanol solvent exchange apparatus 64
Figure 39 Vacuum chamber with Saturated A. nodosum 65
Figure 40 Vacuum chamber apparatus on hot-plate 65
Figure 41 Vacuum pump and cold trap 66
Figure 42 Liquid nitrogen cold trap 66
Figure 43 Diagram of SEM and its operational principle[65] 69
Figure 44 Representation of the process of X-ray emission in an EDX/SEM system[66] 70
Figure 45 (a) A variety of different solid adsorbent structures [68], (b) granulated or pelletised adsorbent graphical representation, (c) monolithic adsorbent structure graphical representation, (d) laminate adsorbent structure graphical representation [72] 76
Figure 46 Mechanisms of spheronisation of cylindrical pellets proposed by Rowe (upper) and Baert (lower) 78
Figure 47 Assembled rig 80
Figure 48 PVSA Sample column C-1 and pressure gauge PG-1 81
Figure 49 Top view of PVSA lab rig piping work 81
Figure 50 PVSA lab rig electrical switchboard and power supply 82
Figure 51 Solenoid valve 82
Figure 52 Air feed inlet supply valve and pressure gauge 83
Figure 53 Vacuum pump and vacuum pressure gauge 83
Figure 54 SEM images of Unexpanded (a) and Expanded (b) A. nodosum powder 85
Figure 55 N2 Adsorption isotherm for A. nodosum expanded particles 86
Figure 56 Pore size distribution graph for expanded A. nodosum particles 87
Figure 57 Features of A. nodosum N2 adsorption isotherm 88
Figure 58 Types of adsorption isotherm and hysteresis loops [90] 89
Figure 59 Type IV isotherms of three mesoporous silica-based CO_2 adsorbents [93] 89
Figure 60 Powder blend (top) and adsorbent paste (bottom) 93
Figure 61 Clay extruder and hexagonal and circular extrusion plates 93
Figure 62 Wet adsorbent pellets 94
Figure 63 Extruded adsorbent paste 94
Figure 64 Dry cylindrical adsorbent pellets (a); Dry cylindrical adsorbent pellets (b); Dry hexagonal prism adsorbent pellets (c); Dry agglomerated adsorbent (bd) 95
Figure 65 Texture Analyser 98
Figure 66 Load cell and base plate of Texture analyser 98
Figure 67 Force v Time graph (compressive strength) for 1mm diameter cylindrical pellets (10 units, Batch 1) 99
Figure 68 Force v Time graph (compressive strength) for 1mm diameter cylindrical pellets (10 units, Batch 2) 99
Figure 69 Force v Time graph (compressive strength) for 3mm diameter Hexagonal Prism pellets (10 units, Batch 1) 100
Figure 70 Force v Time graph (compressive strength) for varied agglomerates (10 units, Batch 1) .. 100

List of Tables

Table 1 Description of processes and costs associated with the technologies of emerging companies in DAC industry 7
Table 2 - The four basic steps of Skarstrom cycle 15
Table 3 Swagelok Sample Columns Technical Specifications[44] 23
Table 4 Swagelok SS Sample Column Pressure-Temperature ratings[44] 23
Table 5 Swagelok SS Tubing technical specifications[45] 24
Table 6 Swagelok SS Tubing Pressure-Temperature ratings[45] 24
Table 7 Swagelok T-Fitting Technical Specifications[45] 25
Table 8 Swagelok Elbow fitting technical specifications[45] 25
Table 9 Swagelok Reducer technical specifications [45] 26
Table 10 Swagelok Female parallel thread connectors[45] 26
Table 11 Swagelok Female NPT connectors[45] 27
Table 12 Swagelok Nut-Ferrule Set Technical Specifications[45] 27
Table 13 SMC Solenoid Valve technical specifications[46] 28
Table 14 Swagelok Poppet Check Valve technical specifications[47] 29
Table 15 Swagelok Poppet Check Valve Pressure Temperature ratings[47] 29
Table 16 Swagelok Bleed valves technical specifications[48] 30
Table 17 Swagelok Bleed Valves Pressure-Temperature Rating[48] 30
Table 18 Swagelok GU Needle Valve Technical specifications[49] 31
Table 19 Swagelok GU Needle Valves Pressure-Temperature Rating[49] 31
Table 20 Vacuubrand Vacuum Pump 32
Table 21 Vacuubrand ME 8 NT technical specifications[50] 32
Table 22 Swagelok Pressure Gauge Technical Specifications[51] 33
Table 23 CO2 Sensor Technical Specifications 34
Table 24 Matrix for HAZOP Risk Evaluation 45
Table 25 Risk rating and acceptability criteria 45
Table 26 Node 1 - Adsorption HAZOP 47
Table 27 Node 2 - Desorption/Purge HAZOP 50
Table 28 BET equation variables 71
Table 29 – Comparison of novel biopolymer adsorbent to literature values. 90
Table 30 Material composition of adsorbent pellet batch 1 (cylindrical) 92
Table 31 Material composition of adsorbent pellet batch 2 (cylindrical) 92
Table 32 Material composition of adsorbent pellet batch 3 (hexagonal prism) 92
Table 33 Calculation of Youngs Modulus for 10 pellets from Cylindrical Batch 1s 102
Table 34 Calculation of Youngs Modulus for 10 pellets from Cylindrical Batch 2 102
Table 35 Calculation of Youngs Modulus for 10 pellets from Hexagonal Batch 1 103
Table 36 Calculation of Youngs Modulus for 10 pellets from Agglomerate Batch 1 103
Table 37 Experimental calculation of Young's Modulus for different Biopolymer Adsorbent particles 104

Acronyms

APS	American Physical Society
ATF	Atmospheric Flux Ratio
BECCS	Bioenergy with Carbon Capture and Storage
BET	Brunauer-Emmett-Teller
CBA	Carbon Based Adsorbents
CCS	Carbon Capture and Sequestration
CDR	Carbon Dioxide Removal
CE	Carbon Engineering
CNCE	Centre for Negative Carbon Emissions
CNHC	Carbon-Neutral Hydrocarbon Fuels
DAC	Direct Air Capture
DACCS	Direct Air Capture and Carbon Sequestration
EDX	Energy Dispersive X-rays
ERI	Environmental Research Institute
FR	Fast Response
GA	Gas Analyser
GHG	Greenhouse Gas
GU	General Utility
HAZOP	Hazards and Operability study
IPCC	Intergovernmental Panel on Climate Change
MFM	Mass Flow Meter
MOF	Metal-Organic Framework
MSA	Moisture Swing Adsorption
NDIR	Non-Dispersive Infrared
NFS	Nut Ferrule Set
NPT	National Pipe Thread
OP	Operation
PCA	Paris Climate Agreement
PCC	Post Combustion Capture
PFD	Process Flow Diagram
PG	Pressure Gauge
PID	Piping and Instrumentation Diagram
SR15	Special Report on 1.5°C
PSA	Pressure Swing Adsorption
PVSA	Pressure Vacuum Swing Adsorption
SA	Surface Area
SEM	Scanning Electron Microscopy
SS	Stainless Steel

STP	Standard Temperature and Pressure
TSA	Temperature Swing Adsorption
TVSA	Temperature Vacuum Swing Adsorption
UCC	University College Cork

Scientific Notation

$	United States Dollar
“	Inch
€	Euro
°C	Degrees Celsius
A	Ampere
Å	Angstrom number
AlO_4	Aluminate
$Ca(OH)_2$	Calcium Hydroxide
$CaCO_3$	Calcium Carbonate
CaO	Calcium Oxide
CO_2	Carbon Dioxide
DC	Direct Current
DEA	Diethanolamine
g	Gram
H_2	Hydrogen
J	Joules
K	Kelvin
KOH	Potassium Hydroxide
m	Metre
MEA	Monoethanolamine
N	Newtons
N_2	Nitrogen
NaOH	Sodium Hydroxide
NH_2	Ammonia
Pa	Pascals
ppm	Parts per million
s	Second
s	Second
SiO_4	Silicate
t	Ton
V	Volts
W	Watt

1. Introduction

1.1 Rationale

The IPCC Special Report on the impacts of global warming of 1.5°C [1] 2018, is a UN-sanctioned document that has accumulated all available knowledge and research on climate change, in the scientific, social, and economic domains, and provides the most robust analysis on the Earth's shifting climate conditions ever produced. The report estimates that human "anthropogenic" activities (when compared to pre-industrial standards) on Earth to date have directly resulted in an average surface temperature increase of approximately 1°C ± 0.2°C.

The overall finding of the report is that climate-related risks to natural systems and human societies are significantly increased at 2°C warming when compared with 1.5°C warming, and should human society not aggressively alter its GHG emissions profile in the coming decade, warming will reach 1.5°C by the middle of the century (*high likelihood,* 90-100% probability) and is virtually certain (99-100% probability) to reach 2°C by 2100. This increase will result in catastrophic impacts on human systems, including health, livelihoods, and food and water security. These impacts will occur through irreversible damage to the biosphere of the planet (*high likelihood)*, including all other terrestrial, freshwater, and marine ecosystems, and their various services to humans.

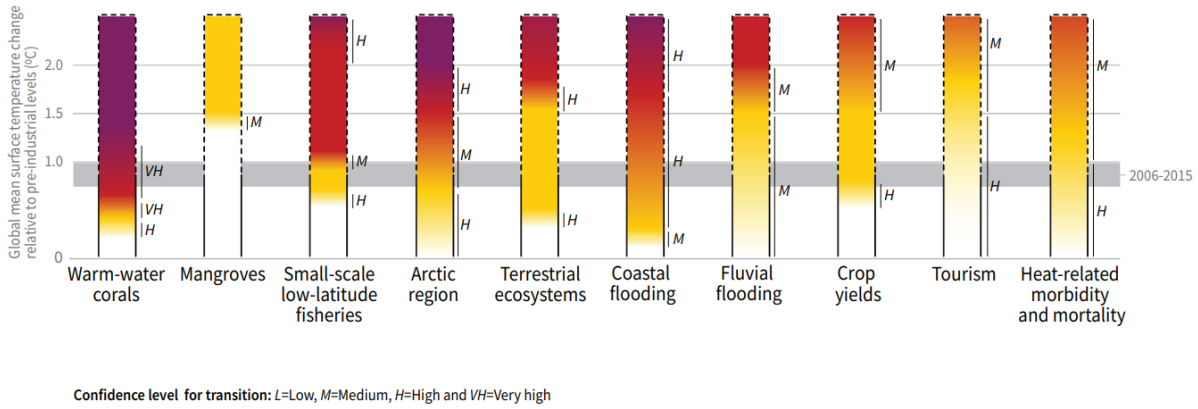


Figure 1 IPCC Visual representation of impacts and risks for selected natural, managed and human systems [1]

Chapter 2 of SR15 [2], entitled "Mitigation pathways compatible with 1.5°C in the context of sustainable development" analyses the potential requirement for Carbon Dioxide Removal (CDR) technologies as the century progresses. The nature and scale ($GtCO_2$ removed) of the CDR technologies to be deployed in emissions pathways consistent with 1.5°C warming levels vary widely, due to the vastly different global emissions profiles that could arise. These variations are largely due to potential societal and governmental attitude shifts. Shifting environmental attitudes are likely to be based on driver amplification (natural disaster, local environmental degradation, etc.), and could precipitate significant policy change, resulting in the drastic reduction of emissions, a point emphasised by Minx et al. [3].

With atmospheric CO_2 levels now at their highest point in approximately 800,000 years[4], and still rising, the requirement for technological solutions for reducing atmospheric or CDR techniques will almost certainly be required. CO_2 removal from the atmosphere is a natural process, with natural terrestrial, geological and ocean reservoirs (known as Carbon Sinks) already removing a portion of atmospheric CO_2 each year. The rapid rise in atmospheric concentrations of CO_2 over the course of the last 100 years is largely a result of the increase in the ratio of anthropogenic emissions of CO_2 to the net CO_2 uptake by natural carbon sinks. This ratio is known as the Atmospheric Flux Ratio (ATF)[1].

Direct Air Capture with Carbon Sequestration (DAC or DACCS) is just one of the CDR technologies being assessed for enhanced atmospheric CO_2 removal. Other examples including Afforestation or Reforestation, Bioenergy Carbon Capture & Storage, Biochar, Enhanced Weathering, Ocean Fertilisation & Soil Carbon Sequestration. Each solution, as is the case with all geoengineering solutions, carries inherent advantages and disadvantages, and it is likely that only through a combination of the solutions will we be able to achieve a sustainable global society. The variety of CDR technologies that are emerging allows governments and societies around the world to introduce a combination of sustainable technologies that are suitable based on geographical and economic factors, as opposed to the one-size-fits-all approach to finding climate solutions.

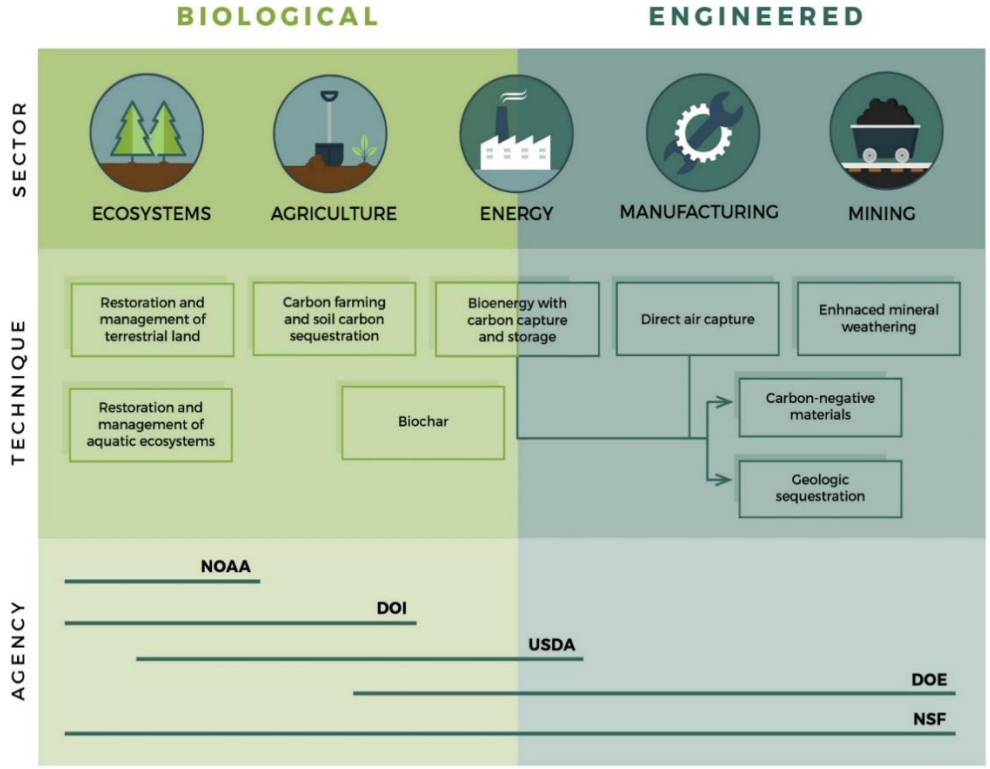


Figure 2 Carbon Dioxide Removal technologies currently being funded by US agencies [5]

This ultimate goal of this research is to conduct engineering research in an effort to aid the development of DAC technologies, through the development of a biopolymer CO_2 adsorbent, and the design and building of a lab-scale PVSA system, which can be used for testing of novel adsorbent materials for CO_2 capacity in future research carried out at UCC.

1.2 Origin and Development of atmospheric CO_2 capture systems

The theoretical inception of atmospheric CO_2 came in the early-to-mid 20th century, with various researchers attempting to further the theoretical understanding and industrial applications of gas adsorption technology. Published in 1947, "Removal of Carbon Dioxide from Atmospheric Air" [6], and ascertained data for the removal of CO_2 from atmospheric air in packed towers using NaOH and KOH solutions.

The earliest examples of atmospheric CO_2 capture systems being deployed can be traced back to early manned spacecraft and submarine missions. Human beings emit roughly 1 kg of CO_2 per day [7] and both environments require the filtration of atmospheric CO_2 to maintain environmental safety for personnel aboard the vessels. The US government utilised single-use lithium hydroxide canisters, to scrub the air aboard the Apollo Spacecraft in the 1950s and 1960s, followed by regenerative zeolite systems in the 1970s for the first space station, Skylab [8]. In the 1980s, their US submarines were equipped with monoethanolamine (MEA) CDR systems that intermittently absorbed and released CO_2 (CO_2 was cooled, compressed and discharged safely) after it was found that continuous exposure to CO_2 levels greater than 1% (1000ppm) precipitated discernible changes in blood pH and affected human ability to retain metallic salts. This is one early example of a regenerative atmospheric CO_2 capture system[9].

Atmospheric CO_2 capture as a technical mitigation strategy for climate change was first proposed as a result of analysis on the diffuse GHG contributing sectors. Transport and agriculture, two of the largest GHG producing industrial sectors, create diffuse emissions that are difficult to capture at the point of release, resulting in huge industries that are near-impossible to decarbonise through conventional means, such as electrification (aviation, livestock production, etc.). A government-funded conference report produced by Klaus Lackner [10] in 1999 recognised the need to create technologies capable of collecting, and either reusing or disposing of CO_2 directly from the atmosphere, that could reduce net GHG emissions without the need for drastic alterations to existing human energy systems (fossil-fuel based). The proposal by Lackner involved thermodynamic analysis of CO_2 removal at atmospheric concentrations using a hydroxide solution ($Ca(OH_2)$), and came to the conclusion that while expensive, Direct Air Capture (DAC) technologies could become of economic interest when countries and governments place an economic value on the sequestration of atmospheric CO_2, which could be precipitated by drastically increased spending on phenomena affected by climate change (i.e. food production, water treatment, disaster relief, etc.).

Since its inception, there has been an exponential increase in the volume of published literature pertaining to DAC and related technologies [11] (i.e. the development of better sorbents for atmospheric CO_2 concentrations, and optimised equipment and processes for industrial systems) and further developments are being made each day.

1.3 Industrial Projects and Developments in DAC Technology

There are a number of companies currently at different stages of process development, attempting to commercialise DAC technologies through the creation of pilot plants and scalable technologies for both CO_2 capture and utilisation. These companies use different sorbents and regeneration processes, as well as operating different strategies for the utilisation of captured CO_2, and therefore offer scope for evidence-based comparison of the various available technologies on a commercial scale. For the purpose of conciseness, only the two companies with fully operational pilot-scale plants will be evaluated.

1.3.1 Carbon Engineering (CE)

CE is a DAC company based in Squamish, British Columbia, Canada. Founded by David Keith, a renowned climate scientist and professor of Harvard University, Massachusetts, USA. CE operates an aqueous hydroxide based capture facility in Squamish, and their CO_2 utilisation strategy is focused on the synthesis of liquid hydrocarbon fuels, a process they call air-to-fuel (A2F) technology. CE, through David Keith and other research-focused employees, has produced a lot of academic literature outlining the operation of their process, including design features, operational costs and full mass and energy balances for each unit operation. Their technical paper published in Joule in August 2018 [12], provides the only detailed end-to-end engineering and cost analysis of a commercial scale (1Mt-CO_2) DAC facility produced to date, and offers insight into the capital and operational costs associated with commissioning and operation of an industrial scale DAC facility.

The development of the CE process was the culmination of nearly a decade of research by Keith and his associates in Harvard that focussed on the development of new, more energy-efficient sorbent regeneration systems and air-liquid contactors for the capture of CO_2 by aqueous hydroxide solutions. The literature establishes the minimum thermodynamic work requirement for sorbent regeneration [13] and argues that the adaptation of the causticization process and heat integration throughout the process drastically reduces the operational cost of the process. The research also provides engineering analysis on the design of more efficient air-liquid contactors that can reduce the capture cost ($/t$CO_2$) as compared with cost predictions put forward in other academic publications, which deem the technology prohibitively expensive [14]. The other key aspect of the Keith & Holmes design is the evaluation of DAC as a potential route for the development of Carbon-Neutral Hydrocarbon Fuels (CNHC), which represents an alternative route to the decarbonisation of the global transport vehicle fleet. Keith, and the other collaborators, argue that CNHC fuels can transform the near-infinite supply of carbon from the atmosphere into high energy density fuels, that are compatible with the current vehicle fleet, and do not require large scale change to human energy infrastructure and transport systems, as seen in other decarbonisation strategies (electrification of vehicle fleet, biofuels or hydrogen) [15]. It is specified that development of CNHC technology for use in tandem with DAC, is a theoretical prospect and not guaranteed to offer a solution to the societal problem of decarbonising the transport

sector, however, CNHC and DAC technologies are at least worthy of a similar amount of funding and research as the alternative decarbonisation strategies. As a result of the academic and industrial development of the CE technology, they evaluate the cost of capture ($/t$CO_2$) as being 94-232$/tCO_2 capture based on their pilot plant[12], which is significantly lower than the previous benchmark cost estimation produced by the American Physical Society (APS), which puts the cost at 500-600$/t$CO_2$[14]. The discrepancy is attributed to the engineering solutions designed by the former which optimise the process of DAC with an aqueous hydroxide solution and use process integration principles to drastically increase energy efficiency, when compared to the technology described in the latter, which is based purely on scientific analysis of minimum energy requirements, and does not include traditional chemical engineering efficiency principles.

While the CE report is based on their pilot plant data, which is at a smaller scale than the proposed facility, their estimation model is robust. Capital costs are based on established industrial equipment that has been identified and adapted (usually through formal collaboration with vendors) to meet the requirements of the process, all stated capital costs include estimations for equipment cost, labour cost and material cost as well as adequate justifications. Operational costs are based around energy and material balances conducted using Aspen Plus process simulation software, which in turn are dependent on both vendor data and data obtained through the operation of the pilot plant [12].

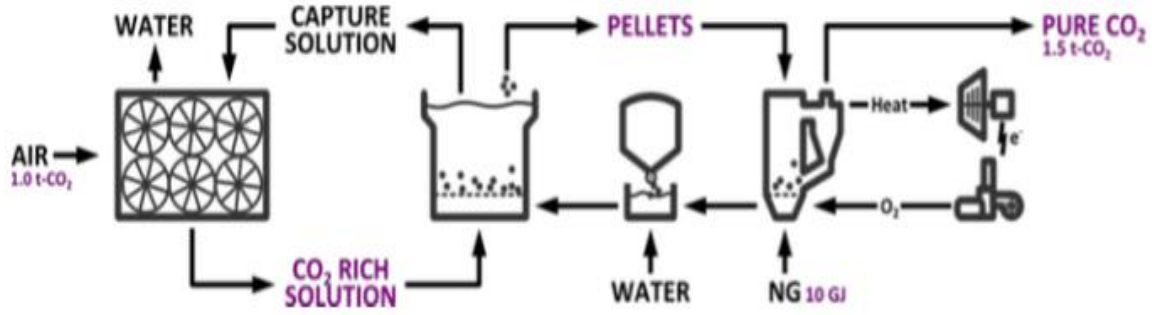


Figure 3 Simplified schematic of the Carbon Engineering capture process (CE)

1.3.2 Climeworks

Climeworks is a Swiss company founded in 2009 by two Swiss researchers, Christoph Gebald and Jan Wurzbacher, as a spin-off company based on their doctoral research theses, which examine novel amine-based solid sorbents (Gebald), and a novel Temperature Vacuum Swing (TVS) process (Wurzbacher) and were conducted in parallel at ETH Zurich [16], [17]. Their capture strategy focuses on the development of solid-amine silica suspended sorbents with high relative surface area and CO_2 capacity, that undergo desorption at low temperatures (approximately 90°C) supplied by low grade heat which uses the principles of both TSA and VSA to achieve an energy-efficient capture cycle [18], [19].

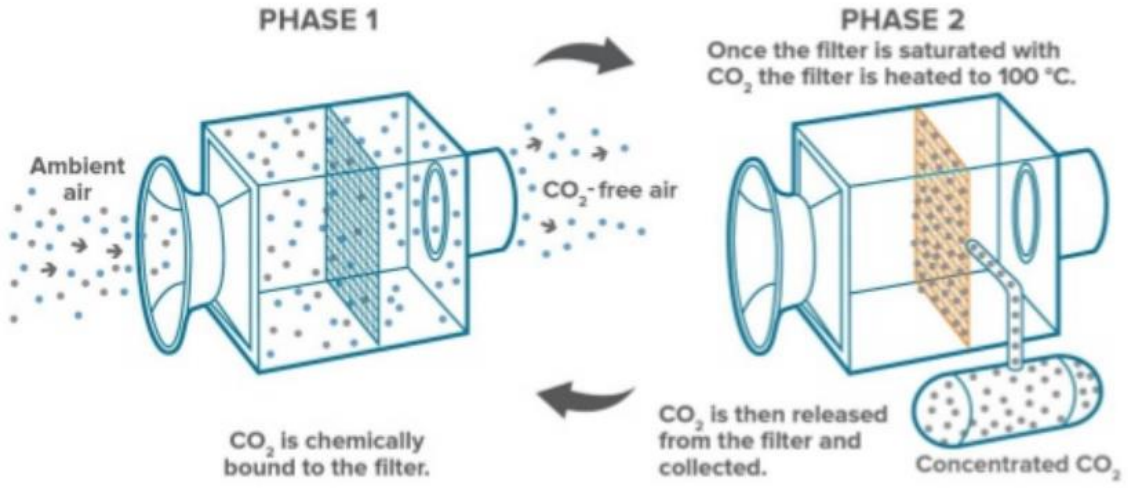


Figure 4 Graphical representation of Climeworks DAC module

The development of the Climeworks process was the result of the academic and industrial developments mate by Gebald and Wurzbacher. Climeworks have three fully operational pilot plants, each with different CO_2 utilisation strategies (DAC with biomass production, DAC with long term sequestration and DAC with fuel production, which is allowing Climeworks to accumulate data on the economic feasibility of DAC as it varies with the downstream CO_2 utilisation process. Their pilot facility located in Hinwil, Switzerland was the first commercial DAC facility to be opened globally (May 2017) and has been in continuous operation since, with a capacity of 900 tCO_2/year. The CO_2 captured by the facility is fed directly to an industrial greenhouse where it enhances biomass growth (tomatoes). Their second DAC facility is a 50 tCO_2/year facility, located in Hellisheidi, Iceland, utilising geothermal energy to provide the heat for desorption of CO_2. The CO_2 captured at this facility is combined with water and injected deep into basalt rock formations, where it reacts with the rock and forms solid carbonate minerals. The sequestered carbon is then monitored to ensure that the injection has been successful, safe, permanent and irreversible. The third plant, launched in Troia, Italy, in October 2018, captures 150 tCO_2/year and operates in parallel to an alkaline electrolyser (1.2MW), which splits water utilising renewable on-site photovoltaic energy and generates up to 240m^3 of hydrogen per hour. The captured CO_2 and H_2 are then chemically combined to form methane which is liquefied and utilised as a liquid vehicle fuel for transport vehicles.

Climeworks do not have the same level of published academic literature as CE by which the end-to-end energy and material requirements of their process can be analysed, so it is difficult to assess the efficiency of their process with accuracy, however, press releases from Climeworks suggest that their capture cost is still in the region of 600-800$/$tCO_2$ which represents a prohibitive capture cost. However, due to the ability of Climeworks to deploy pilot plants in 3 different regions, with three distinct CO_2 capture strategies, they have achieved a high level of funding (approximately €30.8m [20]) and are using the pilot plants to collect data in an attempt to reduce the capital and operational costs of the process.

Company	Process type	Sorbent Material	Estimated Capture Cost ($/t-$CO_2$)
Climeworks [21]	TSA	Solid-Supported Amine	600-800
Carbon Engineering [12]	Calcination	Liquid Hydroxide Solution (NaOH)	94-232
Global Thermostat[21]	TSA	Solid -Supported Amine	10-35[1]
Centre for Negative Carbon Emissions, Arizona State University[21]	MSA	Amine based ion-exchange resin	30-200
Infinitree(Carbon Sink)[21]	MSA	Amine-based ion exchange resin	30-200[2]
Skytree[22]	TSA/VPSA/MSA[3]	Solid-Supported Amine	N/A

Table 1 Description of processes and costs associated with the technologies of emerging companies in DAC industry

[1]Estimate made by Carbon Engineering based on their process at the scale of 1Mt/y.
[2]Infinitree cost estimate based on that of CNCE as the technology was developed by researchers at ASU with similar operational principles.
[3]Information gained from pending patent, which does not specify exact regeneration method, although VPSA system is most likely.

2. Materials & Methods:

The methodology for this research is as follows:

1. Conducted a comprehensive literature review:
   - Created a list of fundamental academic sources pertaining to the research topic.
   - Read these articles and expanded the list of sources to include both citations and dependent articles.
   - Began to separate sources into folders based on the area of research.
   - Collated and summarised relevant information from key academic sources.
   - Review relevant websites and patents.
   - Review relevant Masters Theses online.
   - Created a master list using reference manager Mendeley.

2. Lab Scale PSA Rig Design:
   - Begin preliminary design of CO_2 capture rig using relevant information sources from the literature review.
   - Preliminary assessment of operating requirements and selection of rig system type based on comparison with alternate system designs.
   - Begin detailed design of rig system.
   - Assess requirements for rig inputs, control systems and measurement systems.
   - Mock-up of PID for lab-scale rig system.
   - Sourcing and purchasing of suitable equipment from vendors.
   - Construction of the rig system in the lab.
   - Design of control scheme for the operation of Skarstrom cycle in the rig.
   - Conducting a safety analysis on the rig using HAZOP and what-if safety principles.
   - Creation of an operating manual for lab rig to inform for future research.

3. Development of expanded surface area biopolymer adsorbent for CO_2 capture:
   - Meeting with Materials Science group in ERI to discuss suitable biopolymer adsorbents for this research.
   - Selection of macroalgae (seaweed) biopolymer to be used in development.
   - Conduct an extended literature review on biopolymer adsorbent material development, analysis and use.
   - Development of experimental methodology for the production of biopolymer adsorbent powder.
   - Assessment of biopolymer adsorbent powder properties using lab powder analysis techniques.
   - The shaping of adsorbent material for use in CO_2 capture rig.
   - Mechanical testing of adsorbent particles.

4. Discussion of results and conclusions of the research project:
    - Clearly outline results of the research including the results of the rig design and build, as well as results of the development of a new biopolymer adsorbent.
    - Discuss how the results compare to the original scope of the research and highlight areas in which the research didn't achieve the goals outlined in the original scope.
    - Write a discussion about the results of the research that has been conducted.
    - Make suggestions for future work, and future research to be conducted in the university, and on a global scale in DAC technologies.

5. Completion and submission of Masters Thesis:
    - Outline plan for Thesis, including chapters and sections.
    - Collate relevant data, information, and work produced throughout the course of the research.
    - Assign data and research to the relevant thesis chapter.
    - Complete writing and editing of the thesis.
    - Submit Thesis to UCC on the required submission date.

3. PVSA System Design:

3.1 Overview

To conduct CO_2 adsorption capacity studies on biopolymer adsorbents, a lab-scale experimental rig was designed to facilitate the analysis of CO_2 capacity in various adsorbents by utilising a PVSA adsorption/desorption cycle in a fixed bed sample column. For improved process cycle times, and taking into account available equipment, it was decided that two fixed bed columns would be used, operating a process scheme known as the Skarstrom cycle [23], which allows for alternate adsorption and desorption cycles in a two-column system.

Adsorption describes the phenomenon of the attraction of molecules of a fluid, typically a gas, to the surface of a solid material. These solids, typically microporous materials with a high ratio of surface area to mass, interact with molecules at their surface through spontaneous chemical attractions such as Van der Waals forces or Ion-dipole bonds, allowing certain fluid molecules to be selectively separated from a mixture of molecules [24].

The principle of PSA is based on the phenomenon of certain components of a gaseous mixture being selectively adsorbed onto the surface of a solid microporous adsorbent, with increased adsorption occurring at super ambient conditions of pressure. When the sorbent becomes saturated and breakthrough[4] occurs, the pressure is lowered to near ambient levels, at which point a portion of the adsorbed component is desorbed and can be removed from the system, allowing for further adsorption-desorption cycles [25]. PSA has been a key technology in gas separation operations since it was first introduced as a heatless fractionation (bulk separation) method for oxygen enrichment, by Charles Skarstrom, for ExxonMobil [26] in 1966. Skarstrom designed a two-bed tandem cycle based on the adsorption isotherms of nitrogen and other gaseous compounds in air. Utilising a zeolite adsorbent (zeolite 5A), Skarstrom developed a system by which N_2 is selectively adsorbed at high pressure, and desorbed at low pressure, in a process by which oxygen is concentrated from 22% (atmospheric) to 60 % (percentage based on volume per cent of the total volume of gas) [27]. The major industrial applications for PSA since its inception by Skarstrom have been oxygen enrichment, hydrogen purification, and air drying. In recent years, PSA, VSA and PVSA processes have been identified as potential candidates for the development of industrial-scale CO_2 capture, from both industrial point sources (CCS), as well as diffuse sources (DAC).

For this research, an experimental system was designed, allowing for analysis on the adsorption capacity in different materials under varied conditions of operations. These variations include the concentration of CO_2 in the feed gas, moisture content in the feed gas, adsorption pressure, desorption pressure, and also with different adsorbent materials. This section will outline the development process for the experimental rig from initial design requirements, equipment procurement, assembly as well as operation of the rig.

[4] Breakthrough denotes the moment when the adsorbent material becomes saturated at a given pressure

3.2 Potential Designs and Sorbent Regeneration Techniques:

While the CO_2 capture efficiency of the sorbent material is an important design variable in practical DAC processes, the operation that dictates the overall energy requirement of the system is the regeneration process. Sorbent regeneration is required to enable their use in large and commercially viable numbers of cycles (single-use capture and sequestration is prohibitively expensive) [28]. Regeneration of the sorbent generally requires large amounts of thermal or mechanical energy input which greatly alters the operational cost of the system and is the centre of a lot of research in DAC.

3.2.1 Pressure/Vacuum Swing Adsorption

Pressure Swing Adsorption (PSA) is generally used for regeneration of physisorbent materials, such as MOFs, Zeolites or Carbon-based adsorbents. PSA is a process based on the loading capacity of CO_2 in a sorbent material as it varies with pressure. Generally, adsorbents exhibit high CO_2 capacity at high pressures and low CO_2 capacity at low pressures. By utilising a controlled pressure swing (decreasing pressure) in a closed system, concentrated CO_2 can be removed from the sorbent material and transferred to another part of the system, at which point the pressure is restored and another cycle of CO_2 capture begins [28], [29].

Similarly, Vacuum Swing Adsorption (VSA) is also a process based on the working capacity of CO_2 in a sorbent material as it varies with pressure. VSA operates in the same manner as PSA, the key difference being that adsorption takes place at atmospheric pressure, and desorption takes place at sub-atmospheric pressures, through the utilisation of a vacuum pump. VSA is widely considered as a more feasible option for DAC technologies as it does not require the compression of inlet gas (excessively large volumes of air for atmospheric CO_2 capture), and relies solely on the depressurisation of the CO_2 capture chamber (adsorbent containing area of the system) to sub-atmospheric conditions, at which point the adsorbate is desorbed from the pores of the adsorbent, allowing CO_2 to be drawn off in a concentrated stream [29]–[31].

Pressure Vacuum Swing Adsorption (PVSA) is simply a combination of the PSA and VSA systems, in which adsorption takes place at super atmospheric pressures and desorption takes place at sub-atmospheric pressures [28].

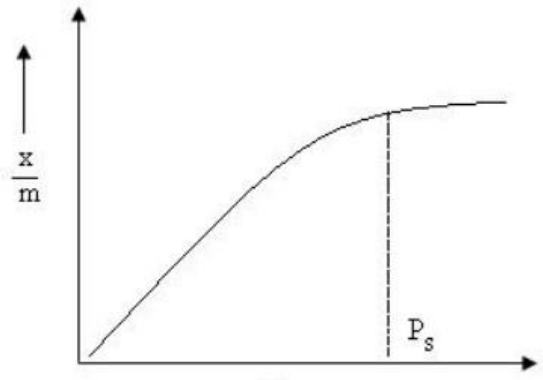


Figure 5 Type I adsorption isotherm showing the ratio of adsorbate(x) to adsorbent(m) as it varies with pressure

3.2.2 Temperature Swing Adsorption

Temperature Swing Adsorption (TSA) is generally used for the regeneration of chemisorbent materials, such as solid amines that are tethered or supported on specially designed structures[14], although research is being conducted into full TSA or combined TSA/PSA systems for physisorbent materials also [28]. TSA is based on the loading capacity of CO_2 as it varies with temperature. Generally, sorbents exhibit high CO_2 capacity at lower temperatures with capacity decreasing as the temperature is increased. In TSA, the saturated adsorbent is heated by a hot inert gas (usually N_2) that is passed over and through the adsorbent (called a hot gas purge) [32], [33]. When the binding energy between the CO_2 and adsorbent is exceeded, desorption occurs allowing for the concentrated CO_2 to be drawn away from the closed system [28].

TSA presents opportunities in solid adsorption processes as the temperature requirement for desorption usually varies from 50-150°C, which can be easily be supplied using waste heat from industrial processes. However, TSA also faces obstacles, including the thermal degradation of adsorbent materials, which greatly reduces their useful life cycle. TSA also faces issues with supplying enough heat for the hot gas purge (gasses have a low specific heat capacity and thus, the process requires very large volumes of gas to be heated and passed through adsorbent) [28], [32], [33].TSA can also be used in combination with PSA or VSA creating PTSA and VTSA, which are being investigated by researchers in an attempt to find the lowest combined energy input requirement for sufficient desorption while maintaining the resilience of the adsorbent material for a long useful lifecycle.

TSA was not considered for this research due to the nature of the sorbent materials being studied. TSA is suitable for chemical adsorbents, which is a branch of adsorption by which reversible chemical reactions occur with CO_2 molecules at the surface of the material. The materials of interest to this particular research are largely physisorbent.

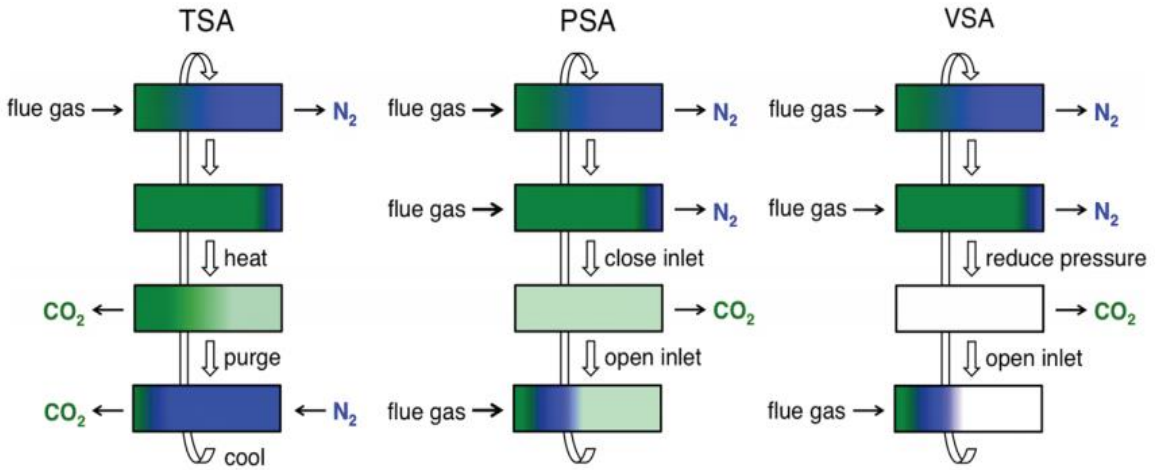


Figure 6 Schematic diagrams of TSA, PSA and VSA processes for regenerating solid adsorbents in fixed-bed columns [29]

3.2.3 Moisture Swing Absorption

Moisture Swing Absorption (MSA) utilises the natural ion hydration process to capture and CO_2 from the atmosphere and selectively release it. Ion hydration occurs in many natural biological and environmental processes [34]. MSA involves the use of a heterogeneous ion exchange resin coated on a solid polymeric support. For example, an amine-based anion exchange resin can be utilised to absorb CO_2 from ambient air in dry conditions, and release the CO_2 when hydrated or exposed to liquid or vapour water [35]. MSA is interesting as it trades the energy input requirement of a TSA or PSA system, merely requiring a water supply, with the latent heat of evaporation providing all of the energy required to drive the cycle [36]. Using water as an energy source has comparatively low energy costs when compared with typical TSA or PSA systems, however, there is a requirement for the air input to be dry, which limits the ability of the technology to be deployed in certain regions of the earth (medium to high humidity areas such as tropical regions), giving rise to further economic and feasibility considerations.

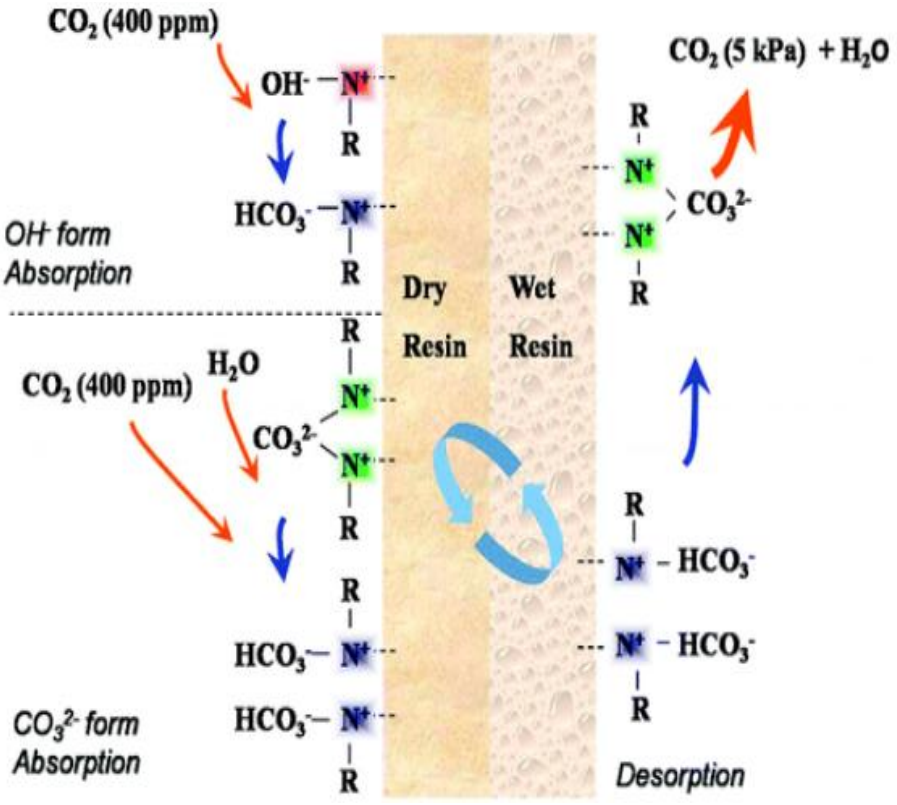


Figure 7 Visual representation of an MSA system for capture of atmospheric CO2 [36]

3.2.4 Kraft Process

The Kraft process is the regeneration process utilised in liquid hydroxide absorption systems. It has been utilised in the paper industry for the extraction of cellulose from wood by using sodium hydroxide. The sodium hydroxide solution adsorption loop can be applied to CO_2 capture processes designed today and utilised in DAC technologies (as described in section 1.3.1). The carbonate, formed when the hydroxide solution comes into contact with the CO_2 present in the air supply, is reacted with calcium hydroxide, in a process known as causticization. Causticization involves the exchange of carbonate ions, which produces calcium carbonate, regenerating the sodium hydroxide which can be recycled to the air contactor for further capture cycles. The calcium carbonate ($CaCO_3$) must then be treated in a calcination process and separated into pure CO_2 which can be compressed and sequestered. The calcination process involves a large application of heat to the $CaCO_3$ solution, which separates it into a pure gaseous CO_2 stream and CaO (lime) (thermodynamic minimum energy input of 179.2 kJ mol^{-1} for calcination or temperatures of between 600-900°C) [11], which drastically increases the minimum energy requirement and eventual overall cost of the entire capture process, given the large volumetric requirements of CO_2 capture from the atmosphere (dilute source). CaO is finally hydrated in a slaking process to reform $Ca(OH)_2$ which is reused in the precipitation step. Fig. 8 shows a process flow diagram representing the modified kraft process designed by Keith and Holmes for CO_2 capture[12].

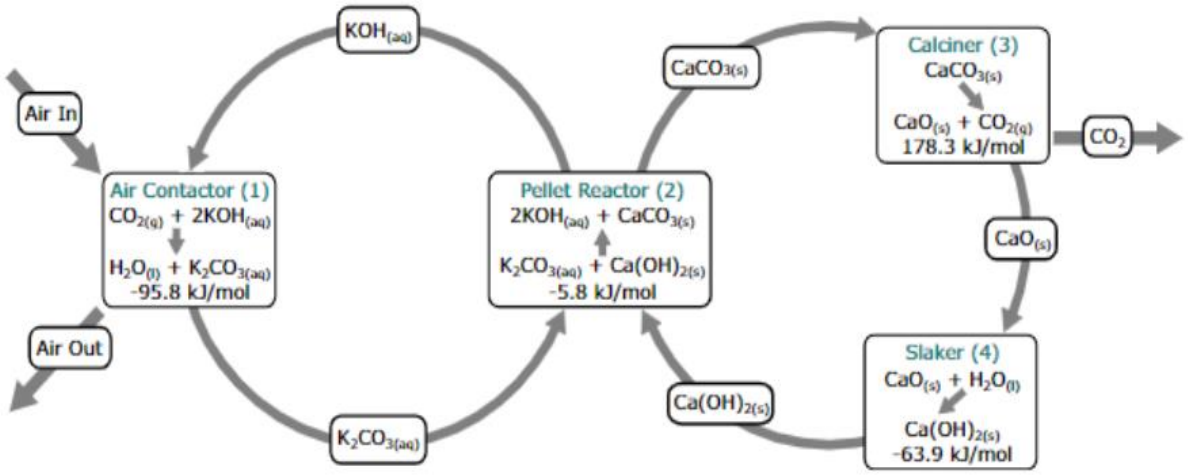


Figure 8 Process Flow diagram of a modified Kraft process for capturing CO_2 from the atmosphere[12]

3.3 Preliminary Design:

This section outlines the process parameters considered during the first phase of the design and commissioning of a CO_2 PVSA experimental rig, operating a Skarstrom cycle. It describes the considerations made prior to detailed design to ensure the operational success and experimental accuracy of the system.

3.3.1 Skarstrom cycle overview:

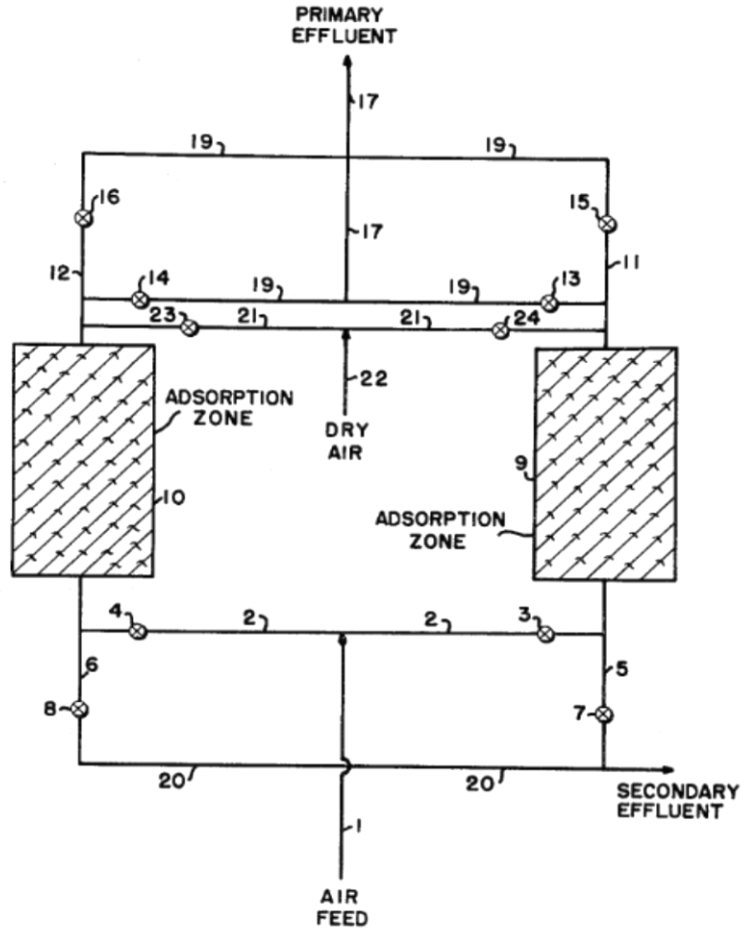


Figure 9 Process patented by Charles Skarstrom [26]

A simplified schematic of the Skarstrom cycle, from the original patent [26], is shown in Fig. 9. The process operates with two identical columns that run in tandem at alternate stages of a four step adsorption-desorption cycle [37].

	Step 1	**Step 2**	**Step 3**	**Step 4**
Column 1 (C-1)	Pressurisation	Adsorption	Blowdown	Purge
Column 2 (C-2)	Blowdown	Purge	Pressurisation	Adsorption

Table 2 - The four basic steps of Skarstrom cycle

3.3.1.1 Pressurisation:

The cycle begins with co-current pressurisation of C-1 using the feed stream. Pressurisation sees the feed mixture introduced at the top of the column at a known flow rate until pressure reaches a pre-defined, super-ambient adsorption pressure (this pressure varies depending on the adsorbent being used).

3.3.1.2 Adsorption:

The column exit valve is opened, and pressure and temperature are maintained at constant levels as the CO_2 rich gaseous mixture is fed through the column at a controlled flow rate. The composition of the gaseous mixture is known, and the heavy component, which is CO_2 for DAC studies, is adsorbed in the column. Downstream of the column, the composition of the lean mixture is analysed before being vented to atmosphere.

3.3.1.3 Blowdown:

The CO_2 content in the lean gas mixture increases sharply when breakthrough occurs due to sorbent saturation, at which point blowdown can begin. Blowdown is a rapid counter-current depressurisation step during which the column pressure is drastically lowered, reducing CO_2 capacity in the adsorbent. A traditional PSA column would typically open the purge vent which equalizes the column bed pressure to atmospheric levels (≈1.1bar). For a PVSA system, a vacuum pump is used to create sub-ambient pressure conditions in the column, which further increases desorption.

3.3.1.4 Purge:

The final step of the Skarstrom cycle is a purge step, in which an inert gas is fed to the bottom of the column and flows counter-current through the column, sweeping the desorbed CO_2 from the adsorbent bed, after which it is vented to atmosphere.

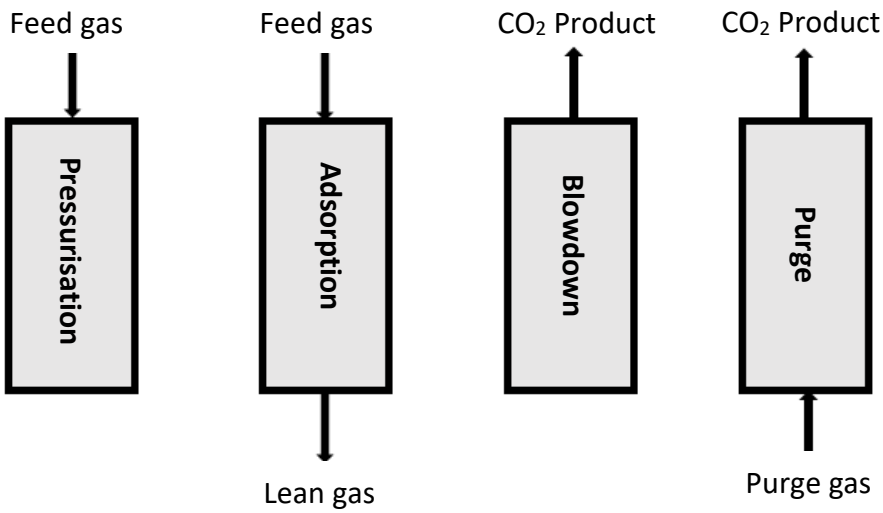


Figure 10 PSA Column operational schematic[38]

3.3.1.5 Operational Pressure

At various stages of the cycle, the columns and equipment are exposed to a range of pressures including sub-atmospheric and super-atmospheric. The rig was designed to be operational without leakage or rupture at pressures exceeding the upper and lower requirements of pressure. First upper and lower limits of pressure in the system were established. Based on literature values for the testing of activated carbons for CO_2 adsorption in PSA systems [37][39][40], 20 bar was chosen as the maximum testing pressure. While the testing for this project was largely conducted at <6 bar, 20 bar was chosen as the maximum design pressure, to allow future research involving new adsorbent materials that necessitated higher operating pressures, to be conducted on the rig. A factor of safety of 3 was employed for the system to ensure that variations in the feed pressure due to unforeseen circumstances, for example, pump malfunction, would not result in leak or rupture. Though it is nearly impossible that the system could become exposed to an excess pressure of this magnitude, it is considered good practice in the design of a pressurised system to employ a large factor of safety. The minimum testing pressure in the system is the ultimate vacuum that the vacuum pump is capable of producing which is specified as 70 mbar absolute. The pressure ratings of the materials and equipment used in the construction of the lab-scale pilot rig are outlined in section 3.7. System pressure is monitored at all times during the cycle by pressure gauges directly downstream of the column (section 3.6) which can measure pressures in the range of vacuum to 5bar, which is suitable for the testing required to be carried out on the rig.

Fig. 11 is a representation of the change in operating pressure over the course of a cycle in a generic PSA cycle.

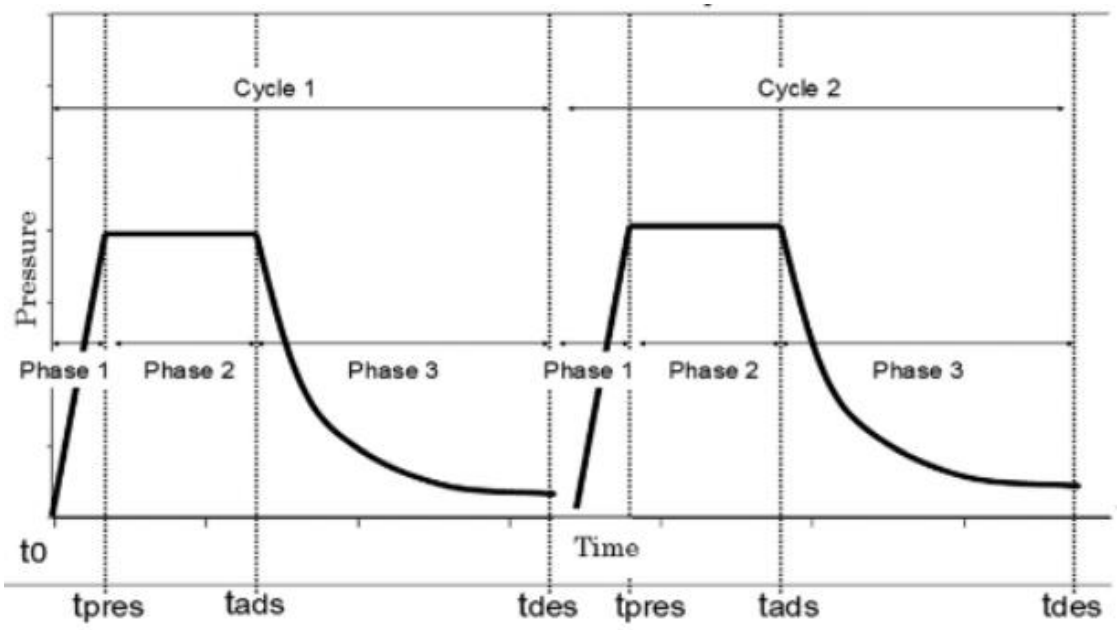


Figure 11 Typical Pressure vs Time graph during PSA cycling[41]

3.3.1.6 Operational Temperature

There were no unique design requirements relating to temperature in the design of the lab-scale pilot rig. The PVSA process employed does not rely on heat energy input to aid desorption and thus, the operational temperature of the rig is low. The operational temperature of the rig was initially given the boundaries 273.5-373.5K (0-100°C). This range was chosen for a number of reasons. Firstly, it was suitable for testing of adsorption capacity of the materials at various near ambient temperatures and also provided a sufficient temperature range to accommodate natural variations in feed or system temperatures. This range was also chosen to facilitate the potential use of the system in future research that might use a combination of PSA and TSA, in the event that the sorbent materials being tested are more effective in a TSA cycle (eg. solid-supported amines). A factor of safety of two was chosen for the operational temperature, meaning that all fluid contacting equipment was designed to be operational up to 200°C, which far exceeds the range in which conventional TSA systems operate, with typical regeneration temperatures in the range of 80-120°C. Solid adsorbent melting points typically range from 140-245°C[42][43], which results in the evaporation of sorbent material, drastically reducing the adsorption capabilities of the system and resulting in replacement of sorbent materials, which can be costly. For these reasons, desorption temperatures in academic and commercial TSA systems rarely exceed 150°C, meaning that the design temperature of this system is suitable should the system be adapted for TSA in future research.

3.4 Alternate Design Schemes:

Two alternate rig design schemes were initially examined before the dual column Skarstrom cycle PVSA system was chosen:

3.4.1 Single Bed PSA System

A single bed PSA system operates PSA in a singular column bed. The operation of the rig follows the typical PSA scheme of pressurisation, adsorption, blowdown and purge, with a simple fluid flow control scheme. The feed source for the system is either compressed air drawn from atmosphere or a known mix of gasses input from pressurised cylinders and a known flowrate via a gas manifold at the inlet. Variable measurement in the system is conducted with standard equipment including pressure gauges and CO_2 sensors.

3.4.2 Single Bed PVSA System

A single bed PVSA system was also briefly considered at the outset of the system design phase, which is the same system as described in section 3.4.1, with the addition of a vacuum pump to create negative pressure. It was decided that a dual column system would be more suitable, as a dual column system allows for more rapid testing of materials, as well as concurrent testing of two different materials. This decision was taken for processing considerations and due to the equipment and materials already available for the rig.

3.5 Detailed Design:

The next step of the rig design process involved the creation of a Piping and Instrumentation Diagram (PID) which is a visual representation of the process design, showing the position of all equipment and instrumentation within the system, as well as all mechanical and electrical lines. The PID was referenced for the purpose of sourcing suitable equipment, and also as a guideline for the physical construction of the PSA Unit. Following construction, the PID was utilised as a source for information in conducting a safety assessment of the rig and producing an operation manual.

3.5.1 Piping and Instrumentation Diagram (PID)

A PID is a prerequisite for the commission and building of any process system or rig. PIDs allow Engineers, Operators, and anyone involved in the building and operation of a process system to gain a detailed understanding of the process equipment being used, the control systems in place, the individual unit operations, and the material and energy flows within the system. They are a central part of the design of any process.

For this PSA system, a PID was created at the beginning of the design process (Fig. 12) using Microsoft Visio. The PID produced is a schematic representation of the equipment and piping used in the rig, and is not a scaled layout. There were a series of design revisions before a final design layout was selected.

The PID (Fig 12) served as the basis for equipment and piping design and purchase, and was used in the evaluation of the construction process and progress. The equipment and piping utilised in the design are outlined in a legend that accompanies the diagram. The legend describes what each symbol represents, and can be used and labelling of equipment is to define the position of each piece of unique equipment in the system.

The PID (Fig. 12) was used to develop the other key aspects of the rig design, including:

1. The development of a control and operation system for the rig.
2. The development of a Hazard and Operability Study (HAZOP) and of a safety system for the rig.
3. The development of an operational methodology and communication documents for the rig.

3.5.2 Feed Sources

The feed source for the system is compressed air, drawn from the atmosphere, and supplied at a maximum of 6 bar pressure. The system was designed to allow for the integration of a gas manifold at the inlet which would allow for the input and mixing of gasses from pressurised containers to create varied gas mixtures of known concentration, should it be required for future research. The addition of a gas manifold and gas mixtures with higher CO_2 concentration would allow the rig to be used with a wider range of adsorbent materials, including adsorbents more suited to CCS applications.

The second inlet feed source is N_2 which is supplied using an industrial gas canister (230bar) available for lab or commercial use. Nitrogen flow rate is controlled using both a purge inlet valve and the canister valve itself.

3.5.3 Flow Control

Flow control in the system is carried out using a series of valves that manipulate fluid flow within the system depending on the requirements of each operational stage. Several different valves were used in the design, including two-way solenoid valves, bleed valves and needle valves, and check valves, which are described in section 3.6.4. Flow in the system is controlled through the manual switching of the valves according to the control schemes described in section 3.7, to meet the flow requirements for each cycle phase. Due to budget considerations, flowmeters were not acquired for the rig. The flow rate of air can be calculated manually using the known values of pressure, and piping specifications, but the system was designed to allow for easy integration of flowmeters if required for future work.

3.5.4 Pressure Control

Pressure control in the system is done manually. The pressure is read on pressure gauges both at the feed inlet, and downstream of both columns, and based on the readings, the pressure in the columns is manipulated by adjusting either the feed inlet valve, or the lean gas outlet valve, or both. Due to budget considerations, automatic pressure control was not designed. In future work, for more accurate pressure control and measurement, pressure transducers and a PID controller could be used to automatically adjust conditions in the system and react to variations in column pressure.

3.5.5 Temperature Control

Temperature control for the system was initially ignored in the design. Room temperature in the lab in which the system was housed was measured over a period of 1 month to be 20 ± 3°C. This variation in temperature was deemed to be acceptable for the level of testing initially required in the system. For future work, it is recommended that a heating jacket or coils be used on both columns, in conjunction with thermocouples, to accurately measure and control the temperature in the columns.

3.5.6 Humidity Control

Humidity control was ignored in this design due to budget considerations. While humidity is an important metric in a PSA system, for this research it was decided that humidity would be taken as atmospheric humidity, and noted before each testing cycle. This was assumed as the gas inlet feed for the design is compressed atmospheric air. For future work, a humidity sensor, integrated with the gas analyser should be used for humidity measurement in the system, and used in tandem with a gas drying unit to control humidity in the inlet feed. For DAC research, using an inlet stream with natural humidity variations is acceptable, as it mirrors real operating conditions. Effective humidity control is more applicable to research in CCS, which requires adsorbent materials that are effective at separating CO_2 at higher concentrations, typically from dry (low water content) gas mixtures (flue gas).

3.5.7 Gas Analysis

Gas analysis in the system is required at both the inlet gas feed and the lean gas outlet or vent stream. To calculate the volume of CO_2 is being removed, and the adsorbent loading capacity, the concentration at of CO_2 in the inlet stream, and the flow rate of air through the system must be measured to calculate the volume of CO_2 entering the column. The concentration of CO_2 in the lean gas vent stream also has to be measured, as well as the flowrate of lean gas out of the system. By calculating the difference between the two values the loading capacity can be ascertained.

It was decided that the CO_2 sensors should be fast response sensors with a high data output rate due to the short cycle times associated with a small scale PVSA system. If the time span in between concentration readings is too long, breakthrough time is measured with less accuracy which has negative impacts on the accuracy of the adsorption isotherm produced.

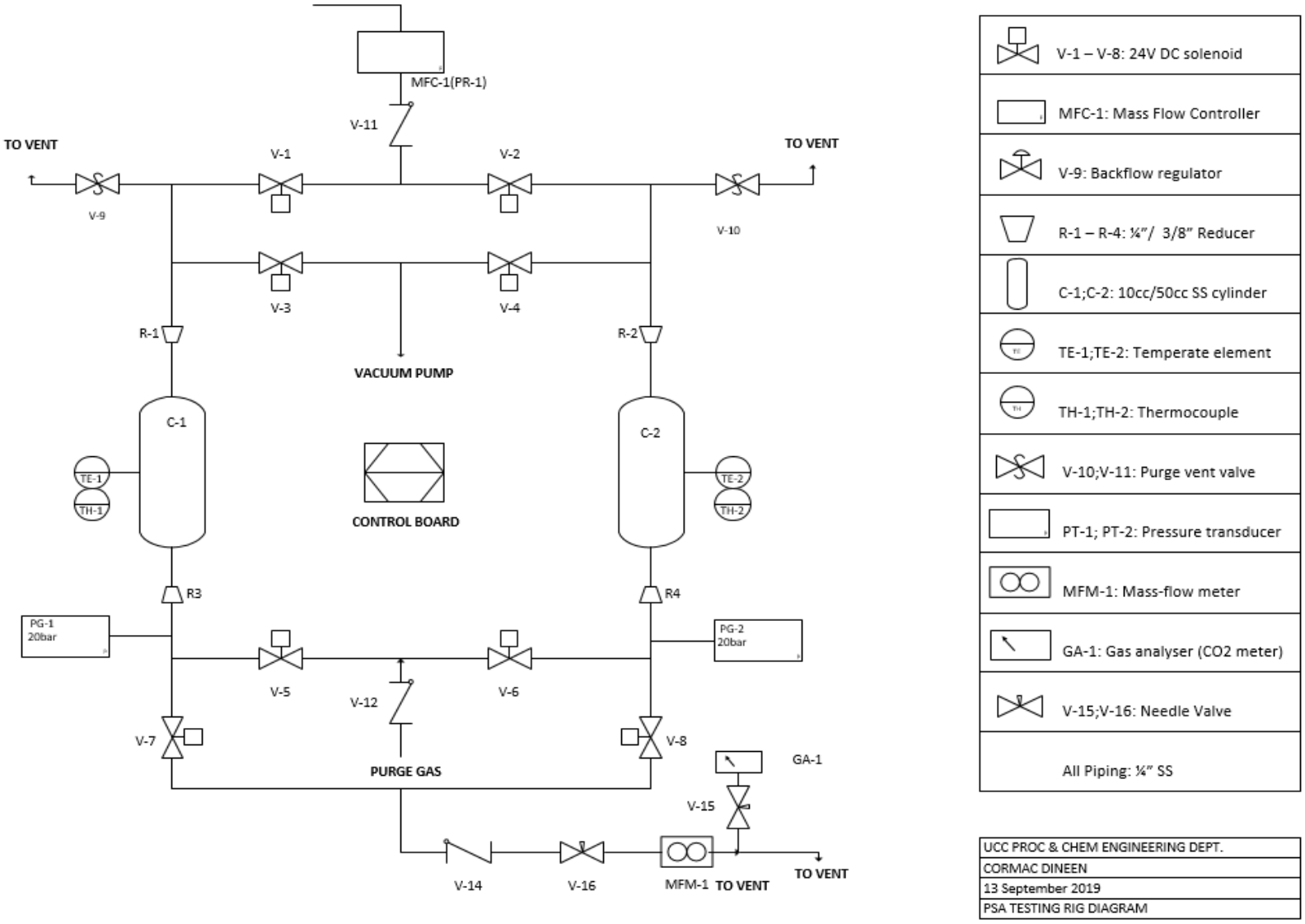


Figure 12 Lab PVSA System PID

3.6 Equipment Selection & Sourcing

Equipment and materials were sourced that were suitable for fulfilling the operational requirements of the process, and of the detailed design outlined in section 3.6.

3.6.1 Sample Columns:

To operate a Skarstrom cycle, two double-ended cylinders were required. The cylinders act as both the adsorption and desorption zone of the process and are central to the operation of the rig. Double-ended cylinders allow for both co-current and counter-current flow of feed gas, purge gas and off-gas.

For the pilot rig, two sets of two columns were acquired. It was decided that two sets of interchangeable columns would be required to allow for variations in the available volumes of adsorbents, which is dependent on a number of factors such as commercial availability of the adsorbent, cost per unit volume, and lifespan of the adsorbent material. By having two sizes of column, the testing process could be adapted to reduce the required quantities of the adsorbent material. This is important as some adsorbents, such as MOFs, are difficult and expensive to synthesise, thus larger sample columns greatly increase the operational cost of the laboratory system. Another benefit of smaller sample columns is the decreased cycle time.

Column A1 and A2 are identical 25cm^3 columns, and column B1 and B2 are identical 50cm^3 columns. The technical specifications of the columns are described in tables 3 and 4.

	Column A1	**Column A2**	**Column B1**	**Column B2**
Material Grade	316L SS	316L SS	304L SS	304L SS
Pressure Rating	68.9 bar	68.9 bar	124 bar	124 bar
Internal Volume	25 cm^3	25 cm^3	50 cm^3	50 cm^3
Bed Height	64mm	64mm	64mm	64mm
Bed Diameter	23.15mm	23.15mm	36.40mm	36.40mm
Volume Tolerance	±5%	±5%	±5%	±5%
Connection Size	3/8”	3/8”	1/4”	1/4”
Connection Type	Tube Fitting	Tube Fitting	Female NPT	Female NPT
Part Code	SS-4CD-TW-25	SS-4CD-TW-25	304L-HDF4-50	304L-HDF4-50

Table 3 Swagelok Sample Columns Technical Specifications[44]

Temperature (°C)	**304L SS**	**316 SS**
-53 to 37	124 bar	68.9 bar
93	93.7 bar	57.8 bar
148	84.7 bar	52.3 bar
204	77.8 bar	48.2 bar
260	72.3 bar	44.7 bar

Table 4 Swagelok SS Sample Column Pressure-Temperature ratings[44]

3.6.2 Piping:

All piping for the rig was chosen to be 1/4" stainless steel piping. This piping was acquired from Swagelok. The pipe sizing selection was made due to the availability of the required fixtures and instruments with 1/4" connections. The technical specifications of the piping used in the rig are described in tables 5 and 6.

Swagelok 316L SS Piping Technical Specifications	
Tube Diameter	0.25"
Wall Thickness	0.035"
Weight	119.053 g/m
Working Pressure	351.63 bar
Part Code	SS-T4-S-035-6ME

Table 5 Swagelok SS Tubing technical specifications[45]

Temperature (°C)	Pressure (bar)
Up to 93	351.63
204	337.31
315	298.66
426	277.57

Table 6 Swagelok SS Tubing Pressure-Temperature ratings[45]

3.6.3 Fittings

The fittings, including all of the joints and connections required for the equipment and instrumentation of the rig, were acquired from Swagelok. Various fittings were required, based on the topography of the rig, and the connection types of valves and instruments, as well as structural and operational considerations for the system. Each type of fixture used in the rig is described in this section, along with its location and use within the system.

3.6.3.1 T-fittings

T-fittings were used at fourteen locations in the rig. T-fittings are used to connect three sections of piping in the rig, which was required in multiple locations throughout the system, in order to enable the Skarstrom operational scheme, which involves the adaption of flow routes in the system with valve changes. T-fittings were also used to enable the connection of analysis equipment to the rig, including the gas analysis instruments and pressure transducers. All T-fittings were acquired from Swagelok, with technical specifications described in table 7.

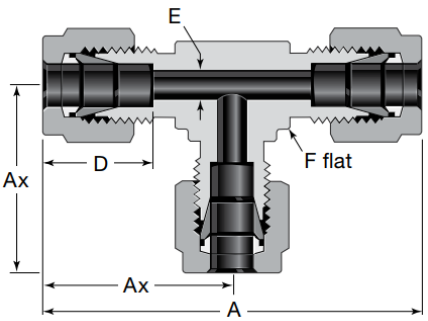


Figure 13 Union T-Fitting

Swagelok T-Fittings Technical Specifications	
Material	316L SS
Connections Size	1/4”
Working Pressure[5]	351.63 bar
Part Code	SS-400-3

Table 7 Swagelok T-Fitting Technical Specifications[45]

3.6.3.2 Elbows

45° Elbows were used at six locations in the rig. 45° elbows are used to connect two sections of piping in the rig to make a perpendicular connection. It was decided that the cylinders would be in front of the valve and instrumentation systems to allow for future installation of a panel, upon which control switches or measurement dials could be mounted to centralise control of the system. Isolating the cylinders at the front of the rig also facilitates the future implementation of temperature control systems, such as a temperature chamber or bath that can be used to directly control the temperature in the cylinders rather than the whole system, removing design and cost considerations. All 45° Elbows were acquired from Swagelok with technical specifications outlined in table 8.

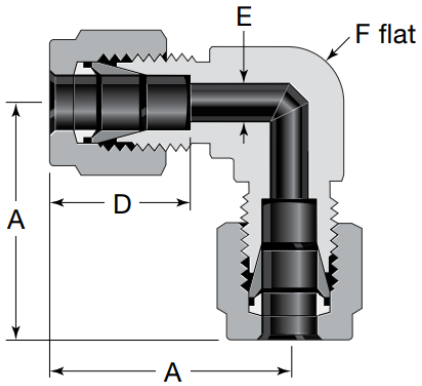


Figure 14 Swagelok 90° Union

Swagelok 90 Elbows° Technical Specifications	
Material	316L SS
Connections Size	1/4”
Working Pressure	351.63 bar
Part Code	SS-400-3

Table 8 Swagelok Elbow fitting technical specifications[45]

3.6.3.3 Reducers

Reducers were used at four locations in the rig. Reducers are used to connect a larger section of pipe with a smaller section of pipe. They were utilised in the rig to facilitate the variation of column sizes between A columns (50cm^3) and B columns (25cm^3). The double-ended B columns were only available with 3/8” connections, which meant that reducers had to be purchased so they could be easily integrated into and removed from the system, which uses with 1/4" piping. The reducers were acquired from Swagelok with technical specifications outlined in table 9.

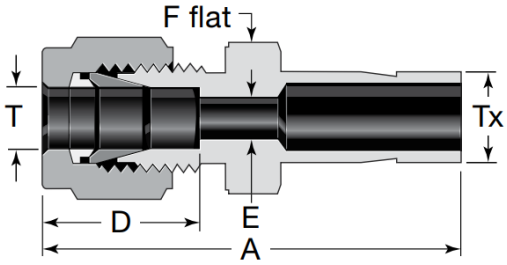


Figure 15 Swagelok Reducer

[5] All Swagelok tube fitting ends are rated to the working pressure of the tubing used in the system

Swagelok Reducers Technical Specifications	
Material	316L SS
Connection 1 Size	1/4”
Connection 2 Size	3/8”
Working Pressure	351.63 bar
Part Code	SS-600-R-4

Table 9 Swagelok Reducer technical specifications [45]

3.6.3.4 Female Parallel Thread Connectors

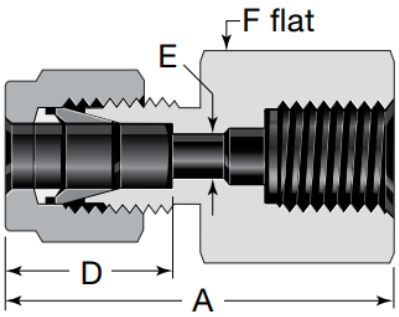


Figure 16 Swagelok Parallel Thread Female Connector

Parallel thread female connectors were required at two locations in the rig. These connectors are were required to facilitate the integration of pressure transducers into the system. The pressure transducers acquired had 1/4" parallel thread male connections which could not be integrated using regular two ferrule-nut pipe fittings. The connectors were acquired from Swagelok and threading was matched to that of the pressure transducers acquired from Manotherm, and allowed them to be integrated into a system primarily consisting of Swagelok equipment. The technical specifications of the connectors are outlined in table 10.

Swagelok Female Parallel Thread Connectors	
Material	316L SS
Connection 1 Size	1/4” tube fitting
Connection 2 Size	1/4" ISO RG Parallel Thread
Working Pressure	351.63 bar
Part Code	SS-600-R-4

Table 10 Swagelok Female parallel thread connectors[45]

3.6.3.5 Female National Pipe Thread (NPT) Connectors

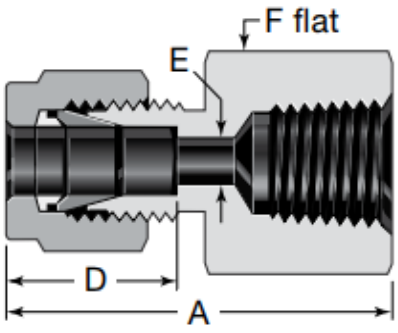


Figure 17 Swagelok NPT Female Connector

Female NPT connectors were used at two locations in the rig. These connectors were required to facilitate the integration of two bleed valves into the rig. The bleed valves were required for the venting of the nitrogen purge stream, however, suitable bleed valves were only available from Swagelok with 1/4" male NPT connections. The two connectors were acquired from Swagelok and connected to the system with the 1/4" pipe fitting. Female NPT

connectors technical specifications are outlined in Table 11.

Swagelok Female NPT Connectors Technical Specifications	
Material	316L SS
Connection 1 Size	1/4” tube fitting
Connection 2 Size	1/4” NPT
Working Pressure	351.63 bar
Part Code	SS-400-7-4

Table 11 Swagelok Female NPT connectors[45]

3.6.3.6 Nut-Ferrule Sets (NFS)

Each connection made in the system requires a nut-ferrule set. The Swagelok NFS (Fig. 18) consists of two-ferrules. The front ferrule creates a seal against the outside diameter of the tubing, and the back ferrule axially advances the front ferrule, locking in the seal. Each fitting purchased from Swagelok comes with an NFS and can be used to fix the fitting to Swagelok piping, however, spare sets were also required to replace sets damaged by errors that occurred in the fitting of the NFS to the piping. The technical specifications of the NFS are outlined in table 12.

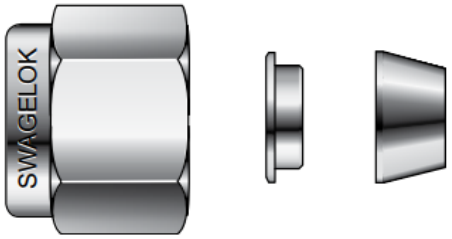


Figure 18 Swagelok Nut and Ferrule Set

Swagelok Nut-Ferrule Set Technical Specifications	
Material	316L SS
Working Pressure	351.63 bar
Part Code	SS-400-NFSET

Table 12 Swagelok Nut-Ferrule Set Technical Specifications[45]

3.6.4 Valves

A series of valves were used in the system, the locations of the valves are described in the PID on section 3.5.1. The valve scheme consists of 13 valves, with different modes of operation, and different purposes. The valves are part of a control scheme that allows the direction of fluid flow within the system to be manipulated, allowing for continuous adsorption and desorption cycling in alternate columns. The types of valve, their purpose, and justifications for their use in the system are described in this section.

3.6.4.1 Solenoid Valves:

Solenoid valves were used at 8 locations within the system. To operate a Skarstrom cycle PSA/PVSA system requires rapid, simultaneous switching of the direction of fluid flow within the system, so that the conditions in each column can be rapidly altered from pressurised (adsorption) to depressurised (desorption/purge). As the system was designed with small sample columns (section 2.1), the system operates with short cycle times, which means that the 8 valves required to create the desired fluid flow need to switch position both instantaneously and simultaneously upon the completion of a cycle phase. Manually operated valves, although inexpensive, were not suitable, therefore actuated valves were considered. Solenoid valves emerged as the most suitable valve type, based on process requirements. Solenoid valves use electrical current to create an electromagnetic field that actuates a plunger, lifting the seal or diaphragm covering the orifice that connects the valve ports. It is possible to get hydraulically or pneumatically actuated valves, but for the purposes of a laboratory system, solenoid valves were deemed most suitable. The solenoid valves were acquired from SMC pneumatics, a company that specialises in vacuum rated control valves and flow equipment. Vacuum rated valves were required for this system as it was designed to operate both PSA and PVSA cycles, allowing for a variety of adsorbent materials to be tested at various conditions of pressure to optimise the cycle. The technical specifications for the valves are outlined in table 13

SMC XSA Series Solenoid Valve Technical Specifications	
Action	Normally Closed
Fluid	Air, Inert Gas
Orifice Diameter (mm)	3
Max Operating Pressure (bar)	1e-5
Min Operating Pressure (bar)	10
Max Pressure Differential (bar)	10
Connection Size	1/4”
Connection Type	Tube Fitting
Fluid Temperature Range (°C)	5-60
Rated Voltage	24VDC
Electrical Connection	DIN terminal
Product Code	XS-A1-22S-5D2

Table 13 SMC Solenoid Valve technical specifications[46]

3.6.4.2 Check Valves:

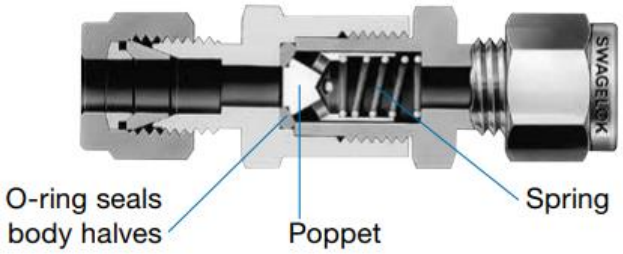


Figure 19 Swagelok poppet check valve

Check Valves were used at 4 locations in the rig to prevent the backflow of fluids. Check valves, also referred to as non-return valves are two-port valves that restrict fluid flow to one direction. They can be used to regulate back-flow in the system. The first location was on the main feed line. The main feed line in the system carries compressed air, drawn from the atmosphere and feeds into the system in the pressure range of 3-6 bar. If the pressure in the feed line dropped due to a system fault such as a line rupture or pump failure, the direction of flow could shift from the pressurised column, back through the feed line, as a result, a check valve was required. The second check valve location is the purge feed line, which is used to introduce nitrogen to the column following desorption to sweep CO_2 from the adsorbent. Nitrogen is introduced from a pressurised tank and as a safety consideration, it was decided that the flow direction would be restricted to prevent the flow of fluids or materials toward the tank. The final check valve location is the lean gas vent line, which is downstream of the column and used to vent the air which has been stripped of CO_2. Due to the nature of a PVSA system, and the vacuum created in the column for desorption, if the solenoid valves failed due to an electrical fault, there would be backflow through the vent line into the columns, which could cause the adsorbent material to be carried away from the columns to various parts of the column. All check valves were acquired from Swagelok. Tables 14 and 15 describe technical specifications.

Swagelok 316SS C-series Poppet Check Valve Technical Specifications	
Action	Unidirectional flow
Fluid	Air, Inert Gas
Orifice Diameter (mm)	3.2
Flow Coefficient (Cv)	0.47
Nominal Cracking Pressure (bar)	0.03
Max Back Pressure (bar)	68.9
Connection Size (Inch)	1/4”
Connection Type	Tube Fitting
Product Code	SS-4C-1/3

Table 14 Swagelok Poppet Check Valve technical specifications[47]

Temperature (°C)	**Pressure (bar)**
-23-37	206
93	177
121	168
148	160

Table 15 Swagelok Poppet Check Valve Pressure Temperature ratings[47]

3.6.4.3 Bleed Valves:

Bleed valves were used at two locations in the rig. Bleed valves allow for the venting of process fluids or pressure bleeding in sections of the process. For the purposes of a laboratory-scale Skarstrom system, a nitrogen purge is required to sweep CO_2 from the sorbent bed following desorption. The nitrogen feed runs counter-current to the gas feed and is introduced through a separate feed line downstream of the columns. After the CO_2 has been swept from the bed, the stream containing CO_2 and nitrogen needs to be vented from the system. To maintain pressure in the column undergoing adsorption, a separate vent line for each column was required.

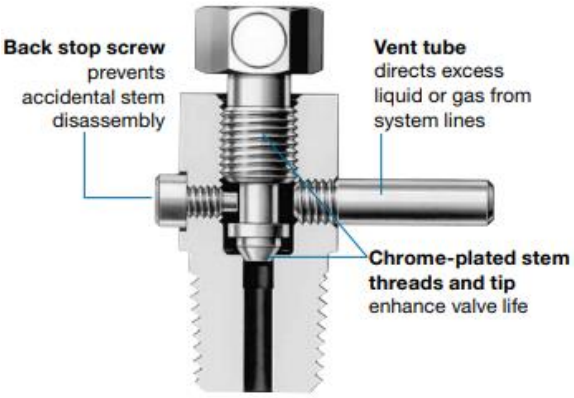


Figure 20 Swagelok bleed valve

Swagelok Bleed Valves Technical Specifications	
Action	Unidirectional flow
Fluid	Air, Inert Gas
Orifice Diameter (mm)	3.2
Flow Coefficient (Cv)	0.25
Nominal Cracking Pressure (bar)	0.03
Max Operational Pressure(bar)	68.9
Connection Size (Inch)	1/4”
Connection Type	Male NPT
Product Code	SS-BVM4-SH

Table 16 Swagelok Bleed valves technical specifications[48]

Temperature (°C)	Pressure (bar)
-23-37	206
93	177
121	168
148	160

Table 17 Swagelok Bleed Valves Pressure-Temperature Rating[48]

3.6.4.4 Needle Valves:

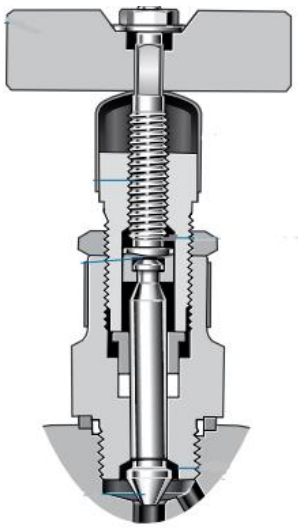


Figure 21 Swagelok Needle Valve

Needle valves were used at two locations in the rig. Needle valves allow for manipulation of flowrate in the system, with a positive shutoff needle that can be used to vary flow coefficient. For this rig, the needle valve was used in a similar manner as a pressure regulator. Installed downstream of the column, at startup, the needle valve remains shut. It is slowly opened using the handle until the desired column pressure is reached. The needle valves allow for a constant and reduced flow of air through the columns while maintaining pressure. A second needle valve is required to control the flow rate of air into the CO_2 sensors. As the CO_2 sensors are designed to read CO_2 concentration in an air sample at 0.5 l/min, running a higher flow rate of air to the sensor could potentially damage or destroy the sensor. The needle valve is closed at startup and opened in quarter turns during the calibration step until a CO_2 concentration is logged on the sensor. When a concentration is being logged it is assumed that the airflow rate is within the operational range for the sensor. If system pressure is being adjusted, the sensor valves are closed fully, prior to adjustment, and opened in quarter turns again, until a concentration is logged.

Swagelok General Utility Needle Valves Technical Specifications	
Action	Positive shutoff
Fluid	Air, Inert Gas
Orifice Diameter (mm)	5.0
Flow Coefficient (Cv)	<0.55
Connection Size (Inch)	1/4”
Connection Type	Female NPT
Product Code	SS-4GUF4-A

Table 18 Swagelok GU Needle Valve Technical specifications[49]

Temperature (°C)	**Pressure (bar)**
0-37	413
93	355
121	322
148	293

Table 19 Swagelok GU Needle Valves Pressure-Temperature Rating[49]

3.6.5 Vacuum Pump

For the purpose of creating a system capable of operating both PSA and PVSA cycles, a vacuum pump was used. The system was designed with an independent line, upstream of the column, which was used could be used for depressurising the sample columns and beginning the desorption process. The pressure relief line included a Swagelok tube fitting and two solenoid valves which can be used to open the line to atmosphere to independently equalise column pressure to atmospheric levels. In the event that a vacuum is required (based on sorbent properties), the pressure relief line is attached to the vacuum pump to create sub-atmospheric pressure in the columns. In the PVSA system, the operation of the vacuum pump is manually cycled as part of the desorption process and is connected to the pressure relief line using flexible tubing. In future, a PLC could be used to automatically cycle the vacuum pump, which would result in reduced cycle time and better reproducibility of results. The vacuum pump was made by a company named Vacuubrand and sold by in Ireland by the company Provac. Technical data was acquired from Vacuubrand and is presented in table 21.



Table 20 Vacuubrand Vacuum Pump

Vacuubrand Vacuum Pump Technical Specifications	
Number of Pump Stages	4
Maximum Pumping Speed	7.3 m^3/h
Ultimate Vacuum	70 mbar
Operational temperature range	10-40°C
Rated Motor Power	0.25 kW
Max back pressure	2 bar(a)
Connection Size (Inch)	1/4”
Connection Type	Hose nozzle DN
Product Code	ME 8 NT

Table 21 Vacuubrand ME 8 NT technical specifications[50]

3.6.6 Pressure Gauges

Pressure gauges were used at two locations in the rig. Pressure analysis was required in the system to analyse the pressure in the columns during the adsorption and desorption cycles. For the purposes of testing the adsorptive capacity of an adsorbent material in a PSA system, it is a necessity that system pressure can be adjusted. This means that sorbate capacity per unit adsorbent (mmol/g) can be analysed at different pressures to find the optimal pressure for adsorption. The rig was also designed to operate a desorption cycle under vacuum (VSA) which required compound pressure gauges that could operate at both positive and negative (vacuum) pressures. The pressure gauge chosen was a Swagelok model with a suitable operational range. For future work, a pressure transducer would be more suitable for this PSA rig as it allows for real-time logging of column pressure. A pressure transducer could also be used with a PLC, to more accurately and effectively control column pressure during the various cycles. Technical data was acquired from Swagelok and is presented in table 22.



Figure 22 Swagelok Pressure Gauges

Swagelok Pressure Gauges Technical Specifications	
Dial size	63 mm
Gauge Fill Fluid	None
Connection	¼” Swagelok tube adapter
Operating Range	-0.1 – 0.5 MPa
Accuracy	±1.0% of span
Operational Temperature Range	-40-60°C
Connection Size (Inch)	1/4”
Connection Type	Swagelok Tube Adapter
Product Code	PGI-63B-MC.5-LAQX-A

Table 22 Swagelok Pressure Gauge Technical Specifications[51]

3.6.7 CO_2 Sensors

CO_2 sensors were used at two locations in the rig. CO_2 sensors were required to assess the CO_2 concentration in the inlet stream in order to calculate the volume of CO_2 input into the system, which is used to calculate the volume of CO_2 removed by the adsorbent. For this system, the inlet stream consists of compressed atmospheric air with a known CO_2 concentration (approximately 400ppm) [1]. It was decided that a CO_2 sensor would be required for the inlet gas stream to allow for the future development of the rig to include a gas manifold, allowing for the input of gaseous mixtures containing varying amounts of CO_2, which renders the system capable of testing a wider array of adsorbents. The second CO_2 sensor was required for the lean gas stream, downstream of the adsorption column. During adsorption, CO_2 concentration in the lean gas stream should be reduced, as CO_2 is being removed from the inlet stream via adsorption in the columns. When the sorbent becomes saturated with CO_2, "breakthrough" occurs, and CO_2 is no longer removed from the gas stream. This manifests as an increase in CO_2 concentration in the lean gas stream as read on the CO_2 sensor, allowing for blowdown and purge steps to begin. The CO_2 sensors are an integral part of the control scheme for the system.

The sensors selected were Non-Dispersive Infrared (NDIR) sensors. NDIR sensors use an infrared (IR) lamp as the key detecting agent. This lamp directs light waves through a sample of the gas, toward an optical filter that covers an IR detector. As the IR light passes through the gas sample, CO_2 molecules absorb a specific band of light (4.2 µm wavelength), and all remaining light is absorbed by the optical filter. The IR detector reads the amount of light absorbed by the filter in the 4.2 µm band and measures the difference between the light emitted by the lamp and the light received by the detector. This result is proportional to the concentration of CO_2 molecules within the sample. Finally, it outputs this as a 4-20mA signal, which can be read using the software package provided with the sensors. The sensors selected were K30 Fast Response 10,000ppm CO_2 sensors. Technical specifications are outlined in table 23.



Figure 23 K30 FR 10000 ppm CO2 sensor

K30 FR 10,000ppm CO_2 sensor Technical Specifications	
CO_2 measurement	NDIR
Measurement range	0-10,000 ppm (0-1%)
Rate of Measurement	2Hz
Outputs	2 Analog, 2 Digital
Accuracy	±30ppm (±3%)
Inlet feed rate	0.5 l/min

Table 23 CO2 Sensor Technical Specifications

3.7 PVSA System Control Scheme

As described in section 3.3, the system operates a Skarstrom cycle. The Skarstrom cycle operates with two sample columns, utilised in tandem in either adsorption, desorption, or purge modes alternately. Due to the need to alternate column operations, it is required to use a series of valves to manipulate the material flow and process conditions within the system. Excluding start-up and shut down, which are dealt with as two separate operations, there are four unique valve schemes used in the operation of the rig to create the required material flows in each column. This equals a total of six control schemes are described individually. The solenoid valves in the system are controlled using a series of 24V DC switches and a power supply, all other valves are controlled manually.

Control of the system and the cycle times are based on the CO_2 concentration in the lean gas outlet stream. When breakthrough occurs, marked by an increase in the value for CO_2 concentration in the lean gas outlet stream, the sorbent material is saturated. This marks the end of the adsorption operation in each column and material (air) flow in the system is re-directed to the other column using the switches to open/close a pre-defined series of the solenoid valves in the system.

The column that has undergone adsorption is now depressurised, using either the vacuum pump or simply by atmospheric equalisation which is controlled manually using the solenoid valves

The six distinct operational control schemes are described below and are the following titles:

1. Start-up
2. Operation 1 (OP1)
3. Operation 2 (OP2)
4. Operation 3 (OP3)
5. Operation 4 (OP4)
6. Shut-down

Valve and equipment control schemes for each operation are described in section 3.9.1-3.9.6.

3.7.1 Start-up

The Start-up operation is a short operation designed to pressurise and saturate C-2 in isolation, to set up the Skarstrom cycle. Once the columns have been filled with adsorbent material they are integrated back into the system, and start-up begins. Prior to start-up, all valves are checked and moved into the off or closed position. Inlet pressure is set to the desired value and the inlet feed tap is opened. Air is directed to C2 by switching V2 to the open position, pressurising C2. To begin airflow through the adsorbent bed, V16, a needle valve downstream of the column, is gradually opened in quarter turns. Pressure in the column will decrease as the valve is opened and the valve is adjusted until pressure reaches set-point for testing. Flow through the column will increase as the valve is opened, and can be read on MFM-1. V15 is a needle valve which controls fluid flowrate to the CO_2 sensor, GA-1. V-16 is opened in quarter turns until sensor registers a data point for CO_2 concentration, which can be read using the GasLab software provided with the sensor, this indicates that the flowrate to the sensor is within operational range.

When breakthrough occurs, which is marked by CO_2 concentration, read in GA-1, becoming equal with CO_2 concentration in the inlet stream, the adsorbent bed in C2 is saturated, and Start-up is completed.

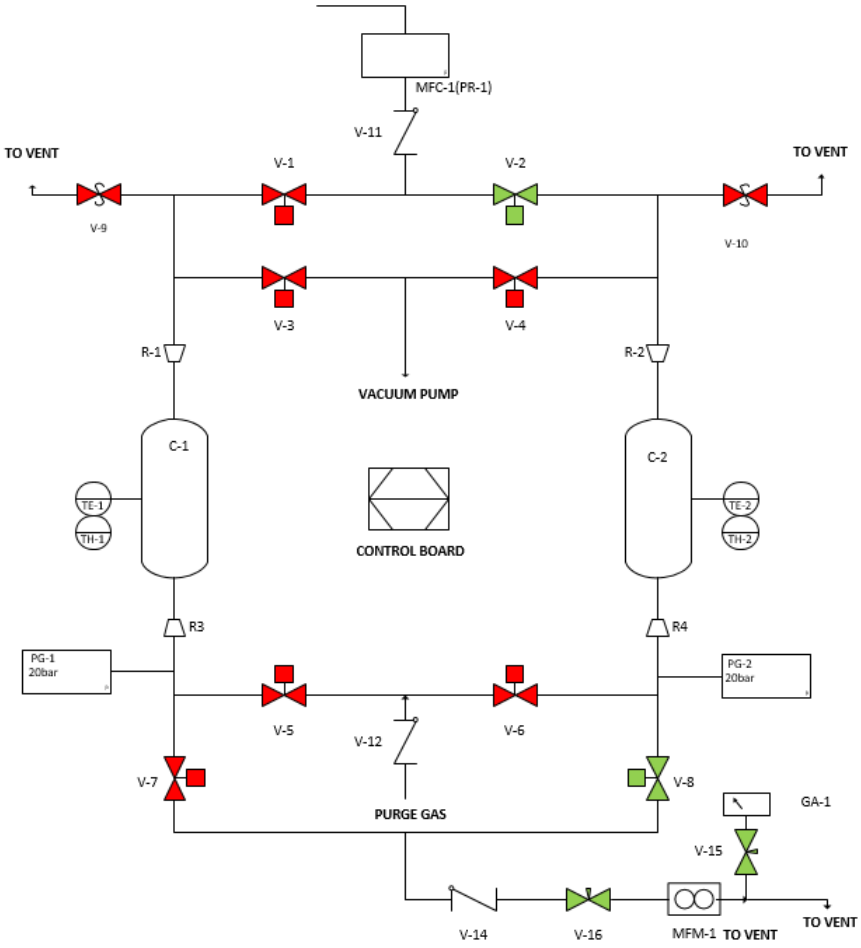


Figure 24 Start-up Control Scheme

3.7.2 Operation 1 (OP1)

OP1 is the first operation of the Skarstrom cycle that is used for data collection. It is the concurrent operation of an adsorption scheme in C-1, and a desorption scheme in C-2. OP1 is controlled by using the switches open or close a series of the solenoid valves within the system, as well as the opening and closing of a series of manual valves within the system. OP1 also requires the operation of certain auxiliary equipment, such as the vacuum pump.

The valve scheme used in OP1 is shown in Fig. 25. If a valve is open, it is shaded in green, if it is closed it is shaded in red. An operation manual is provided in section 3.9 which outlines the process steps and the correct operational sequence.

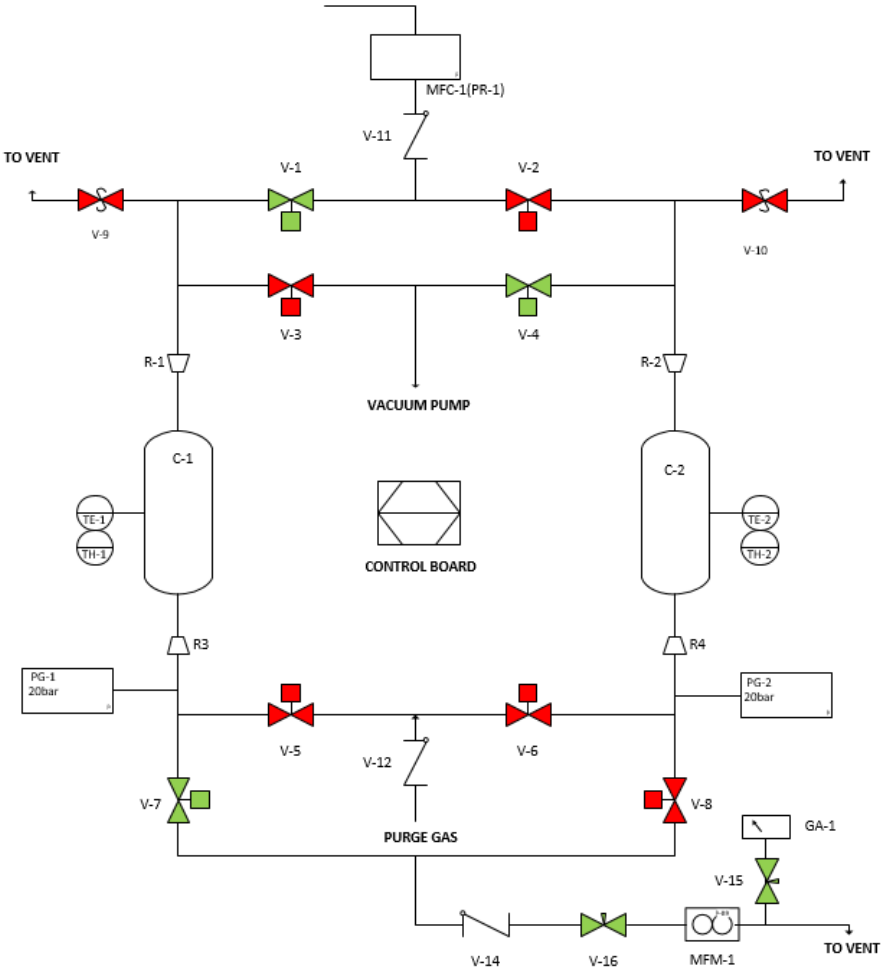


Figure 25 Operation 1 Valve Control Scheme

The cycle time for OP1 is based upon data gained from the relevant measurement systems. The OP1 cycle is very short, and only requires the length of time required to depressurise the saturated column (nearly instantaneous), which is analysed using PG-2. For a Skarstrom cycle to operate correctly, the adsorption cycle time for each column must coincide with the desorption and purge cycles in the other column, so adsorption in C-1 remains constant throughout OP1.

3.7.3 Operation 2 (OP2)

OP2 is the second operation of the Skarstrom cycle. OP2 consists of a continuation of the adsorption phase in C-1 and the execution of a purge phase in the C-2. Having undergone depressurisation to atmospheric or sub-atmospheric conditions, the CO_2 present in adsorbent bed in C-2 is now desorbed and must be swept from the column so a new adsorption cycle may be carried out. A series of valves within the system are changed to redirect fluid flow in C-2 allowing for an N_2 purge stream to be introduced downstream of the column. The purge stream sweeps the CO_2 from C-2, exiting at the top of the column and being vented from the system through manual purge valve V-10.

The valve control scheme for OP2 is shown in Fig. 26, with open valves shaded in green and closed valves shaded in red.

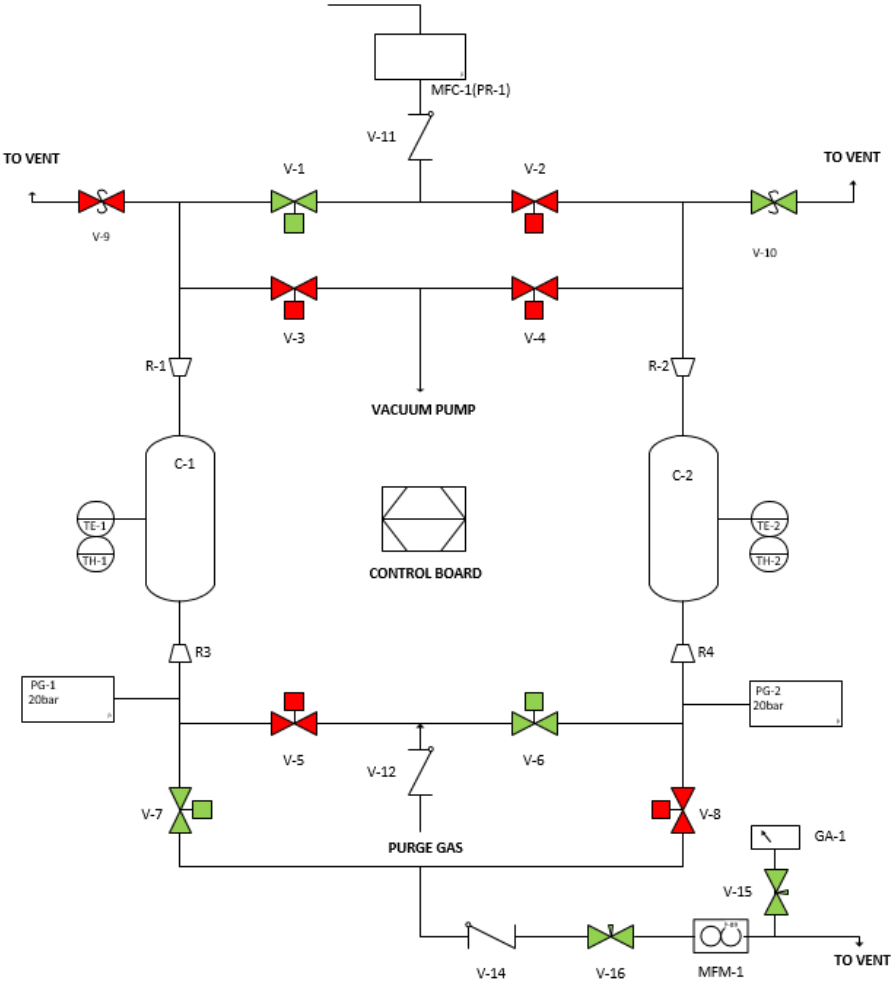


Figure 26 Operation 2 Valve Control Scheme

The cycle time for OP2 is dependent on the length of the adsorption cycle in C-1. The cycle time is based upon data gained from the relevant measurement systems. The CO_2 sensor GA-1 outputs a CO_2 concentration from the lean gas outlet stream which can be read in real-time using the accompanying GasLab software. When adsorption C1 is complete, CO_2 concentration in the outlet stream rises, becoming equal with the inlet stream, indicating that the sorbent is saturated. The valves are changed (see section 3.9) and OP3 begins.

3.7.4 Operation 3 (OP3)

OP3 is the third operation of the Skarstrom cycle. OP3 consists of the beginning of an adsorption phase in C2 and a desorption phase in C1. It is the mirror or alternate operation of OP1 (section 3.4.2), mimicking all of the operational and control conditions but conducting adsorption and desorption in alternate columns.

The valve control scheme for OP3 is shown in Fig. 27, with open valves shaded in green and closed valves shaded in red.

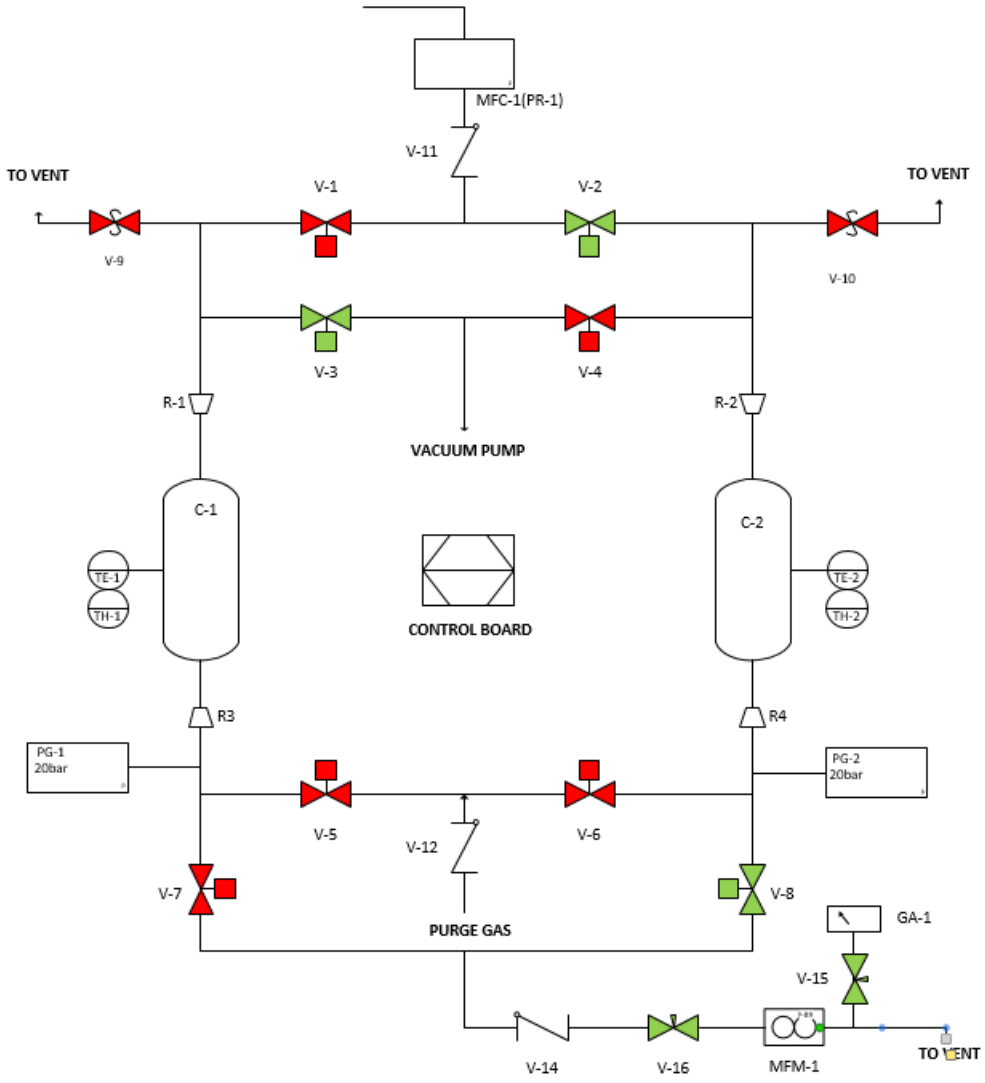


Figure 27 Operation 3 Valve Control Scheme

The cycle time for OP3 is very short, it mimics the length of OP1 which is based on the time required to depressurise C-1 containing the saturated adsorbent bed (nearly instantaneous). Pressure in the column is measured using PG-1, and when the pressure in the column reaches the pre-defined value, based on the adsorbent material, the operation is complete.

3.7.5 Operation 4 (OP4)

OP4 is the final operation of the Skarstrom cycle. OP4 consists of a continuation of the adsorption phase in C-2 and the execution of a Purge phase in the C-1. It is the mirror or alternate operation of OP2 (section 3.7.3), mimicking all of the operational and control conditions but conducting adsorption and purge in alternate columns.

The valve control scheme for OP4 is shown in Fig. 28, with open valves shaded in green and closed valves shaded in red.

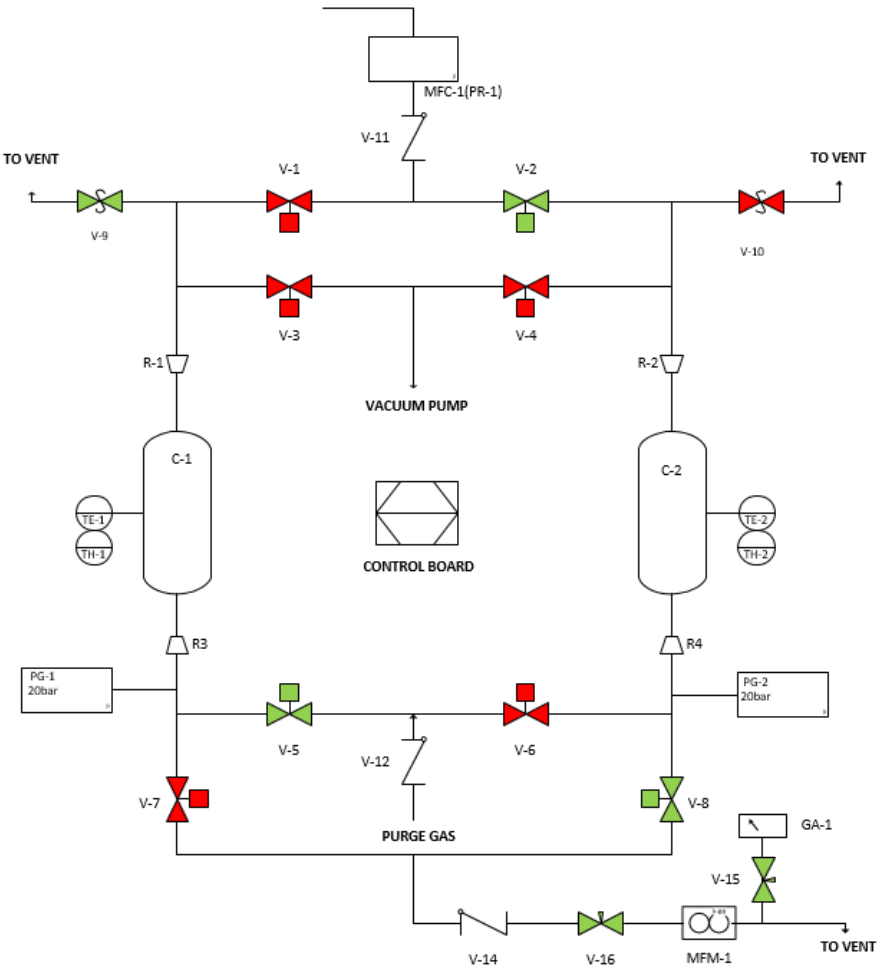


Figure 28 Operation 4 Valve control scheme

The cycle time for OP4 is dependent on the length of the adsorption cycle in C-2. OP4 mirrors or mimics OP2 in cycle length, and is based on the time taken for the adsorbent bed in C2 to become fully saturated. The CO_2 sensor GA-1 outputs a CO_2 concentration which can be read in real-time using the accompanying GasLab software. When adsorption C2 is complete, CO_2 concentration in the outlet stream rises, becoming equal with the inlet stream, indicating that the sorbent is saturated. At this point, the Skarstrom cycle is complete, all four phases have occurred and the cycle is repeated. The valves are changed and inlet fluid flow is directed to C-1 to begin OP1 again. This cycle can be repeated numerous times to collect numerous data sets on the CO_2 capacity of the sorbent.

3.7.6 Shut-down

The shut-down operation is used to end the Skartsrom testing cycle and safely shut down all equipment. It is a simple procedure designed to depressurise the system safely and ensure the correct position of all valves, to ensure that the start-up operation can be easily and safely carried out to begin a new testing cycle.

The valve control scheme for Shut-down is shown in Fig. 29, with open valves shaded in green and closed valves shaded in red.

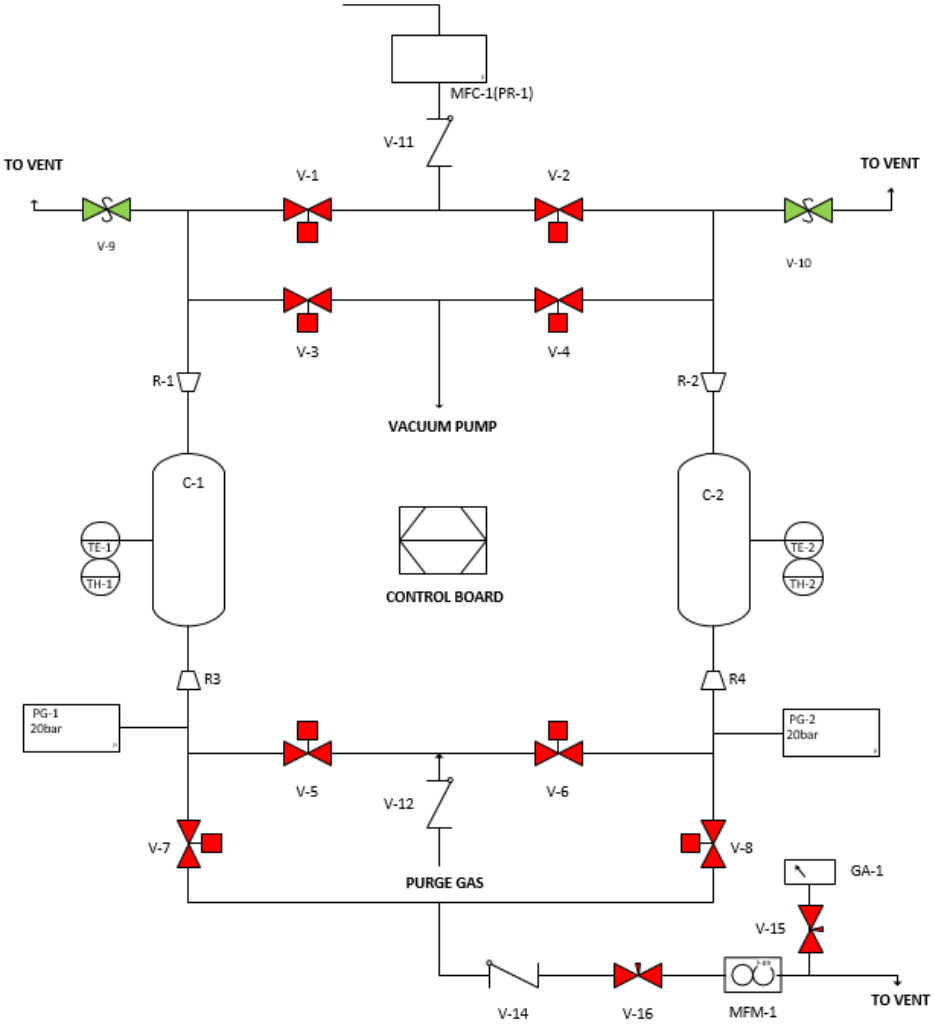


Figure 29 Shut down Valve Control Scheme

Once Shut-down has occurred, GA-1 one should be disconnected from the system and stored according to manufacturer guidelines. V-9 and V-10 can be manually closed. The columns, C-1 and C-2 containing the adsorbent should be carefully removed from the system. The adsorbent material should be removed carefully from the columns and disposed of safely, and the columns should be cleaned and stored.

3.8 PVSA System Safety Analysis

Due to the nature of experimental research, precautions had to be taken to ensure lab safety throughout the design, construction and operation of the lab-scale PVSA system. To assess system safety, and introduce adequate safety measures, a Hazards and Operability Study (HAZOP) was conducted.

3.8.1 HAZOP

A HAZOP is a systematic, industry-standard safety method for identifying hazards within a proposed process system and ascertaining measures of prevention or minimisation of the identified hazards. Hazard identification in a HAZOP is usually conducted on the basis of a "what if" scenario. A "what if" question asks for the possible outcomes of deviation from the designed operating conditions within a system[52]. It was decided that for the purpose of the laboratory rig design, a HAZOP would be conducted as the primary safety measure. The risk rating of any given process fault is calculated as a product of its likelihood and its consequence. The risk rating evaluation methodologies are described in tables 24 & 25.

3.8.1.1 Node Evaluation

To conduct a HAZOP, the system or process must be examined in nodes. Nodes are small and logical portions of a system which encapsulate one individual operation of the process, including the groups of equipment necessary for that operation[53]. As the lab-scale PSA system is small, it was only necessary to divide the system into two individual nodes, representing the unique material flows associated with adsorption and desorption within the system. For the purposes of conducting the HAZOP, the adsorption and desorption nodes were assumed to be the same for each column and were analysed once only.

Node 1 (Fig. 30) encompasses material and energy flow through all equipment that is used during normal operation of the adsorption phase of the Skarstrom cycle. It was assumed that there were no significant differences that required separate nodes for adsorption in C-1 and C-2.

Node 2 (Fig. 31) encompasses material flow through all equipment that is used during normal operation of the blowdown and purge phases of the PSA cycle. Once again it was assumed that there were no significant differences that required separate nodes for desorption in C-1 and C-2.

3.8.1.2 Parameter Evaluation

To conduct a HAZOP the safety of the system must be assessed on the basis of variation in key parameters using what-if analysis to identify safety weaknesses. The parameters chosen for evaluation in conducting safety analysis for this lab system were Temperature, Pressure and Flow. Three pre-defined variations, "More", "Less" and "None" were analysed for each of these parameters.

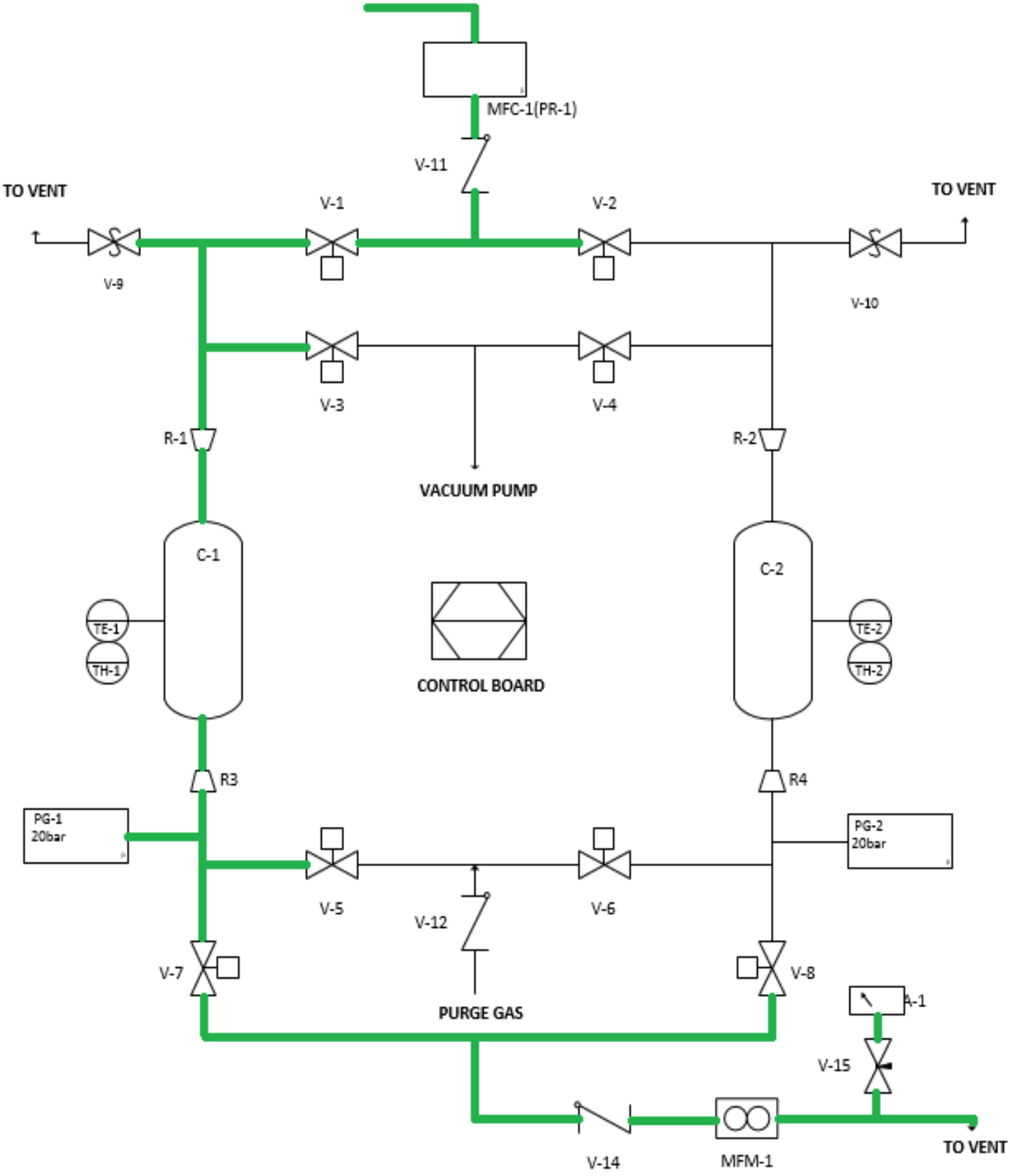


Figure 30 HAZOP Node 1 - Adsorption

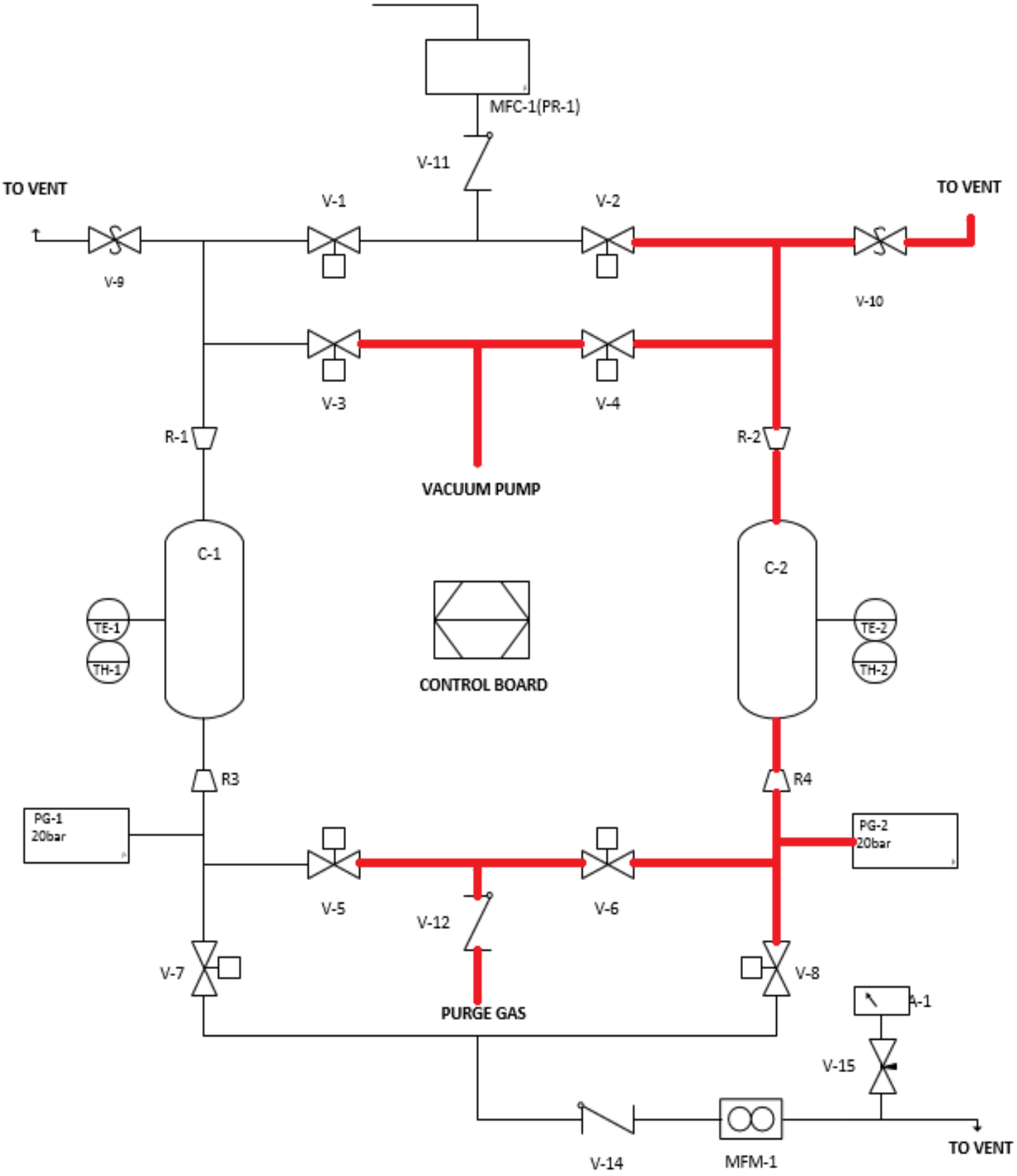


Figure 31 HAZOP Node 2 - Desorption

Likelihood	Consequence Severity				
	Insignificant (1)	Minor (2)	Moderate (3)	Major (4)	Severe (5)
Almost Certain (5)	II	III	III	IV	IV
Likely (4)	II	II	III	III	IV
Possible (3)	I	II	II	III	IV
Unlikely (2)	I	II	II	II	III
Rare (1)	I	I	II	II	III

Table 24 Matrix for HAZOP Risk Evaluation

Risk Rating	Unit	Action Required
Acceptable	I	The risk is considered acceptable and no further action is required.
Acceptable with Controls	II	The risk must be controlled using available measures to make it acceptable.
Undesirable; Mitigation Required	III	Significant safety measures should be introduced to mitigate the risk and make it acceptable.
Unacceptable Level of Risk	IV	Risk should be avoided by process redesign; if process redesign is impossible, a series of safety measures should be introduced to mitigate the risk.

Table 25 Risk rating and acceptability criteria

Project: **Lab Scale PVSA rig**

HAZOP Engineer: Cormac Dineen

Date: Jun-19

NODE: **1: Adsorption Stream C1**

Parameter	Deviation	Possible cause	Consequences	Existing Safeguards	Likelihood Rating (1 to 5)	Consequence Rating (1 to 5)	Risk Ranking with existing safeguards	Extra safeguards required	Risk Ranking with added safeguards	Comment
Flow	More	Pump Fault; Valve Failure; Gauze Failure.	Loss of Material; Damage to equipment.	Max supply pressure of 6 bar	2	1	I	None required	n/a	Check MSDS for any adsorbents used in the system
	Less	Supply Failure; V-10 left open.	No Consequences	n/a	n/a	n/a	none	n/a	n/a	
	None	Inlet valve shut-off; Air Supply Pump Trip:	No Consequences	n/a	n/a	n/a	none	n/a	n/a	
	Reverse	V-3 left open.	Adsorbent lost in direction of vacuum; Damage to vacuum pump.	Non return valve; Operation Manual.	1	2	I	None required	n/a	
		V-8 left open.	No Consequences		2	1	I	None required		

Parameter	Deviation	Possible cause	Consequences	Existing Safeguards	Likelihood Rating (1 to 5)	Consequence Rating (1 to 5)	Risk Ranking with existing safeguards	Extra safeguards required	Risk Ranking with added safeguards	Comment
	Other	V-2 left open.	Cycle disrupted and data loss							
		V-5 left open.	Contamination of Purge gas supple	Non-return valve; low-pressure inlet; Operation Manual	2	1	I	None required	n/a	Unlikely to have enough inlet pressure to contaminate purge supply
Pressure	More	Regulating valve opened too much or V-15 fails.	More pressure to CO2 sensor GA-1, Sensor damaged or destroyed.	V-16 regulating valve; Operation Manual	1	2	I		n/a	
	Less	Inlet valve shut-off	No Consequences	n/a	n/a	n/a	none	n/a	n/a	
	None	V-3 left open.	No Consequences	n/a	n/a	n/a	none	n/a	n/a	
Temperature	More	Heated jacket malfunction	Adsorbent lost due to heat degradation	Temperature sensors	1	1	I	n/a	n/a	
	Less	None	No Consequences	n/a	n/a	n/a	none	n/a	n/a	

Table 26 Node 1 - Adsorption HAZOP

Project:	**Lab Scale PVSA rig**
Team Members:	Cormac Dineen
Date	Jun-19
NODE:	**1: Purge Stream C2**

Parameter	Deviation	Possible cause	Consequences	Existing Safeguards	Likelihood Rating (1 to 5)	Consequence Rating (1 to 5)	Risk Ranking with existing safeguards	Extra safeguards required	Risk Ranking with added safeguards	Comment
Flow	More	Purge tank inlet valve failure	Adsorbent carried out of the column and into the upstream piping system; Damage to equipment.	Gauze placed above the adsorbent bed at top of the column	2	1	I	None required	n/a	Check MSDS for any adsorbents used in the system
	Less	Supply Failure	CO2 remains in adsorbent bed; Data set lost	n/a	1	1	I	n/a	n/a	Ensure Supply tank does not run out during a Testing run
	None	Supply Failure	CO2 remains in adsorbent bed; Data set lost.	n/a	1	1	I	n/a	n/a	Ensure Supply tank does not run out during a Testing run
	Reverse	Backflow into the supply tank	Supply contamination	Non-return valve; High-	1	2	I	None required	n/a	Highly unlikely to occur

				pressure supply tank						
Parameter	**Deviation**	**Possible cause**	**Consequences**	**Existing Safeguards**	**Likelihood Rating (1 to 5)**	**Consequence Rating (1 to 5)**	**Risk Ranking with existing safeguards**	**Extra safeguards required**	**Risk Ranking with added safeguards**	**Comment**
	Other	V-2 left open.	Purge flow through inlet feed pipe	Non-return valve	1	1	I	None required	n/a	
		V-5 Left open	Purge flow through adsorption column; Lost data set	None	2	1	I	None required	n/a	
		V-8 Left open	Purge gas in outlet stream; Lost data set	None	2	1	I	None required	n/a	
Pressure	More	Supple tank valve failure	High-pressure condition in the system	The pressure rating of the equipment	1	1	I	None required	n/a	
	Less	Supply tank valve fault	Inadequate purge; Lost data set	None	1	1	I	None required	n/a	
	None	Tank valve fails shut	Inadequate purge; Lost data set	None	1	1	I	None required	n/a	
Temperature	More	Heated jacket malfunction	Adsorbent lost due to heat degradation	Temperature sensors	1	1	I	n/a	n/a	

	Less	None	No Consequences	n/a	n/a	n/a	none	n/a	n/a	

Table 27 Node 2 - Desorption/Purge HAZOP

3.9 PVSA System Operation Manual

This section includes the instructions for the operation of the lab system.

3.9.1 Start-up (C-1 Adsorption)

For start-up, the system undergoes a unique procedure:

1. Input sorbent containing sample cylinders into the system.
2. Turn on the power supply and use 24V DC pre-set.
3. Ensure all switches are in the off position.
4. Attach air input line to V-13 (check valve).
5. Open the tap and set inlet air pressure to 2 bar.
6. Adjust V-15 (needle valve) to ensure air-flow to the sensor does not exceed 0.5 l/m.
7. Calibrate CO_2 sensor using background calibration setting (400ppm).
8. Turn off the air supply.
9. Disconnect air input line form V-13 and connect to V-11.
10. Open the tap and set to desired inlet pressure.
11. V-1 Switch ON.
12. V-7 Switch ON
13. Monitor outlet gas CO_2 concentration from GA-1.
14. Read pressure from PG-1.
15. Read air flowrate at inlet and outlet from FM-1 and FM-2.
16. When CO_2 concentration as read on GA-1 returns to approximately 400ppm, breakthrough has occurred and start-up operation is complete

3.9.2 Operation 1 (OP1) – C2 Adsorption/C1 Blowdown

OP1 is the procedure that redirects inlet airflow through C-2 to begin adsorption and simultaneously begins blowdown in C-1 which contains CO_2 saturated sorbent:

1. V-1 Switch OFF.
2. V-7 Switch OFF.
3. V-2 Switch ON.
4. V-8 Switch ON.
5. VP-1 Switch ON.
6. V-3 Switch ON.
7. Read negative pressure shown on PG-3.
8. V-3 Switch OFF.
9. Read negative pressure shown on PG-1.
10. VP-1 Switch OFF.
11. Monitor outlet gas CO_2 concentration from GA-1.
12. Read positive pressure shown on PG-2.
13. Read air flowrate at inlet and outlet shown on FM-1 and FM-2

3.9.3 Operation 2 (OP2) – C2 Adsorption/C1 Purge

Operation 2 is the procedure that begins a nitrogen purge to remove desorbed CO_2 from the sorbent bed in C-1 and simultaneously continues adsorption in C-2:

1. V-9 OPEN.
2. Purge gas supply ON
3. Read positive pressure shown on PG-1
4. V-5 Switch ON
5. Read positive pressure shown on PG-1
6. Monitor vent gas CO_2 concentration from GA-2
7. Purge gas supply OFF

3.9.4 Operation 3 (OP3) – C1 Adsorption/C2 Blowdown

OP3 is the procedure that redirects inlet airflow through C-1 to begin adsorption and simultaneously begins blowdown (depressurisation) of C-2 which contains CO_2 saturated sorbent:

1. V-2 Switch OFF.
2. V-8 Switch OFF.
3. V-1 Switch ON.
4. V-7 Switch ON.
5. VP-1 Switch ON.
6. V-4 Switch ON.
7. Read negative pressure shown on PG-3.
8. V-4 Switch OFF.
9. Read negative pressure shown on PG-2.
10. VP-1 Switch OFF.
11. Monitor outlet gas CO_2 concentration from GA-1.
12. Read positive pressure shown on PG-1.
13. Read air flowrate at inlet and outlet shown on FM-1 and FM-2

3.9.5 Operation 2 (OP2) – C1 Adsorption/C2 Purge

Operation 2 is the procedure that begins a nitrogen purge to remove desorbed CO_2 from the sorbent bed in C-1 and simultaneously continues adsorption in C-2:

1. V-10 OPEN.
2. Purge Gas supply ON
3. Read positive pressure shown on PG-2
4. V-5 Switch ON
5. Read positive pressure shown on PG-1
6. Monitor vent gas CO_2 concentration from GA-2
7. Purge Gas supply OFF

3.9.6 Shutdown

For shutdown the system undergoes a unique procedure:

1. Close inlet air tap and shut air supply OFF.
2. (close valves for gas analysers)
3. Disconnect GA-1 and GA-2 and store.
4. V-9 OPEN.
5. V-10 OPEN.
6. V-1 to V-8 ON.
7. Allow pressure to equalise.
8. V-1 to V-8 OFF.
9. V-9 OFF.
10. V-10 OFF.
11. V-15 OFF.
12. Disconnect air input line.
13. Disconnect Vacuum Pump line.
14. Disconnect Purge Supply line.
15. Turn off the power supply
16. Remove the sample cylinders.
17. Clear sorbent material from sample cylinders using pressurised air and store cylinders.

4. Development of a Carbon-Based Adsorbent for DAC

4.1 Overview

Alongside the development of an experimental system for testing CO_2 adsorption capacity (section 3), a secondary goal of this research was to develop a CO_2 adsorbent material with potential applications in DAC technologies, that could be tested using the experimental system. The operating scheme of the system is a PSA cycle, which is used for physisorbent adsorption materials. There are a number of families of physisorbent materials, including MOFs, Zeolites and Carbon-Based Adsorbents (CBA), which are described in detail in section 4.2.2. For this research, a CBA powder was developed in the lab, and pelletised, for testing in the lab system.

Carbon Based Adsorbents have become an area of attention for the synthesis and development of renewable or "green" sorbents for CO_2 adsorption. The wide availability of inexpensive agricultural and industrial waste biomasses has stimulated interest in CBA, and a significant amount of research has been carried out on the development of effective CO_2 sorbents from these biomasses. The term CBA includes all carbon derived materials, with modified or unmodified surfaces, that exhibit adsorptive properties. There are a number of families of material that fall into the category of CBA including activated carbons, pyrogenic carbons, carbon nanomaterials, and metal-carbon composites. All of these families are derived from a wide array of carbon-containing substances and are prepared in various ways, with varying degrees of potential in CO_2 capture applications.

By utilising carbon sources for the development of new CO_2 adsorbent materials, it is possible to drastically reduce the high processing costs associated with the processing of synthetic or inorganic adsorbent materials. Carbon materials are readily available in very large quantities as a waste product of a range of industrial processes, they represent an inexpensive alternative to highly processed and complex sorbent materials, such as MOFs or solid supported amines. By creating adsorbent materials from a variety of biomasses, it is possible to ascertain the most effective polymer groups for CO_2 capture applications.

This research attempts to develop a carbon biopolymer adsorbent material, derived from a naturally occurring native Irish Seaweed, Ascophyllum nodosum. The adsorbent produced was a powder consisting of a porous carbon nanomaterial with a significantly expanded surface area. The adsorbent material also had a variety of naturally occurring amine groups, which are of interest and benefit in CO_2 adsorption.

Due to time constraints and sourcing issues, full testing of the material in the system was not carried out before the conclusion of the research, however, the surface characteristics of the sorbent material were analysed, and the material was pelletised for use in the PSA system. The laboratory work carried out is described in this section.

4.2 Sorbent Families used in DAC Technologies

The most important design consideration for any new DAC process is the adsorbent material used to selectively separate CO_2 from the atmosphere air stream. A substantive amount of literature exists in the area as the sorbent material is the process component that dictates the overall energy requirement of the system (based energy required for regeneration of sorbent). The research frontier in DAC is currently at the establishment of new sorbents that exhibit high CO_2 selectivity and loading capacity at atmospheric conditions of temperature, pressure and humidity [14]. Current research involves systems that utilise both absorptive and adsorptive materials, and there are certain families of materials which are the centre of focus.

4.2.1 Chemisorbents

Chemisorption typically involves absorbent materials that bind CO_2 through reversible chemical reactions [54], [55], [56]. Chemisorption means bulk chemical reactions between the CO_2 and the chemisorbent material, as opposed to surface interactions like the Van der Waals or Ion-dipole reactions which occur in physisorbents. An example of a chemisorbent absorption reaction, capable of selectively removing CO_2 from a gaseous mixture, is the reversible exothermic reaction of solid calcium oxide (CaO) and gaseous CO_2[57]:

$$CaO + CO_2 \leftrightarrow CaCO_3 \tag{4.1}$$

The absorption mechanism involves the diffusion of CO_2 into the pores of the solid CaO powder, followed by the reaction scheme described in equation 4.1. The reaction can be reversed through the application of heat. This reaction scheme is just one of the many chemisorbent reaction mechanisms available for the capture of atmospheric CO_2.

4.2.1.1 Aqueous Hydroxide Solutions

Aqueous hydroxide solutions are a family of chemisorbent materials that can react with and selectively remove CO_2 from a gaseous mixture. Hydroxide solutions (OH^-) such as sodium hydroxide (NaOH), potassium hydroxide (KOH), or calcium hydroxide (CaOH) are strong bases, which means they dissociate in water to form and OH^- ion and solvated anions[14]. The OH^- ion reacts with H_2O and CO_2 from the atmosphere to form a carbonate ion which can be further processed through a calcination and slaking step to regenerate the absorbent. Hydroxide solutions generally show excellent CO_2 selectivity at low partial pressures of CO_2 (atmospheric) which is favourable for DAC technologies, however, this high selectivity is due to a strong affinity between sorbent and sorbate. This strong affinity produces a strong binding energy, which in turn creates a very large energy penalty in the regeneration process (calcination step)[11].

Fig. 32 shows a process flow diagram of an atmospheric CO_2 capture process that utilizes an aqueous hydroxide solution as an absorbent.

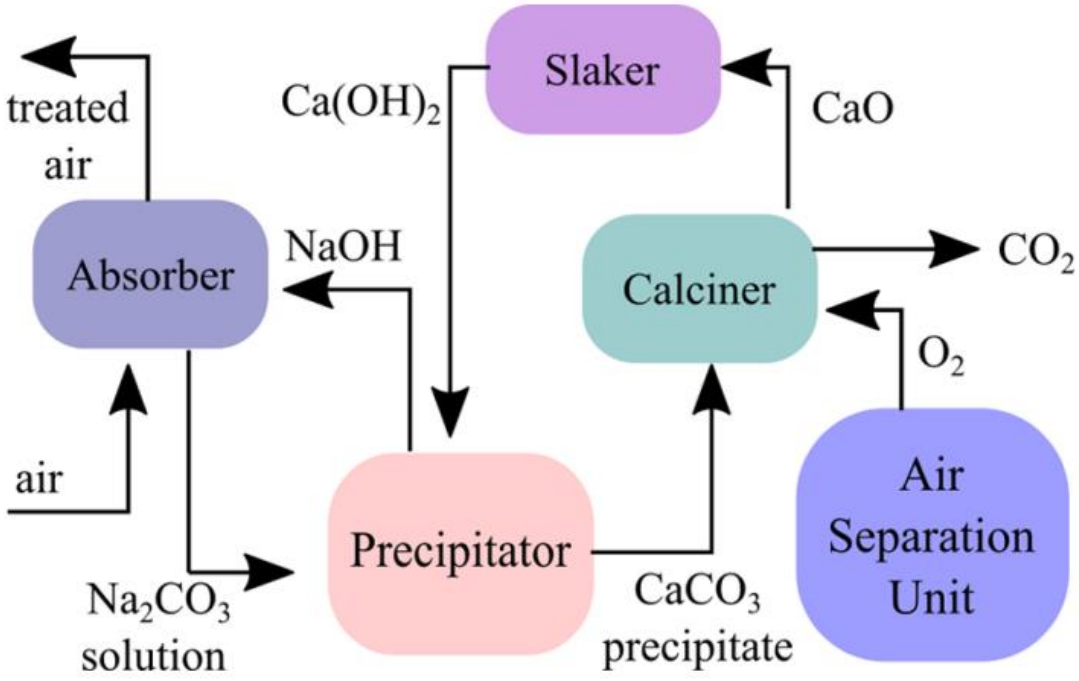


Figure 32 PFD of a DAC process using an aqueous hydroxide solution (NaOH)[11]

4.2.1.2 Solid Amine Sorbents

Another commonly used family of chemisorbents are amine-based solid adsorbents. These are any NH_x bearing organics and polymers that chemically bind CO_2 at atmospheric conditions [56] and thus are another good candidate for DAC. Differing from industrially established post-combustion CO_2 separation processes, which use aqueous amine solutions such as monoethanolamine (MEA) and diethanolamine (DEA), amine-based solid adsorbents are more suitable for atmospheric CO_2 separation as they do not incur the same energy penalty for absorbent regeneration. The amine-based sorbent is immobilized and impregnated in or coated on a solid support such as silica, mesoporous material or activated carbon fibres which are designed to optimise air contact by maximising the surface area of the amine sorbent [28]. Solid sorbent amines face issues with fouling, and the effects of temperature and humidity can severely degrade both the sorbent and the support thus, most of the research in the area is now focused on extending their lifecycle.

Due to there being a large number of amine group adsorbents, the reaction scheme for each of the absorbent material is different and varies in complexity. (4.1) describes a generic reaction between CO_2 and aqueous ammonia.

$$CO_2 + 2NH_{3(aq)} + H_2O(NH_4)_2CO_3 \quad (4.2)$$

4.2.2 Physisorbents

Physisorbents are adsorbent materials that bind CO_2 at the surface of the sorbent material, typically with weak surface interactions such as Van der Waals forces. The weaker binding energy reduces the energy requirements for regeneration, which in turn reduces the overall energy requirements for the capture process. Physisorbents are somewhat overlooked as sorbents for DAC processes due to their low selectivity for CO_2 over H_2O and N_2 at atmospheric concentrations (ultra-dilute) and low partial pressures of CO_2 [11]. Having an adsorbent material with selectivity for H_2O presents further energetic and cost considerations for DAC such as dehumidification of the atmospheric inlet gas stream to avoid uptake of H_2O instead of CO_2[28]. A lot of research is currently being conducted into physisorbent materials for CO_2 applications due to the lower costs and higher degree of tailoring achievable.

4.2.2.1 Zeolites

Zeolites are solid porous aluminosilicates (materials consisting of aluminium, silicon and oxygen), with high surface areas (m^2/g) and micropore volume (cm^3/g) which are utilised industrially in post-combustion CO_2 capture. The zeolite framework is organised as interlocking tetrahedrons of SiO_4 and AlO_4. Pores exist in the zeolites into which gaseous molecules (CO_2) can penetrate, at which point they are captured by an ion-dipole reaction between the metal cation and the gaseous molecule[56]. In general, zeolites are not considered as a viable adsorbent material for DAC due to their poor efficiency in humid conditions (atmospheric).

4.2.2.2 Metal-Organic Frameworks (MOFs)

MOFs are a relatively new family of solid adsorbent structures that consist of transition metal ions and bridging organic ligands. MOFs have attracted a lot of academic attention in recent years in relation to DAC due to their tuneable pore-size, which indicates that they could be further developed to exhibit high CO_2 selectivity at atmospheric concentrations of CO_2. Both the constituent metal joints and organic linking material of the individual MOF can be varied to adapt its physical properties, particularly pore size, and this means that there is a large number of unique MOFs that can potentially be developed [58]. Furthermore, the organic linking material that binds the transition metal ions, can be adapted to increase CO_2 capture capacity and selectivity. For example, the organic ligand has the potential to be functionalised CO_2 selective materials, such as nitrogen-based amine groups which increase the CO_2 capacity of the substance by orders of magnitude[56]. MOFs also have the advantage of being applicable to both Post Combustion Capture (PCC) technologies deployed at power generating facilities to capture CO_2 from flue-gas (higher CO_2 concentration in gaseous stream), as well in DAC, depending on the physical and chemical properties of the unique MOF[11], [14], [59], [29]. The major disadvantage is that before MOFs can be considered as commercially deployable in DAC systems, substantial developments must be made in two areas – (a) The development of highly thermostable MOFs with low water selectivity, and (b) The techniques available for the synthesis of commercial-scale batches of novel MOFs[29].

4.2.2.3 Carbon-Based Adsorbents

CBAs are porous adsorptive materials derived from carbonaceous materials such as agricultural biomasses, woods, coals and other various organic materials primary consisting of carbon atoms. As mentioned in the section 4 overview, there are a number of different families of material within CBA, including activated carbons, pyrogenic carbons, carbon nanomaterials, and metal-carbon composites. Each family of materials within CBAs has different properties and different levels of utility in atmospheric CO_2 capture systems. CBAs are highly porous substances with excellent surface area properties (generally 500-1500 m^2/g) which can be used in various gas separation operations including CO_2 removal. Like other physisorbents, gaseous molecules are attracted to the surface by Van der Waals interactions, which makes the available surface area an important parameter in assessing the adsorption capacity of the material.

Pyrogenic carbon materials are low-cost, simple materials such as charcoal, charred biomass, agrichar and biochar. The process of creating pyrogenic carbon involves the pyrolysis/carbonization of biomass. The biomass, generally either plant or animal matter, is exposed to high temperatures (350-900°C) in an oxygen-starved environment[60]. The pyrolysis process increases the carbon content and decreases the content of oxygen and other volatile components of the biogas. The pyrolytic transformation produces a material with a high surface area and porosity, capable of CO_2 adsorption. The adsorptive properties of the final pyrogenic carbon are dependent on the properties of the bio-feedstock used in the process, as well as the conditions during pyrolysis (the heating rate of the material).

Activated Carbons are low-cost materials derived from biomass in a similar manner as pyrogenic carbons. Activated carbons undergo pyrolysis, and are subsequently physically or chemically “activated”, which involves expanding the surface area, or adding surface functional groups such as amines, to increase the absorptive capacity of the material[60].

Carbon nanomaterials, which are of particular importance to this research, are any carbon-based materials, derived from biomasses, with small particle size and high surface area. These materials do not undergo pyrolysis to increase their carbon content, they are just processed into smaller, porous substances with a higher surface area. They retain functional surface groups present in the original biomass, but also carry the disadvantage of retaining volatile compounds, which can impact their usefulness in industrial adsorption systems.

There is a lot of research currently being conducted into CBAs as potential DAC sorbents due to the sustainable nature of the substances, their hydrophobicity (resistance to water) and the low cost when compared to other solid adsorbents such as zeolites or solid-supported amines [61]. Naturally occurring biopolymers and their derivatives are of particular interest to this research.

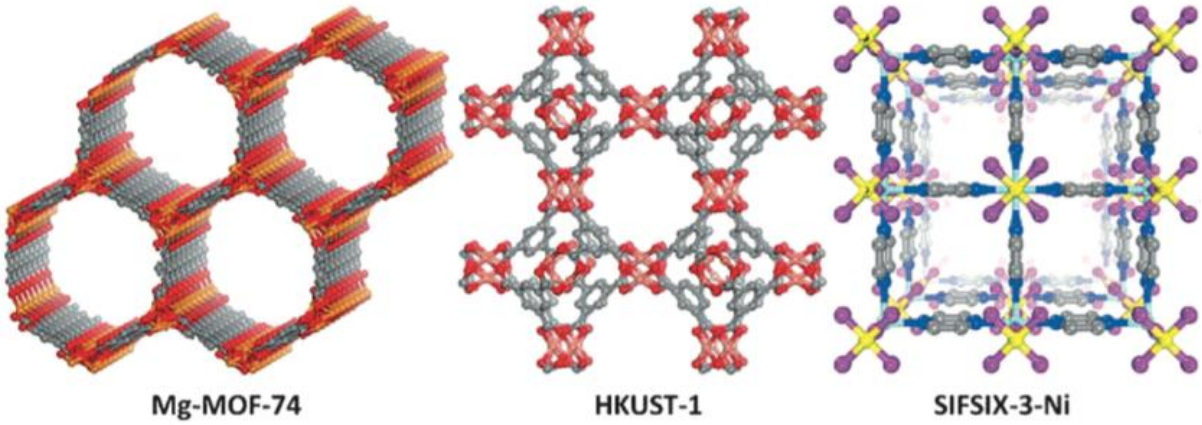


Figure 33 Graphical representation of structures of three common MOFs [54].

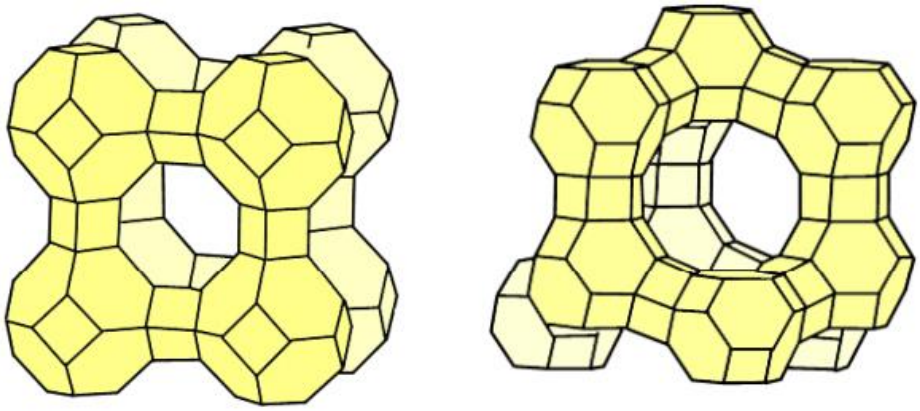


Figure 34 Graphical representation of typical zeolite structures, zeolite A and faujasite [62]

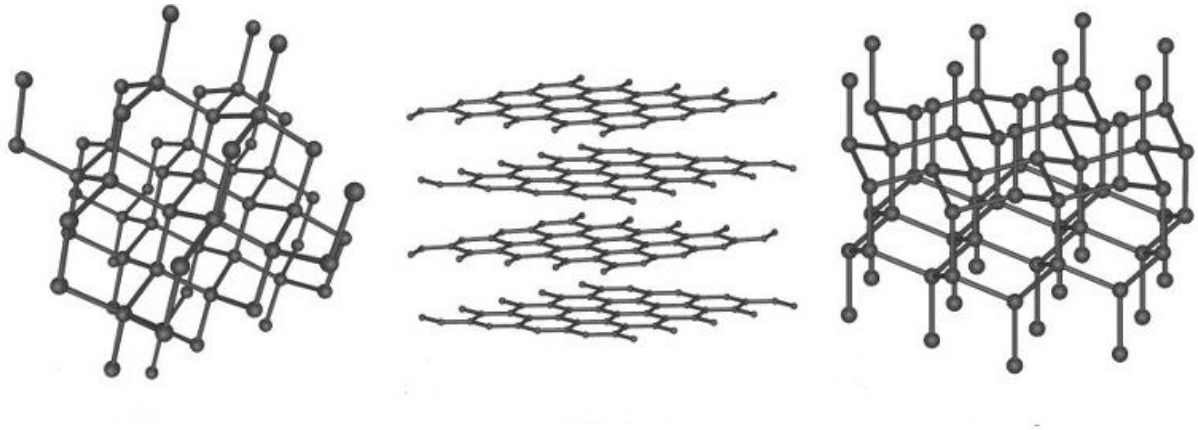


Figure 35 Graphical representation of typical carbon-based structures

4.3 Experimental Method for Development of a Biopolymer Adsorbent Material

This section outlines the experimental method for the development of a biopolymer adsorbent. The development of the adsorbent was done under the guidance and instruction of Dr Eoin Flynn of the Materials Science group in the Environmental Research Institute. The development involved expanding the surface area of a native Irish macroalgae to create a physisorbent material with high surface area, capable of adsorbing CO_2 in a PVSA system.

4.3.1 Material Selection

Ascophyllum nodosum, also known as "knotted wrack" or "knotted kelp" is a cold water macroalgae species from the family Fucales, common to the Northern Atlantic Ocean. It is a brown seaweed, found abundantly at sheltered coastline sites, where it becomes a dominant algae species in the littoral zone. It has been harvested widely in countries along the European Northern Atlantic coastline (Ireland, Scotland, Iceland and Norway) for use in the production of alginates, organic fertiliser, and high-quality seaweed feed for animal consumption [63].

There is no accurate data on the annual world harvest of this seaweed, however, rough estimates exist based on the annual production of animal meal from seaweed, almost entirely consists of A. nodosum. A study in 1968 [64] put the annual harvesting of A. nodosum in Norway at 50,000 tonnes (wet weight). Based on this level of harvesting in Norway, and taking into account that A. nodosum is now harvested in greater quantities also for alginate and fertilise, it is estimated that the global harvest now exceeds 200,000 tonnes [63]

Due to the abundance of A. nodosum along the coastline of Ireland, it was deemed as an excellent candidate for use as "green" carbon source, to use in the synthesis of a carbon-based adsorbent for testing in the PVSA lab system designed in this research.



Figure 36 Wet (left) and Dried (right) sample of A. nodosum

4.3.2 Material Sourcing, Primary Processing and Size Reduction

A. nodosum was harvested, wet, in West Cork, Ireland. The wet fronds were spread out on a drying rack and dried at room temperature (18°C-23°C) for approximately 5 days. After 5 days the samples were deemed dry enough and the size reduction steps were carried out. The purpose of the size reduction steps was to obtain a sample of A. nodosom powder with particle size in a known range of 75-150 µm, which could be processed using experimental techniques to create a sample of A. nodosum with an expanded surface area.

4.3.2.1 Rough Particle Size Reduction (<5mm)

1. Roughly 300g of dried A. nodosum sample was torn roughly into 5-10cm strips.
2. 3-5 strips were loaded into a food processor (Russell Hobbs 25920 Go Create).
3. The food processor was operated in consecutive 3-5 second pulses.
4. Samples were assessed visually after processing, and when particle size was approximately 5mm, rough size reduction was complete.
5. The processed sample was transferred into a glass container using a funnel.
6. Steps 1-5 were repeated until the entire the seaweed sample had been processed.

4.3.2.2 Fine Particle Size Reduction (75-150 µm)

1. Approximately 5g of A. nodosum (<5mm) sample was placed into a coffee grinder (Krups, Type F203).
2. The coffee grinder was operated in consecutive 3-5 second pulses.
3. The sample was pulsed in coffee grinder between 10-15 times, with 3 second breaks in between pulses, to avoid overheating the coffee grinder motor.
4. The sample was visually inspected to ensure that it was now a powder.
5. A 150 µm round sieve was placed on a piece of paper, inside a rectangular tray.
6. The sample was poured out of the grinder, onto the 150 µm sieve.
7. Steps 1-6 were repeated until the sieve had a top layer of A. nodosum powder.
8. The tray and sieve were shaken back and forth for approximately 30 seconds.
9. The sieve was lifted up, and rejected material was transferred into a labelled, empty container using a funnel.
10. The pass-through was collected on a sheet of paper under the sieve and transferred into a labelled, empty container.
11. The rejected matter was transferred back into the coffee grinder using a funnel, and steps 2-6 were repeated.
12. Steps 1-11 were repeated until all of the A. nodosum samples had passed through the 150 µm sieve, and had been transferred into the labelled container.
13. To limit the particle size range, the entire sample of A. nodosum powder was passed through a dual-block sieve, with a 150 µm sieve on top of a 75 µm sieve.
14. All powder that passed through the 150 µm sieve but was rejected by the 75 µm sieve was transferred into a clean, labelled container and consisted entirely of particles in the 75-150 µm range.

4.3.3 Surface area expansion

The next step of the adsorbent synthesis process is the expansion of the effective surface area of the seaweed particles. The expansion is done through the addition of deionised water. The deionised water causes the particles to swell in size, increasing the surface area of the particles. This is followed by a solvent exchange, which is a lab operation that can be used to change the solvent, without taking the solute out of solution. Deionised water is exchanged for ethanol, which is a more volatile compound that can easily be evaporated off at low temperatures. This allows for the seaweed particles to be dried without significantly altering their structure.

1. Add 200ml (149.66g dry weight) of the seaweed particles (75-150 µm) to a clean dry container (2l glass bottle)
2. Add 1200ml deionised water (4:1 – 6:1 ratio, volume of deionised water to the volume of dry seaweed).
3. Leave the suspension to settle for 2-4 hours, allowing the seaweed particles to expand (expanded volume approximately 800ml).
4. Add 10ml 85% wt glycerol to the container as a cross linking-agent, to make the particles less water-soluble, resulting in less material loss during the solvent exchange. It also can be added as an agglomerating agent (used as a powder shaping method).
5. Leave suspension to settle for approximately 24 hours (see Fig. 37)
6. Remove the free deionised water (approximately 800ml in first exchange) in 25 ml portions using a pipette (taking care not to disrupt settled seaweed) and discard.
7. Replace with the same volume of 96.5% pure Ethanol (approximately 800 ml) and let the suspension settle for approximately 24 hours.
8. Remove the free liquid again (approximately 800ml) in 25 ml portions using a pipette and discard).
9. Replace with the same volume of 96.5% pure Ethanol (approximately 800 ml) and let settle for approximately 24 hours.
10. Repeat steps 6-9, 8 times, taking care not to disrupt the settled seaweed.
11. The solvent exchange is repeated 8 times as this was the calculated number of repetitions required for the solvent composition to be <1% deionised water.
12. After 8 exchanges, the excess solvent in the container is decanted and discarded leaving only the saturated seaweed particles.
13. Seaweed particles are saturated with ethanol (>99%) and can now move on to the next processing step, vacuum drying.

4.3.4 Vacuum Drying

For the particles to retain their expanded surface area, they must be dried under vacuum. Drying the particles at atmospheric pressure causes them to contract as they dry, which reduces the surface area of the particles. Water was exchanged for ethanol (section 4.3.3) due to its lower boiling point, and the boiling point is further lowered under sub-atmospheric conditions of pressure. By removing the ethanol in a vacuum chamber, the temperature requirement for drying is significantly reduced, which reduces the risk of degrading or damaging the A. nodosum particles, due to prolonged heat exposure. A cold trap, containing liquid nitrogen is used in this experimental setup. The cold trap is used to freeze the ethanol that is removed from the particles, to stop it flowing into the diaphragm pump and destroying it. This section outlines the experimental steps required for vacuum assisted drying.

1. Decant the layer of liquid (>99% ethanol) above the saturated seaweed particles, (approximately 800ml) and discard as waste in sink.
2. Fill a cold container with liquid nitrogen from the dewar.
3. The final 50ml of liquid top-layer is removed using a pipette to avoid product loss.
4. Set up the vacuum chamber apparatus as shown in Fig. 39.
5. Get a clean dry petri dish, and fill both base and lid to approximately 1cm depth of seaweed and ethanol mixture.
6. Place the petri dishes into the vacuum chamber as shown in Fig. 38.
7. Place the lid onto the vacuum chamber ensuring that a seal is created, and place the vacuum chamber on the hotplate.
8. Attach an oil sample in a 20ml glass beaker to the side of the chamber, and place the temperature probe in the oil. The probe cannot be placed directly into the vacuum chamber as it would break the vacuum.
9. Make the temperature probe set-point to 35°C (for evaporation of ethanol) and plug the probe into the correct outlet on the hotplate.
10. Fill the cold trap with liquid nitrogen (approximately -170°), see Fig. 40.
11. Attach tubing to the vacuum pump (Vacuubrand ME 4R) shown in Fig. 41.
12. Turn on the vacuum pump, and read pressure shown on vacuum chamber pressure gauge.
13. The seaweed sample should take approximately 8-10 hours to dry.
14. Check the temperature in the vacuum chamber every 40 minutes to ensure the probe is at the desired set point.
15. Check the cold trap every 40 minutes to ensure that it still contains liquid nitrogen.
16. Check the particles (observed through the transparent lid) to see if they are dry.
17. The suspension, when dried becomes a powder with a light brown colour, which should be clearly recognisable through the lid of the vacuum chamber
18. The adsorbent powder is transferred from the petri dishes to a labelled container.

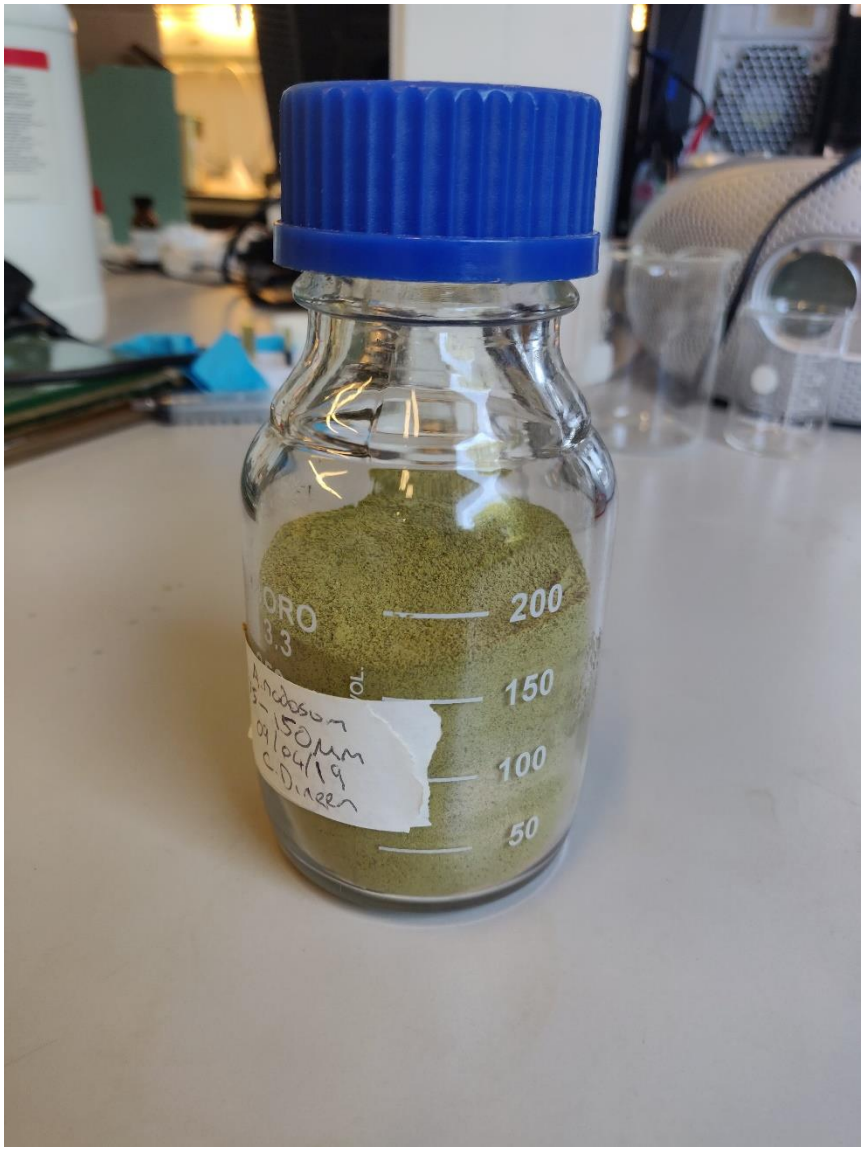


Figure 37 A.nodosum particles 75-150

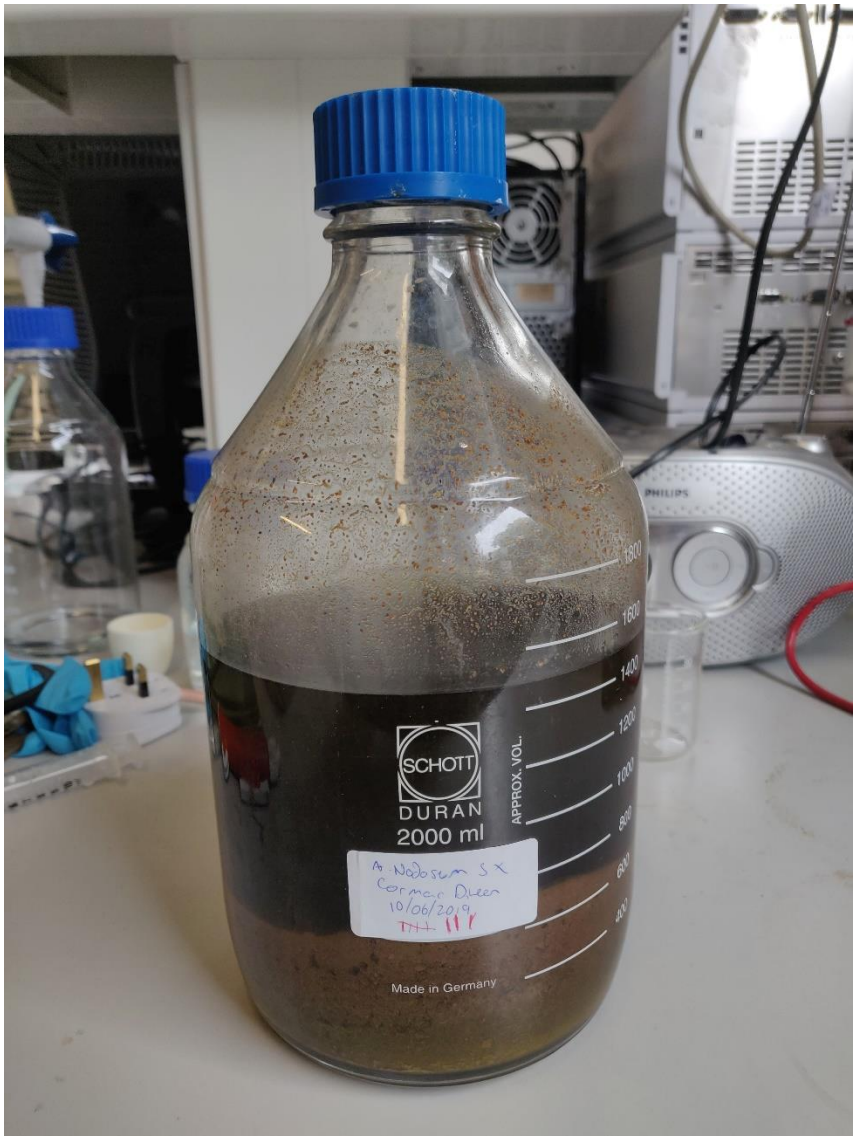


Figure 38 A. nodosum & Ethanol solvent exchange apparatus



Figure 39 Vacuum chamber with Saturated A. nodosum



Figure 40 Vacuum chamber apparatus on hot-plate

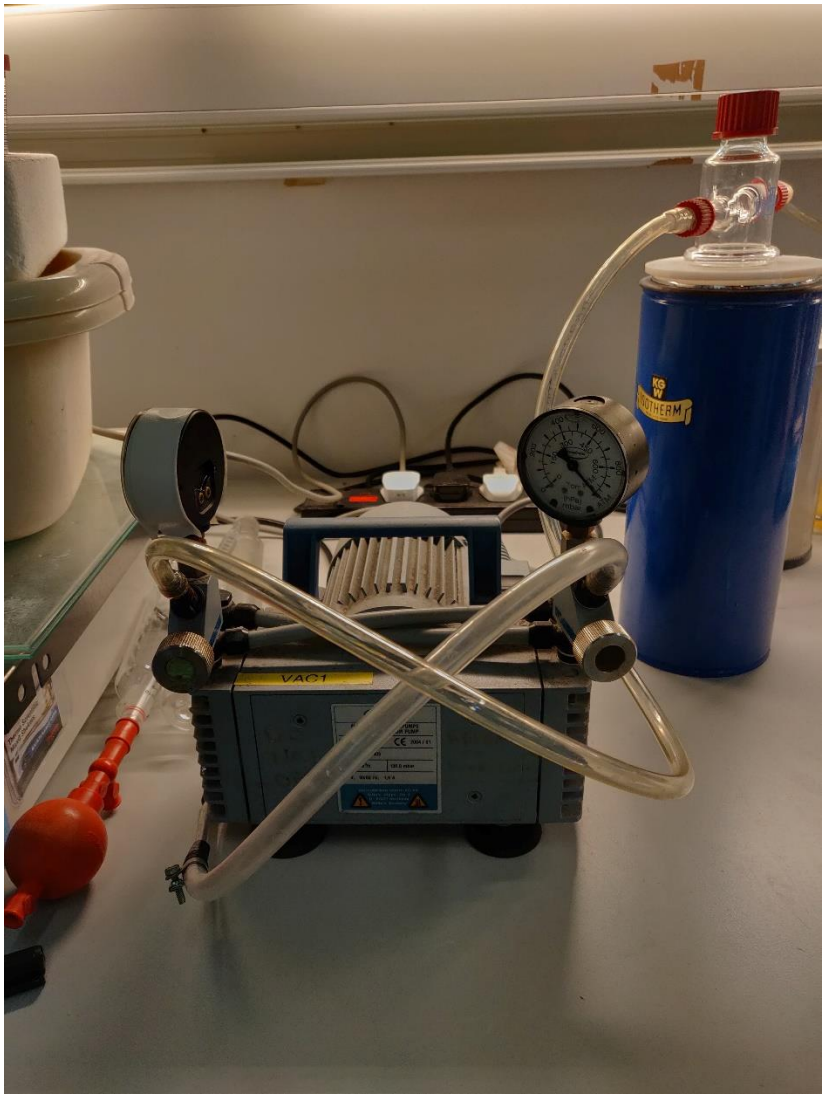


Figure 41 Vacuum pump and cold trap

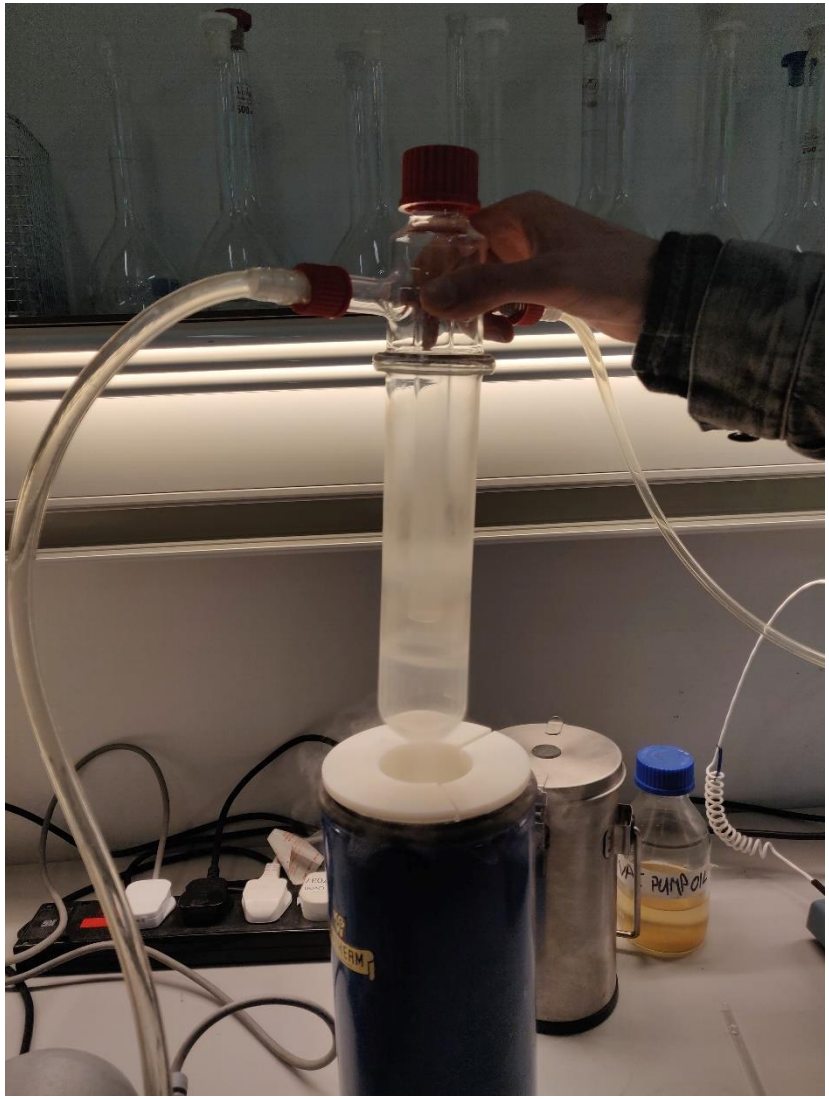


Figure 42 Liquid nitrogen cold trap

4.4 Experimental observations

Throughout the experimental procedure, several observations were made.

4.4.1 Size Reduction Observations

Firstly, during the initial rough-size reduction step, it was noted that grey particles, typically 2-3 times the size (visual observation) of the seaweed particles, (green-brown colour) were dispersed randomly amongst the seaweed particles. Upon further examination of the dried A. nodosum fronds, it was noted that small grey masses sometimes appeared at the root of the frond, where the specimen had been attached to rock or some other stabilising object. As these grey masses, which presumably comprised of some sort of rock, or rock derivative, could compromise the properties or composition of the eventual A. nodosum powder, it was decided that all visible grey particles would be removed. The remaining fronds had the root removed to reduce the possibility of rock particles ending up in the final adsorbent.

Secondly, as described in section 4.3.2.2, a particle size range was established for the finished powder. To establish a particle size range, the particles were passed through a sieve tower consisting of a 150 µm round sieve and a 75 µm round sieve. Any particle that passed through the 150 µm sieve, and was rejected by the 75 µm sieve, was confirmed to be in the 75-150 µm particle size range. During the sieving process, it was noted that a significant amount of material had also passed through the 75 µm sieve. This material was discarded, and not included in the sample that was used in the SA expansion step. The significant quantity of particles with a size <75 µm, that passed through the sieve, indicated that it was possible that more particles of this size could become trapped between particles in the correct size range and not pass through the sieve. Therefore, even though the sieving process was conducted thoroughly, it was noted that the sample most-likely contained a small quantity of particles <75 µm in size.

4.4.2 Surface Area Expansion Observations

During the surface area expansion, the particles were suspended in 1200ml water, after which a series of exchanges occurred. In an exchange, approximately 800ml of liquid was removed and replaced with 800ml of ethanol (>99%). After the first exchange, 10ml of glycerol was also added to the container as a cross-linking agent, to aid in the settling of the seaweed after each exchange. After the second exchange, it was noted that a brown-red substrate had formed, floating near the surface of the ethanol-water mixture in the container. During the third exchange, the substrate was removed from the container and examined, turning out to be a very low-density (floating), brown-red, semi-solid structure. A definite explanation for the formation of this substrate was not achieved, however, it is assumed that the substrate was simply the product of some additional constituent of the seaweed powder, potentially a microorganism present on the surface, being bound together by the glycerol, and separating from the solid seaweed sediment in the container, floating to the top of the liquid mixture.

4.4.3 Vacuum Drying Observations

During the vacuum drying step, two petri dishes, containing approximately 1cm depth of the saturated seaweed particles were placed in a metal vacuum chamber (Fig. 38) which was connected to a vacuum pump, and heated to 35°C using a hotplate. Each batch of adsorbent was then dried under vacuum and checked every 40 minutes to assess dryness. This was done by visual observation through the transparent, hard plastic lid of the vacuum chamber. Over the course of the drying process, it was noted that one of the petri dishes was drying faster than the other, observable by noting a lighter colour in the petri dish, consistent with a drier powder. The second batch of two petri dishes yielded the same result, with one petri dish appearing to dry faster than the other dish. After consideration, it was decided that this phenomenon was occurring due to the condensation forming on the lid of the chamber dripping down onto a specific area of the vacuum chamber floor. Either variation in the manufacturing process, or wear due to use, had rendered the lid of the vacuum chamber non-uniform, with a slight deformation at a specific point on the lid. As condensation formed on the underside of the lid, gravity carried it toward the deformation, which resulted in dripping only occurring at a particular point, rather than uniformly throughout the chamber, or not at all. For the subsequent batches, the petri-dishes were positioned away from the deformation in the vacuum chamber, and the discrepancy in drying time between the two petri dishes was not observed. It is not known if the varied drying time affected the properties of the final powder properties, as the petri dishes were not analysed individually, due to time considerations.

It was also observed that there were slight variations in the colour of the adsorbent powder particles produced from batch to batch. The colour of the particles in each of the two petri-dishes dried in one vacuum drying batch was observed to be the same. However, over several batches, the colour of the finished powder was observed to vary. Instances of both lighter and darker batches occurred, with no observable trend from batch to batch (i.e a consistent lightening of powder colour). It is not known precisely why a variation in powder colour arose, however, a few theories were proposed. Firstly, it is possible that a variation in the drying conditions could cause a variation in the colour. The position of the vacuum chamber on the hotplate, or variations in the atmospheric temperature on the day of drying, could affect drying rate, and theoretically cause some minute change in powder colour. The other possible explanation could be variation in the seaweed particles taken from the solvent exchange container. As the solvent exchange was a settling process, smaller, or less dense particles could settle at the top of the saturated seaweed mass. As the saturated seaweed was not mixed prior to drying, and simply poured from the container into the petri-dishes, it is possible that there was a certain particle profile that varied throughout the saturated seaweed mass, giving rise to variation in final dried adsorbent properties, including colour. However, if this was the case, it is thought that some colour trend should have arisen, either manifesting as a consistent trend toward lighter shades of brown, or darker shades of brown in each consecutive batch, rather than the seemingly random variation that actually occurred.

4.5 Product Analysis

After the experimental processing of the adsorbent material, product analysis was carried out on samples of the adsorbent to gain data on its properties. The analysis carried out included typical testing used to ascertain information about the surface morphology, chemical composition, and structure of the adsorbent material. The data gathered was used to understand the properties of the material as a potential adsorbent material for atmospheric CO_2 capture. Three types of testing were carried out by members of Dr Eoin Flynn's team in the Environmental Research Institute of UCC:

1. Scanning Electron Microscopy
2. Scanning Electron Microscopy/Energy Dispersive X-Rays (SEM/EDX)
3. Brunauer-Emmett-Teller (BET) Surface Area Analysis

The results of the product analysis are included in section 5 of this research.

4.5.1 Scanning Electron Microscopy (SEM)

The Scanning Electron Microscope focusses a high energy electron beam on the surface of the testing material. The electron beam interacts with the surface of the material, producing signals that can be adapted, to form an image that provides information about the surface morphology and composition of the sample.

The electrons are emitted from an electron source, which consists of a solid material such as a tungsten filament, which emits electrons when heated [65]. The electrons are accelerated and attracted by the anode and their path is controlled by a lens. When electron beams strike the sample, the sample scatters the beam, producing characteristic x-rays and secondary electrons. The signals generated are transformed into a 2-D image which typically magnifies an area of the sample up to by a factor of up to 30,000. The image produced is typically a high resolution, computerised image that can be used for analysis [65].

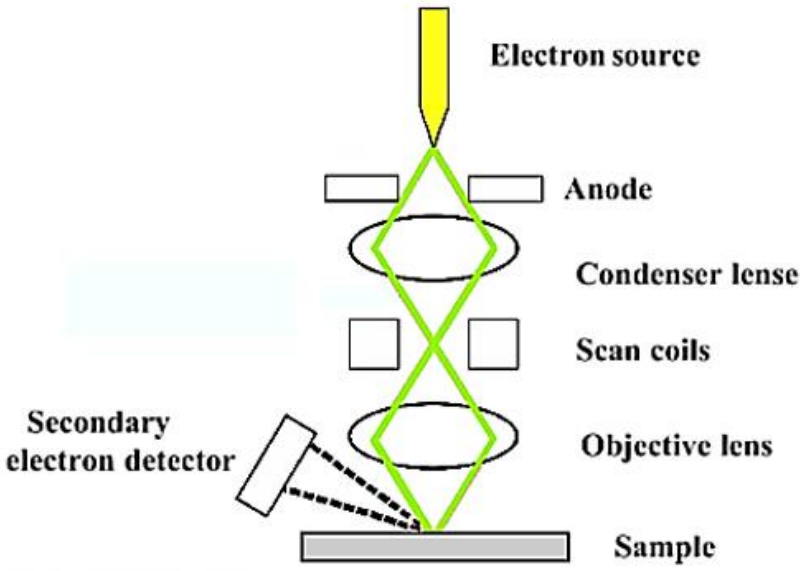


Figure 43 Diagram of SEM and its operational principle[65]

4.5.2 Energy Dispersive X-rays (EDX) in conjunction with SEM

Along with backscattered electrons, secondary electrons and any other transmitted electrons, X-rays are also transmitted in SEM and are used to generate signals and images of the sample. When the electron beam in the SEM comes in contact with the sample product, it transfers its energy to the sample. This results in the transmitted electrons already described, but also in X-ray emissions. X-rays occur when high energy electrons in the sample, fill holes left behind by transmitted electrons in lower energy shells, resulting in the emission of the energy difference in the form of X-rays. As the energy difference between the shells of an atom is a unique property in every element, it allows the observer to identify the elements that are present by measuring the energy emitted in these X-rays [66].

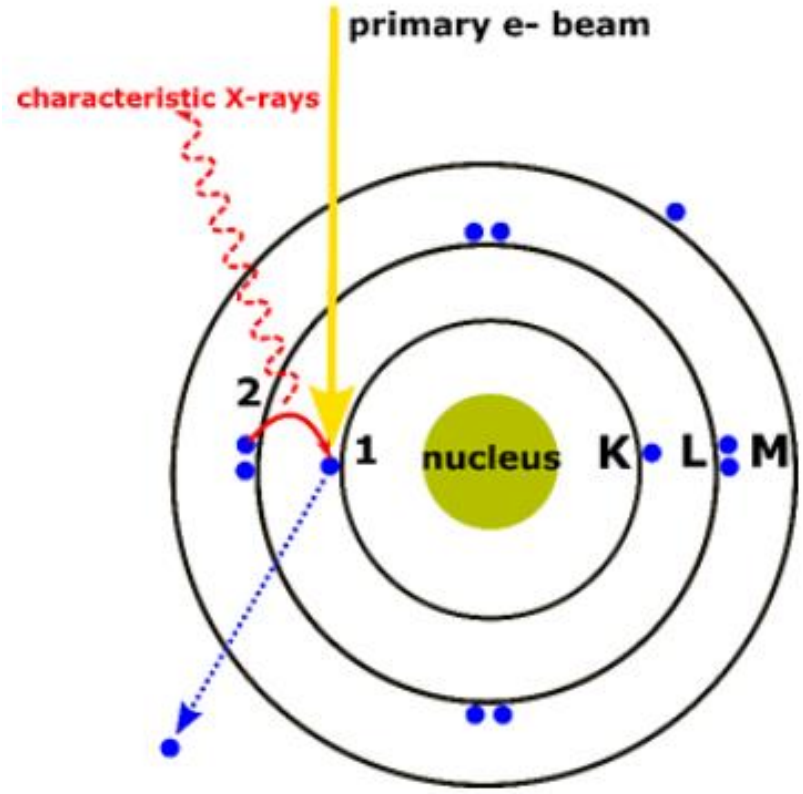


Figure 44 Representation of the process of X-ray emission in an EDX/SEM system[66]

The X-rays are detected by specialised pieces of equipment called detectors that are made of silicon, positioned at an angle, in very close proximity to the product sample. The EDX analysis converts the X-ray energy emitted from the sample into a signal that creates data that consists of a spectrum of peaks that correspond to the constituent elements of the sample. The EDX data can also not only be used to analyse the type of elements present in the sample, but it can also be used to calculate the percentages of each element that comprise the sample[66].

4.5.3 Brunauer-Emmett-Teller Analysis (BET)

BET Analysis is the most widely utilised scientific technique for characterising and analysing the surface area of a material. It is named after the three scientists (Stephen Brunauer, Paul Emmett & Edward Teller) who proposed the theory of multimolecular adsorption to calculate the surface area of a material [24]

The first step of BET analysis is outgassing. Outgassing is the process by which any gasses that have been physically adsorbed on the surface of the substance during manufacture, storage or handling, are removed. Outgassing is achieved by applying a vacuum and introducing a purge stream of inert, dry gas, which is swept over the sample, removing any gasses of vapours previously adsorbed on the surface, which could interfere with BET results.

Following outgassing, the adsorbate gas is introduced into the system. The typical adsorbate is nitrogen, which is introduced at a known volume and a known temperature (usually 77.15K, the boiling point of nitrogen). The nitrogen condenses on the surface of the sample in a monolayer[6] and when saturation occurs, no more nitrogen can be adsorbed on the surface. The volume of nitrogen adsorbed, the partial pressure of nitrogen, the temperature, and the mass of the sorbent or sample material are now known, and these values can be correlated, using a set of equations, to find the surface area of the sample particles. BET analysis can also be used to find other particle properties such as pore volume, pore area and pore distribution, which provide further insight into the expected behaviour of a substance as an adsorbent.

The data points gained during experimental BET analysis are input into the BET adsorption isotherm equation (4,1) which is as follows to ascertain the values of surface area the material:

$$\frac{1}{[V_a(\frac{P_0}{P}-1)]} = \frac{C-1}{V_m C} \times \frac{P}{P_0} + \frac{1}{V_m C} \tag{4.1}$$

Where:

Variable		Unit	Description
$\mathbf{V_a}$	=	ml	The volume of adsorbed gas at STP
$\mathbf{P_0}$	=	Pa	Saturated pressure of adsorbate gas
P	=	Pa	The volume of adsorbed gas at STP
$\mathbf{V_m}$	=	ml	The volume of adsorbed gas required to produce a monolayer of adsorbate gas on the surface of the adsorbent
C	=	N/A	A constant related to the energy of adsorption for monolayer; indicates the magnitude of adsorbent affinity for adsorbate.

Table 28 BET equation variables

[6] Monolayer is assumed

4.6 Pelletisation and Shaping of Adsorbent Material

One of the basic principles involved in the design of an adsorbent gas treating system is the physical structure and mechanical strength of the adsorbent material. The physical structure of the adsorbent particles is crucial as it affects other key process parameters such as fluid flow, adsorption rate and system pressure. Fluid flow through any packed bed invokes a pressure drop, associated with friction between the passing fluid and the solid particles. In powder technology, as per Darcys Law, and the Kozeny-Carman Equation, smaller particles, with lower porosity such as the fine seaweed powder adsorbent material produced in section 4.3, invoke a larger pressure drop across the bed [67], requiring a greater energy input into the system. For a large, regenerable adsorbent bed, retaining a particle size of 75-150 µm is impractical due to the large pressure drop across the bed, which makes it very hard to create fluid flow, drastically reducing the operability of the system. To solve this problem, the microporous adsorbent particles must be shaped into larger, macroscopic pellets or masses, designed to reduce pressure drop in the bed while retaining adsorbent functionality. Shaping the particles allows for higher flow rates through the bed and more rapid mass transfer, which is essential in the operation of a gas separation process.

Generally, methods for the structuring of adsorbent materials have been invented by private companies for their own processes, and thus not much academic literature exists on adsorbent structuring. However, recently there has been an increased interest in the field of microporous material structuring. Structuring and pelletising are of particular interest in a variety of renewable engineering applications such as gas sweetening in hydrogen and methane, and also CO_2 capture in the context of flue gas and atmospheric adsorption.

The major consideration in the structuring of the microporous adsorbent material is producing a structure that has sufficient mechanical strength for use in a gas separation system. The structure has to be capable of resisting both chemical and physical attrition due to conditions arising during the separation, such as separation temperature, pressure, or the presence of a contaminant in the fluid phase that could weaken the structure. The performance of the structured adsorbent, therefore, does not depend entirely on the adsorption capacity of the primary adsorbent material. It depends on multiple operating conditions, such as the properties of the structural additives, the interaction of several parameters such as the gas diffusion kinetics, the mechanical strength, the void fraction, the volumetric capacity the heat transfer properties and the pressure drop across the adsorption bed. These factors must be taken into consideration when selecting a suitable structuring method and optimising the PSA process.

4.6.1 Typical PSA adsorbent structures

There are a number of adsorbent structure types that have been used industrially for PSA and gas separation technologies. When optimising a gas separation or PSA system, variations of these structures are experimented with until the most effective structure, which is dependent on the adsorbent properties and the process requirements, is found. This section examines some of the different types of adsorbent structures used in industrial processes.

4.6.1.1 Randomly packed Beads, Pellets and Granules

Discrete randomly packed beads, pellets and granules, are some of the most conventional structures used across all processing industries, including gas separation technologies. All three structures consist of a bed of numerous individual shaped units of the adsorbent material or powder, which are held together by processing the powder with a binding agent. The performance level of beads, pellets and granules in gas separation technologies is usually high due to the rapid mass transfer that is achievable. These small discrete masses achieve a high level of mass transfer due to their small size and high relative surface area, however, a trade-off occurs as smaller particles create a larger pressure drop across the adsorbent bed. A large mechanical energy input is required to overcome the pressure drop, and this is a serious consideration in a gas separation process which has a high volumetric throughput of air like the DAC process. DAC requires a large volumetric flow rate of air due to a dilute concentration of adsorbate in the inlet stream (CO_2 in atmospheric air), and because of this, the pressure drop across the bed becomes an important variable. There are several well established industrial methods for the shaping of porous powders into beads, pellets and granules. Typical shaping methods include extrusion, spheronisation and wet and dry granulation[68].

4.6.1.2 Monolithic Structures

Monoliths are an adsorbent structure type that have received a lot of attention in gas separation processes in recent years, and particularly in CO_2 capture technologies. They consist of the adsorbent material either shaped into, embedded in, or coated on a structure which consists of one large support with numerous parallel channels, through which fluid can flow. These channels can be created in a variety of various shapes, including round and honeycomb, with the geometry of the structure designed to maximise contact between the fluid and solid phases, which maximises mass transfer. The key advantage of monolithic adsorbent structures, as opposed to traditional pellet or bead structures, is the significantly reduced pressure drop across the bed. It has been found that the pressure drop across the bed in monolithic structures was between 3-5 times lower than that of a packed bed of pellets[69]. This makes monolithic adsorbent structures very appealing for atmospheric CO_2 capture systems. While the separation efficiency is superior in pellets, it is harder to rapidly pressurise and depressurise the entire system in order to process large volumes of air, making monoliths advantageous. Two of the most promising commercial DAC projects, Climeworks and Global Thermostat, make use of monolithic adsorption structures for air contacting.

One of the key problems associated with monolithic structures lies in the manufacturing of a structure with high adsorbent density at the surface[68], which reduces the functionality of the system. Monoliths also face resistance to mass transfer at the surface, and a lower residence time of fluid particles in the bed than a conventional packed bed, which makes it hard to maintain separation efficiency. The key areas of research in monolithic adsorption structures is the tailoring of the structure to individual application based on the properties of the adsorbent and the adsorbate, and the development of higher density (mol adsorbent/cm^2 of structure surface) structures that increase separation efficiency.

4.6.1.3 Laminates

Laminate adsorbent structures are a relatively new development in adsorption, and gas separation operations and consist of a bed made from a series of thin adsorbent sheets arranged very closely together. They are a close relative of monoliths, with the key difference being that rather than one continuous adsorbent structure, a laminate structure consists of many discrete units. Recent developments in laminates have also introduced corrugated or furrowed sheets, which can increase the overall surface area of the sheets and improve separation efficiency.

The laminate sheets themselves are generally produced by adding a binding agent to the adsorbent material and then coating the mixture on a specially designed external support. Laminates composed entirely of adsorbent material can be produced but have inherent processing difficulties. As seen in monolithic adsorbent structures, laminates face issues with low adsorbent density on the surface, as well as maldistribution of the adsorbent material, due to the difficulty in producing uniformly thin laminate sheets. However, if the processing difficulties can be overcome, laminates show good potential in PSA systems, particularly rapid-cycling, high throughput systems like atmospheric CO_2 capture. With laminate structures, the pressure drop can be controlled by varying the spacing between each laminate. Mass transfer efficiency is inversely proportional to space in between, allowing for a good amount of control in the operation of laminate containing systems. In theory, a laminate adsorbent system could vary the spacing continuously, according to variations in the feed throughput or composition, to optimise adsorption, however, in practicality, the spacing would be predetermined and uniform. The key design consideration is balancing the importance of the decrease in pressure drop across the bed with the decrease in mass transfer efficiency. This can also be done by creating laminates of different shapes, for example, woven mesh or spiral-wound configurations which are currently being developed, with potential for utility within CO_2 capture systems.

4.6.1.4 Other Structures

There are several other structure types that have been explored in the context of other gas processing industries but haven't yet been widely utilised for gas separation or PSVA systems.

Foam adsorbents or ceramic foams are used widely as catalyst supports or liquid filters, but have not yet been properly utilised for gas separation purposes[68][70], and are not applicable to biopolymer adsorbents such as expanded seaweed particles. In this technique, the adsorbent material is used to create a ceramic slurry. The slurry is coated on a polymeric sponge, with excess slurry removed, followed by heat treatment. At very high temperatures the polymeric sponge disintegrates, and what remains is a hardened ceramic skeleton. This method is potentially suitable for zeolites, or other inorganic adsorbents comprising of silica, which are not degraded by high-temperature thermal treatment[71]. The resultant solid foam structure is a high surface area, high porosity adsorbent structure. Foam structures exhibit a reduced pressure drop across the bed when compared to the traditional, packed bed adsorbents. Foams also have the advantage of large, randomly structured flow channels which allows for radial mixing, which does not typically occur in the laminar flow channels of monolithic and laminate adsorbent structures.

Fabric adsorbent structures are another promising development in sorbent technology. A close relative of monolithic structures, the fabrics comprise of thin interwoven fibres made partially from the adsorbent material. They can be fabricated in various configurations depending on the properties of the adsorbent or the nature of the process. By tailoring the fabric adsorbent structure based on specific process requirements, fabric structures can exhibit good mass transfer and pressure drop qualities. In fabric structures, the pressure drop across the adsorbent bed is directly related to the manner in which the fabric is assembled, whether it is mesh, parallel fibre sheets, or spiral wound. Fabrics are also advantageous due to their flexibility, and high mechanical strength, which results in mechanical attrition of the adsorbent bed due to high volumetric throughput, an important consideration in atmospheric CO_2 capture[68].

4.6.1.5 Structure Selection for this Research

The adsorbent structuring method chosen for this research was pelletisation. The key considerations in making this selection were the properties of the adsorbent material, a seaweed-derived biopolymer, and the process requirements of the experimental system designed in section 3. The decision to make pellets was taken due to the risk of denaturing or destroying the adsorbent during the processing steps required for the fabrication of other structures. As a biopolymer, exposure to high temperatures, or abrasive processing operations, could destroy the activity of the adsorbent. It was decided that a simple pelletisation process carried the least risk. The pressure drop associated with a packed bed of pellets would be a processing consideration in a high throughput commercial CO_2 capture process but was not considered in the context of this research. The adsorbent bed (volumes of <25cm^3 in each of the columns) in the lab-scale PSA system meant the pressure drop across the bed was not a significant concern, therefore, pellets were considered suitable. Finally, as a practical consideration, the adsorbent bed had to be introduced through a 1cm opening at the top of each column and this was only possible with pellet structures.

Various methods of pelletising the adsorbent were explored in an effort to optimise surface area, porosity, and mechanical strength, and these methods are described in section 4.62. Fig. 44 shows a variety of adsorbent structures:



Figure 45 (a) A variety of different solid adsorbent structures [68]*, (b) granulated or pelletised adsorbent graphical representation, (c) monolithic adsorbent structure graphical representation, (d) laminate adsorbent structure graphical representation* [72]

4.6.2 Powder Shaping Methods

There are various commercial powder shaping methods used throughout powder processing industries that can be applied to DAC and adsorbent technologies, for the purposes of this research, only pelletisation using extrusion was used.

4.6.2.1 Pelletisation using Extrusion Method

The extrusion method for pelletisation is one of the most common forms of powder shaping and processing. It involves the addition of a plasticiser and/or binding agent which allows the powder to be transformed into a clay, after which it is extruded and spheronised. It is a popular processing method in the pharmaceutical industry where bulk active pharmaceutical powders must be shaped into highly spherical and highly consistent units of a known dosage [73], [74].

The steps in the Extrusion-Speheronisation process are as follows[73]:

1. Powder Blending: The active powder ingredient (adsorbent) is blended with a binding or plasticising agent and a filler, in known ratios, to produce a powder blend.
2. Wet Massing: Water, or another suitable hydrating liquid, is added to the powder blend and mixed to form a paste or clay-like wet mass.
3. Extrusion: The wet mass is put into an extruder, which usually consists of a chamber, which is covered with a screen or die, containing an orifice of known shape and diameter, and a piston. The wet mass is then pushed through the screen or die into long extrudates. Finally, the long l extrudate is cut into a series of individual particles of the same length either manually or using specialist equipment.
4. Spheronisation: The individual pieces of the extrudate are loaded into a mixer or spheroniser which consists of a cylindrical chamber with a rotating frictional base plate. As the base plate rotates, frictional forces between the extrudates and the chamber wall eventually turn them from cylindrical particles to spherical particles of uniform size. The size of the spheres is based on the properties of the extrudate and the spheronisation conditions, such as base plate rpm or the impeller size.
5. Drying: The final spherical pellets are dried to remove the moistening liquid. Pellets can be air-dried, but in industrial applications typical pellet drying processes use either ovens or fluid bed dryers.

The spehronisation process is not fully understood and different methods of particle shaping have been proposed [74][75], starting with cylindrical extrudate and ending with spherical units. Each containing different stages of plastic deformation which leads to the eventual spherical shape, these methods are shown in Fig. 45.

For the purposes of this research, spheronisation of the pellets was not carried out due to the absence of suitable lab equipment to carry out the process.

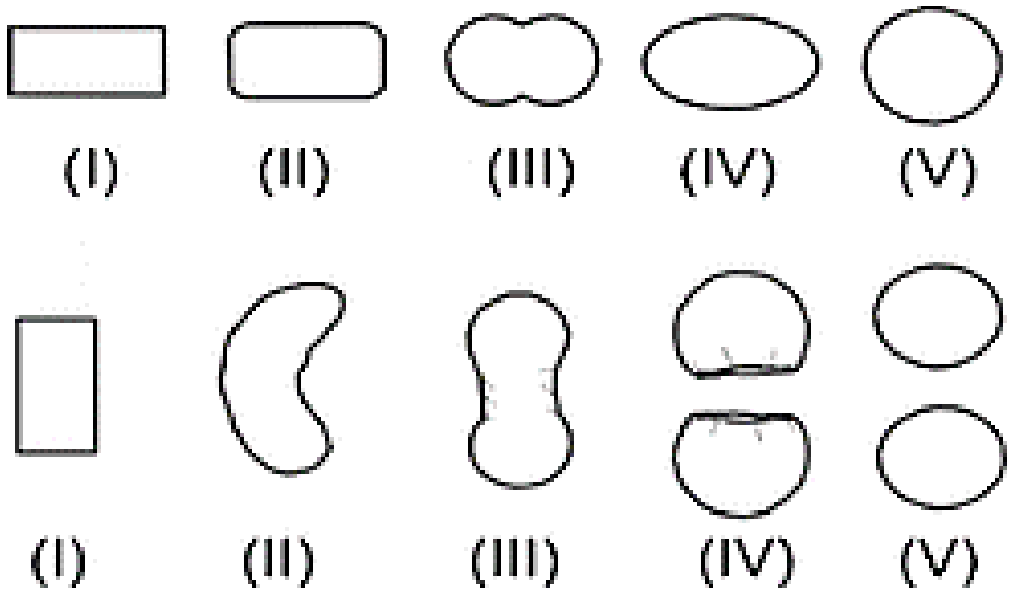


Figure 46 Mechanisms of spheronisation of cylindrical pellets proposed by Rowe (upper) and Baert (lower)

4.6.2.2 Pelletisation Experimental Methodology:

The final step of the experimental method for the development of a CO_2 adsorbent was the pelletisation of the powder product. The rationale for powder shaping is explained in further detail in section 4.6, and the experimental method is further explained in section 5.2.3.

1. Weigh the adsorbent powder sample and note weight.
2. Add 15% (by weight of adsorbent powder) of methylcellulose, and 15% (by weight of adsorbent powder) of bentonite.
3. Mix the powders together in a beaker to create powder blend.
4. Add deionised water dropwise until the powder blend forms into a paste.
5. Add the paste to the extruder (Makin's Professional Ultimate Clay Extruder).
6. Attach extrusion plate with the desired orifice and extrude paste into 25-30cm lines.
7. Cut lines using laboratory knife into pellets approximately 3mm long.
8. Let pellets dry at room temperature for 24 hours.

5. Results

This section compiles the results of this research, including the design and development of a lab-scale PVSA system, and the development of a new biopolymer adsorbent material for CO_2 capture.

5.1 Rig Design Results

After the design process outlined in section 3.1-3.5, the equipment was sourced and the lab-scale PVSA system built in the lab. Due to supplier issues, the CO_2 meters had not been sourced at the time of writing, meaning that CO_2 adsorption testing of the adsorbent material produced could not be conducted. The system was instead tested using plastic ball bearings, of similar size to a pelletised adsorbent, to ensure that fluid flow and pressure control through the system operated as designed.

Fig. 47-53 show the results of the PVSA system design and assembly.

5.2.1 Mechanical Assembly

Pipe cutting, fitting and fixturing was done by hand with the assistance of Paul Conway, the department technical officer. All fixtures were attached to the pipework using supplier instructions and Swagelok ¼" fittings, as described in section 3.6. Every section of pipe used in the rig, that had been cut by hand, was deburred and polished to ensure consistent fluid flow throughout the entire system. Non-uniform, or rough sections of piping can arise during cutting and cause issues with fluid flow to occur. Sections of rough piping can retain contaminants that are present the fluid or in the adsorbent material, and could impact the accuracy of testing carried out on the rig, or the operation of the rig itself.

Fig. 47-53 show images of the PVSA system after the purchase and assembly of the equipment. Missing from the images of final assembly are the CO_2 sensors, which have not been sourced at the time of writing, and P-2, a pressure gauge for C-2 which was not yet acquired due to budgeting considerations.

5.2.2 Electrical Assembly

Electrical assembly and wiring were done with the assistance of John Barrett, the department electrical officer. The solenoid valves require 24V DC current to operate. The valves were wired connected to switches on a switchboard and wired to a power supply. Each solenoid valve was independently wired to its own switch, corresponding to the numbering of the solenoid valves in the rig. Upon startup, the power supply is set 24V DC current using a pre-set function. Having completed these steps, all 8 solenoid valves can be operated in 2-way control (on/off) by using the designated switch on the switchboard.

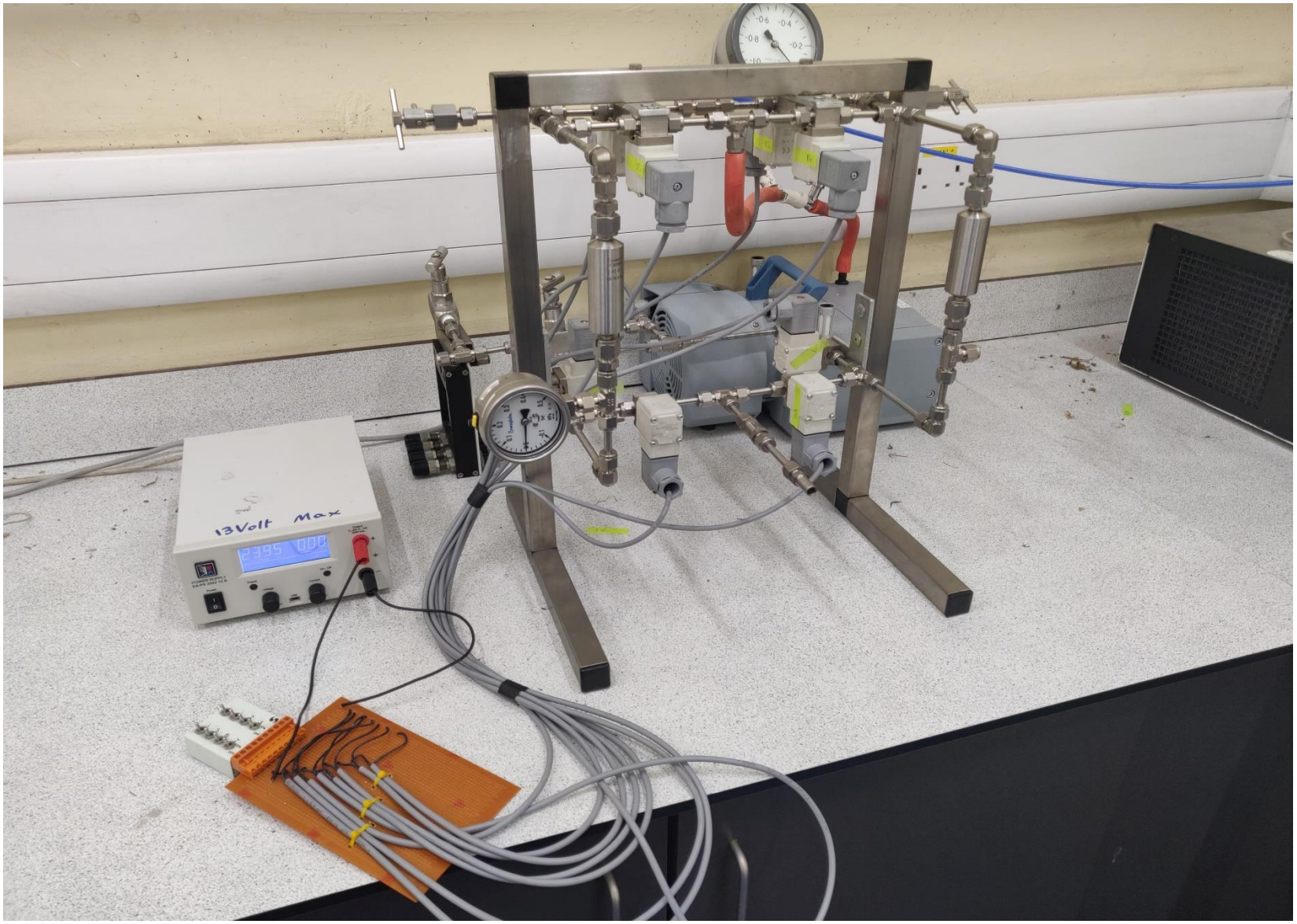


Figure 47 Assembled rig

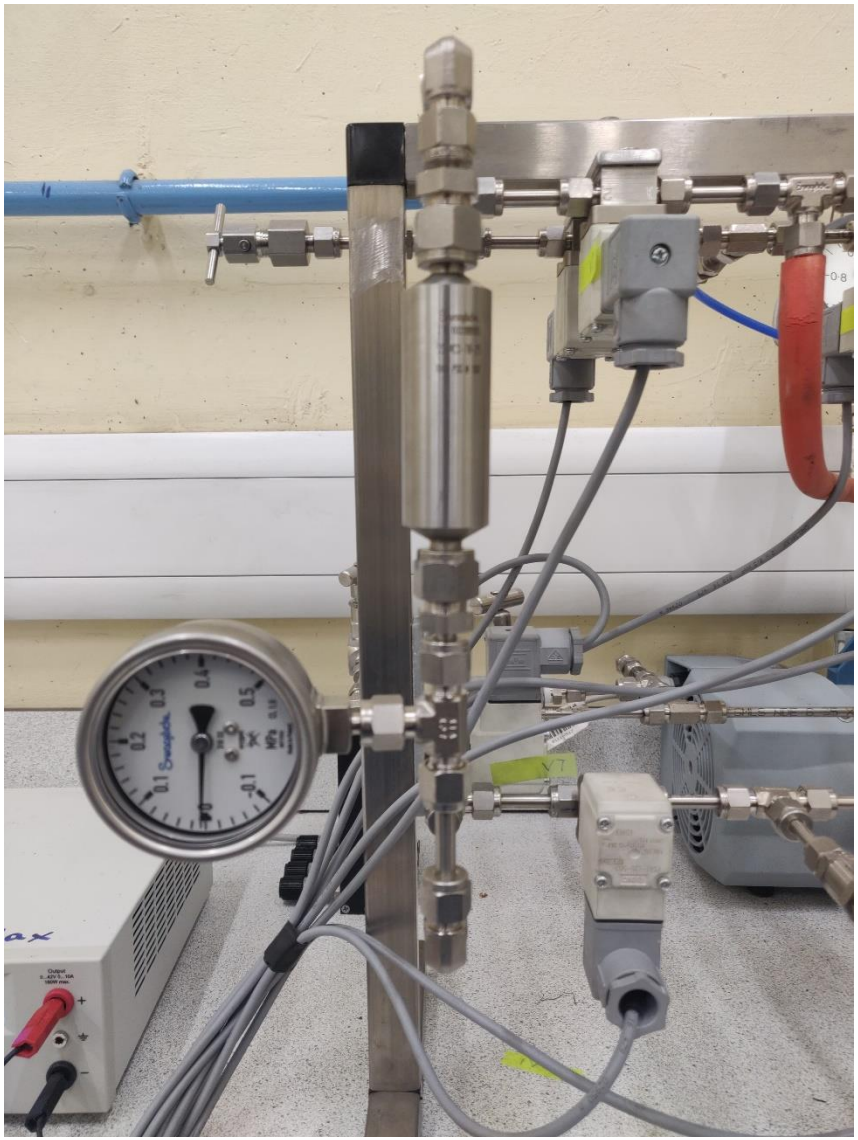


Figure 48 PVSA Sample column C-1 and pressure gauge PG-1

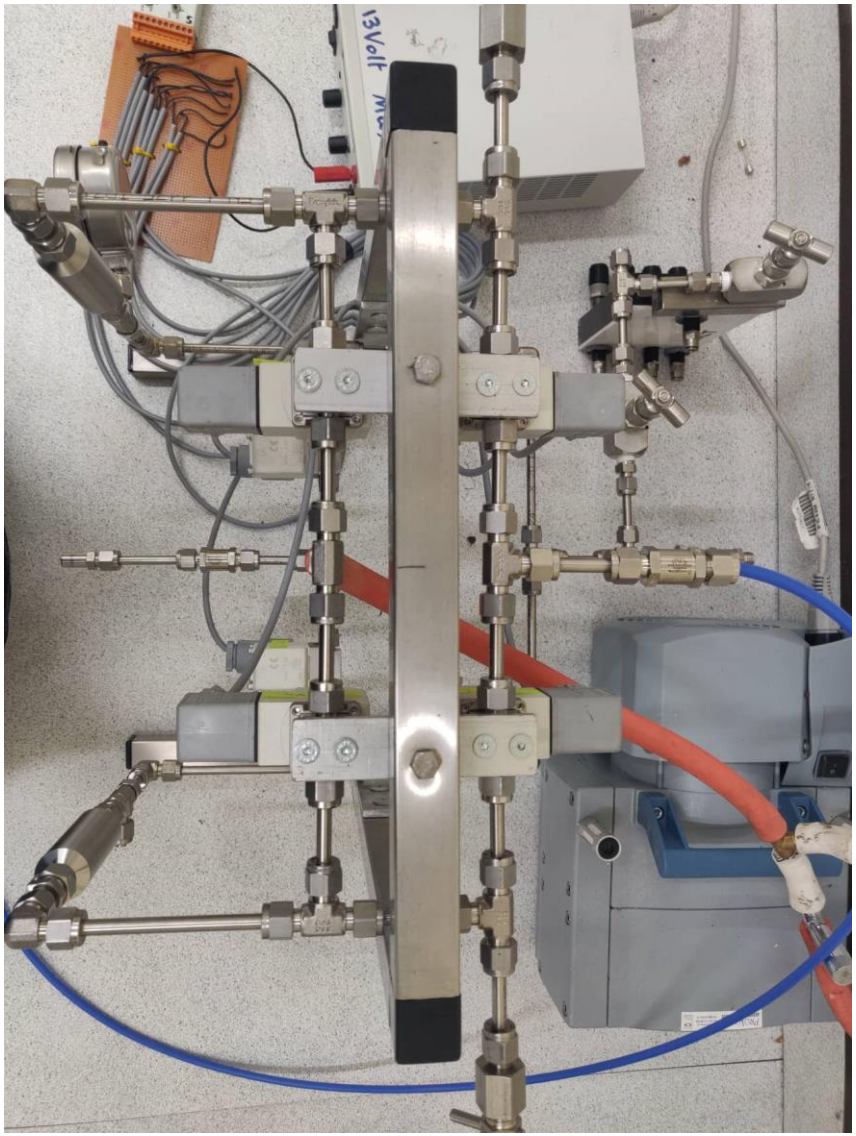


Figure 49 Top view of PVSA lab rig piping work

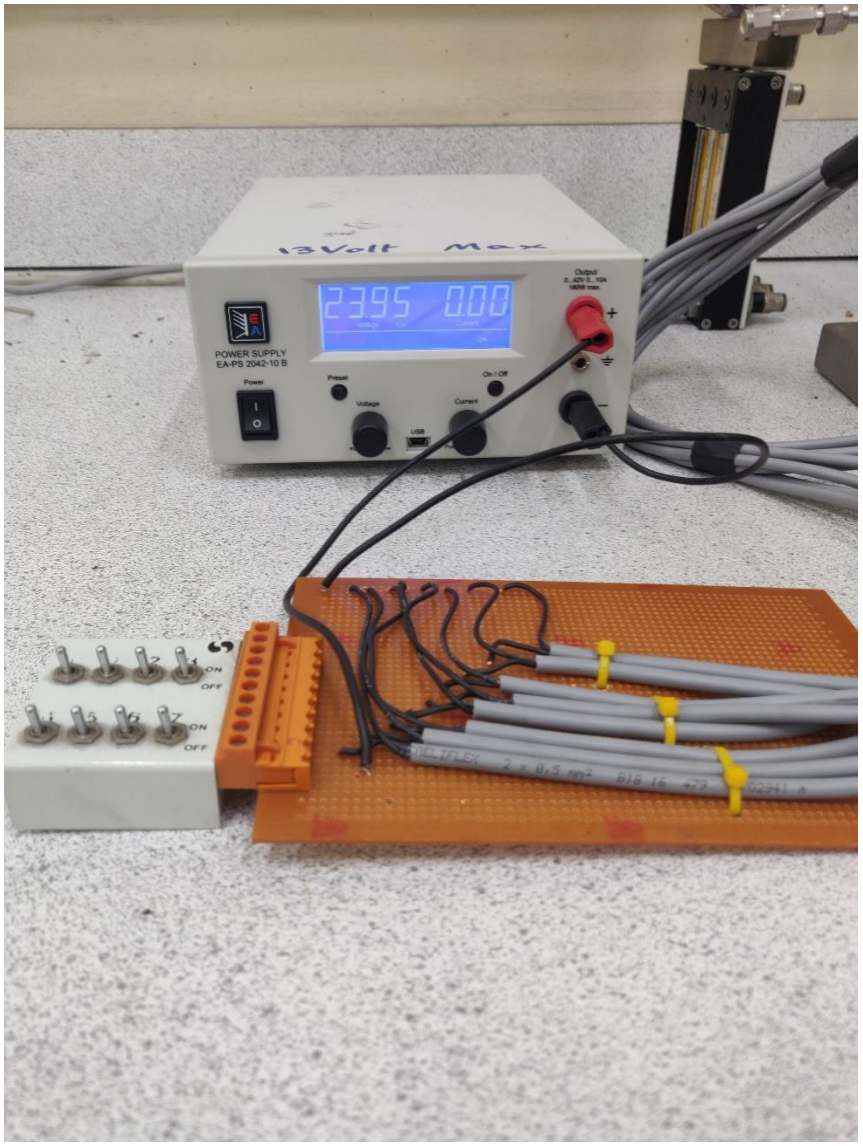


Figure 50 PVSA lab rig electrical switchboard and power supply

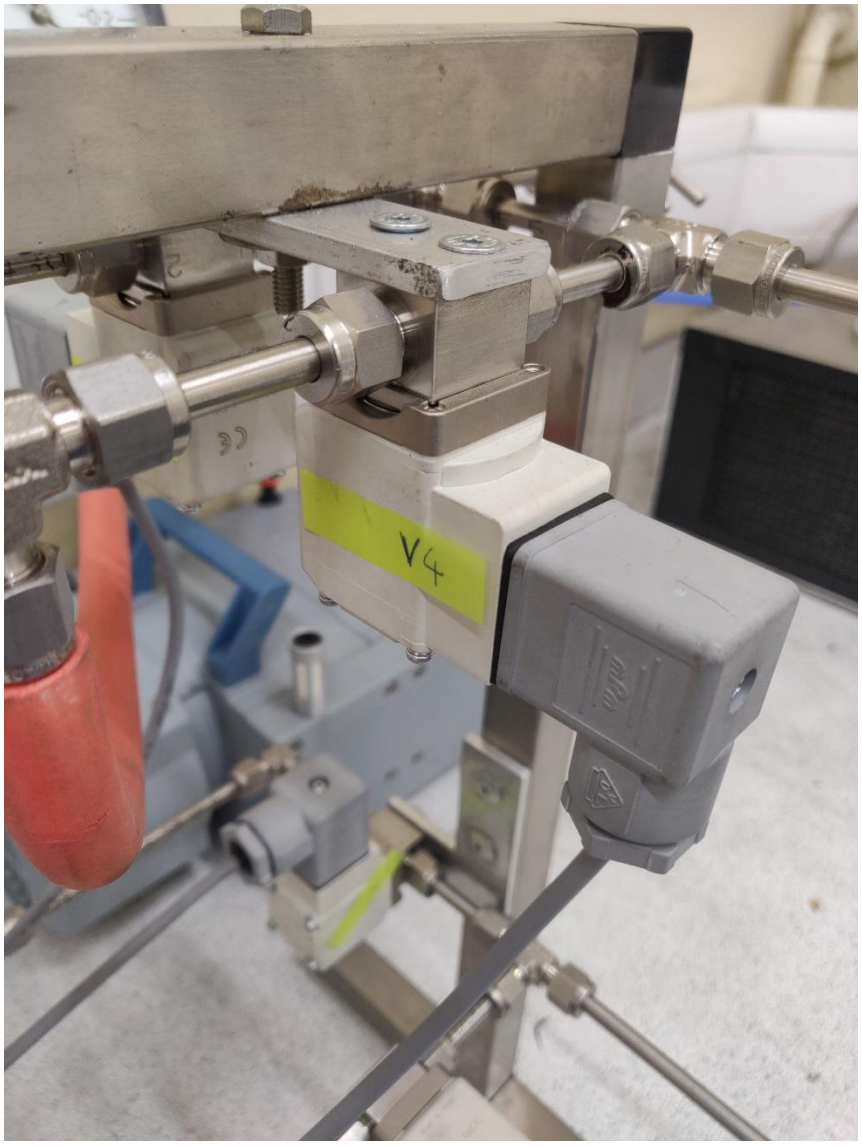


Figure 51 Solenoid valve



Figure 52 Air feed inlet supply valve and pressure gauge

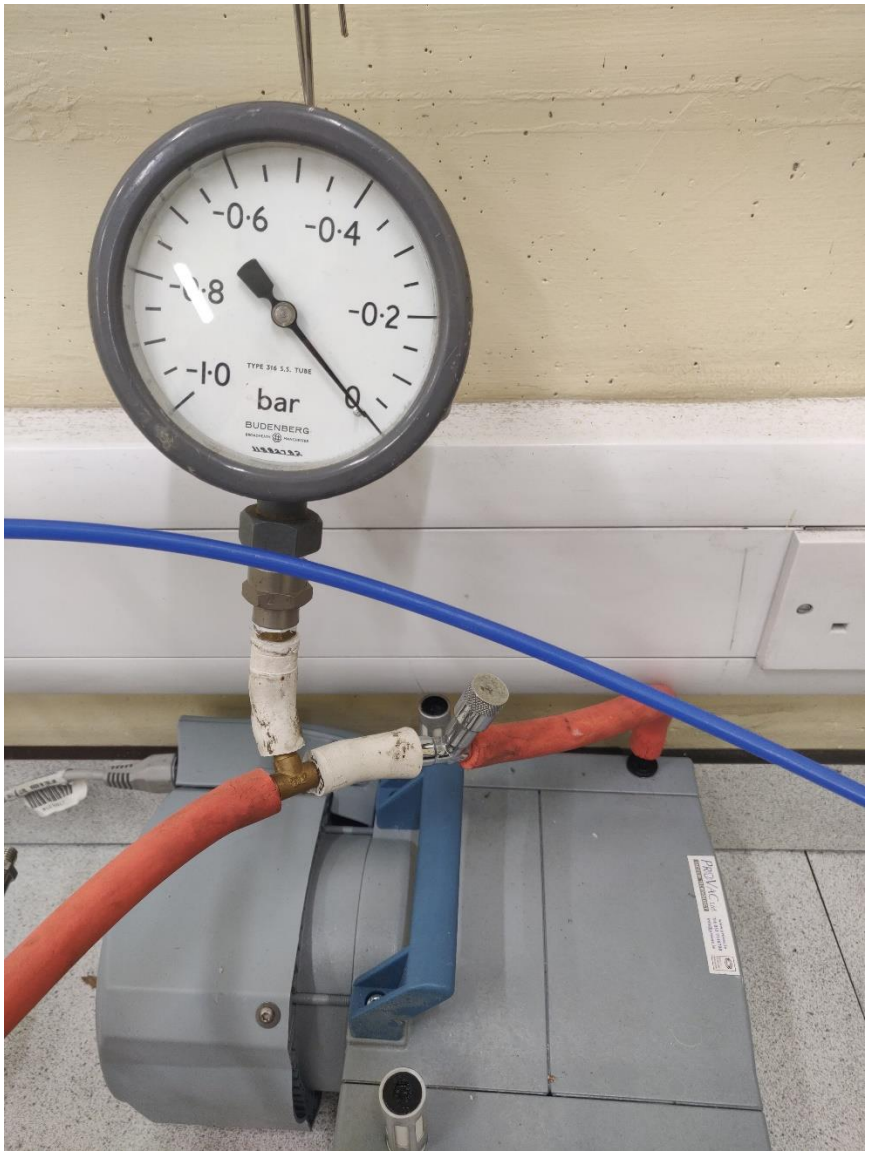


Figure 53 Vacuum pump and vacuum pressure gauge

5.2 Development of Biopolymer Adsorbent Results:

The final adsorbent powder product was tested using equipment in the Environmental Research Institute of UCC. Testing of the material was carried out by Dr Eoin Flynn, and members of his Materials Science Research Group.

Particles of the macroalgae A. nodosum were examined before and after the experimental procedure was carried out and the results are compared in this section.

5.2.1 SEM Results:

SEM analysis of the particles revealed a drastic change in the surface morphology of the A. nodosum particles after experimental processing. Fig. 54 shows side by side images of the surface of the unexpanded (a), and expanded (b) A. nodosum particles, with a magnification factor of approximately 2000. In the image (b), it can be clearly observed that the surface morphology is significantly altered when compared to the image (a). Image (a) shows a surface consisting of slit-like pores, with no observable trend in pore size or pore distribution. The surface of the material in the image (a) appears to consist of solid, smooth shapes distributed randomly throughout the image, with large pores appearing as fissures between these structures. Image (b) shows a more uniform surface morphology. The surface of the material (b) appears to consist of thin spiral structures, with a relatively uniform pore size and distribution throughout the image. The surface in the image (b) appears to be mesoporous, with pores sizes somewhere in the range of 2-50 nm, as opposed to the macroporous surface in the image (a) with pore diameters exceeding 50nm. From a visual perspective, image (b) immediately represents a more porous, high SA adsorbent material when compared to image (a), which represents a typical surface morphology of an untreated biopolymer. The increased surface area was confirmed with BET testing, which showed an increase in SA in material (b) by a factor of 4490.0 times that of the SA in material (a).

5.2.2 BET Results:

BET analysis was conducted on unprocessed and processed A. nodosum samples to produce the nitrogen adsorption/desorption isotherm. BET analysis showed an initial surface area of 0.023 m^2g^{-1} for the unexpanded sample of A. nodosum, and a final surface area of 103.270 m^2g^{-1} for the expanded sample, which represents an increase by a factor of 4490.00 times the initial SA, indicating that the SA expansion procedure was a success.

Fig. 55 shows the Nitrogen adsorption isotherm for the expanded sample of A. nodosum powder. The graph shows that the particles have a type IV adsorption isotherm which is consistent with a mesoporous solid adsorbent [76] in which multilayer adsorption occurs at low pressures and also capillary condensation (a condensation of adsorbate in the pores) occurs at higher pressures. The shape of the isotherm could also indicate the existence of micropores (less than 2nm in size). The analysis conducted does not rule out the existence of micropores, so the finished product is evaluated as a microporous-mesoporous solid.

The BET analysis also included results on the pore size distribution, which is graphed in Fig. 56. The results show that the final, expanded A. nodosum particles exhibited the average pore volume and pore diameter of 0.420 cm^3g^{-1} and 113.236 Å

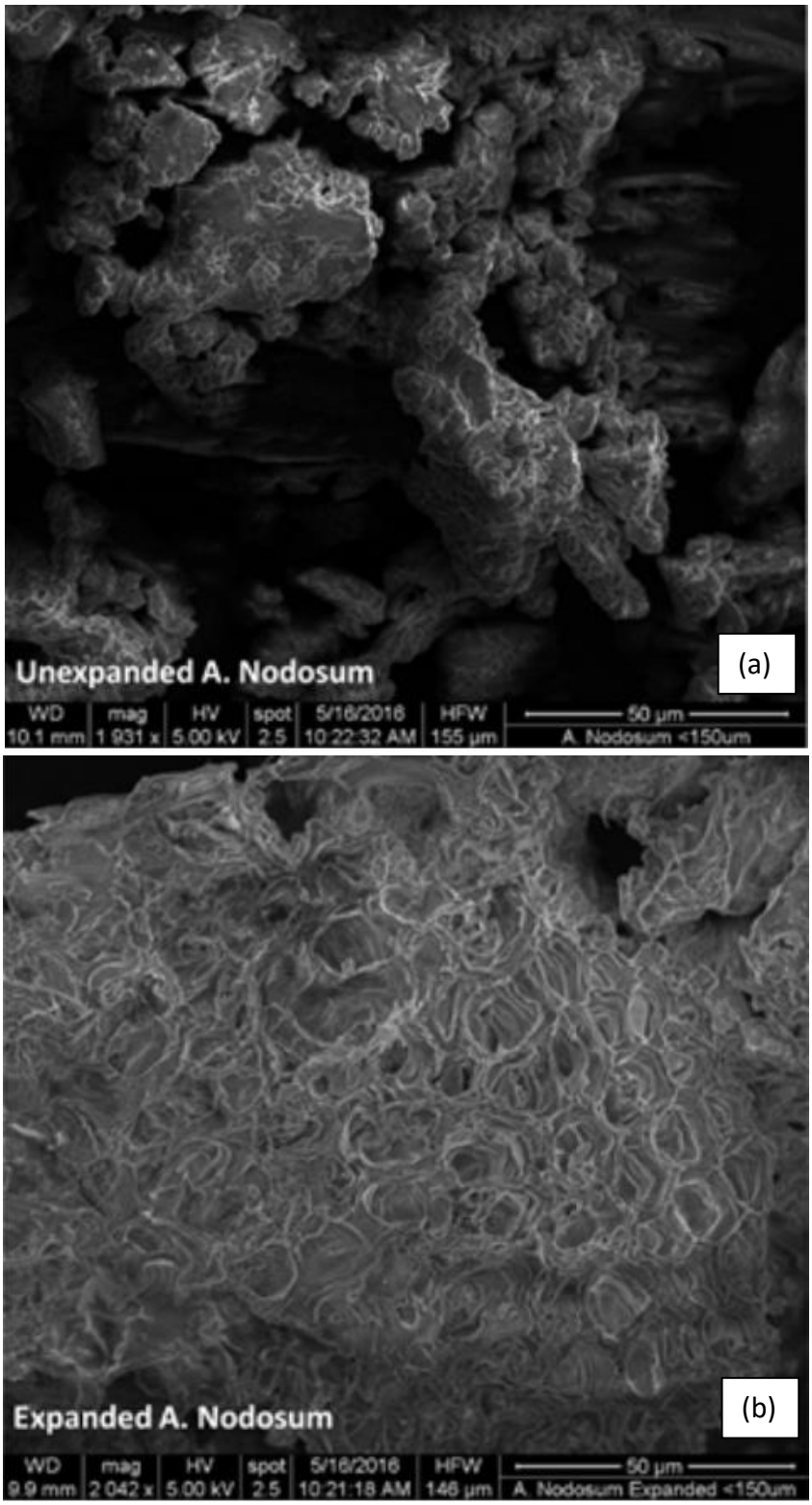


Figure 54 SEM images of Unexpanded (a) and Expanded (b) A. nodosum powder

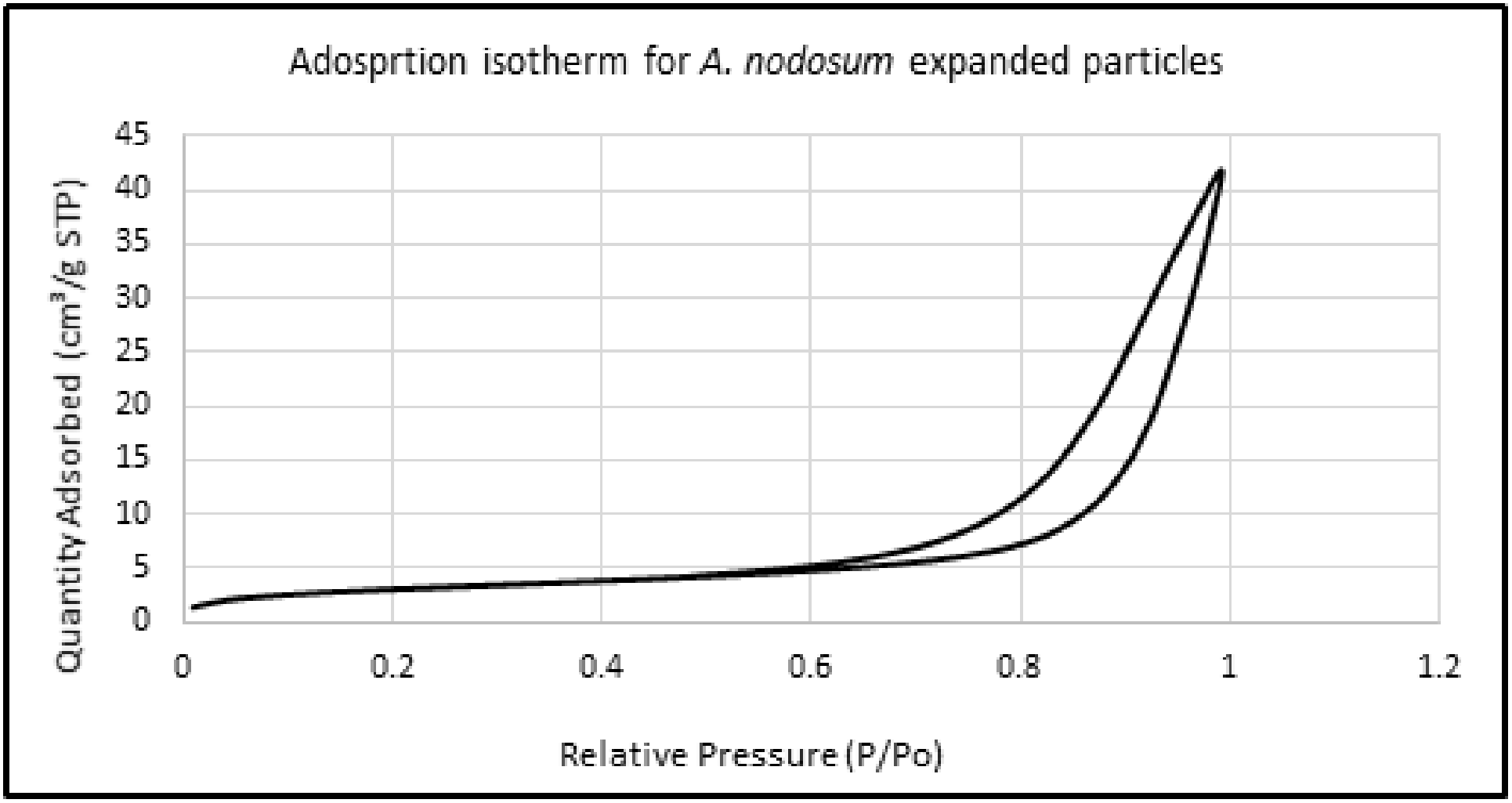


Figure 55 N2 Adsorption isotherm for A. nodosum expanded particles

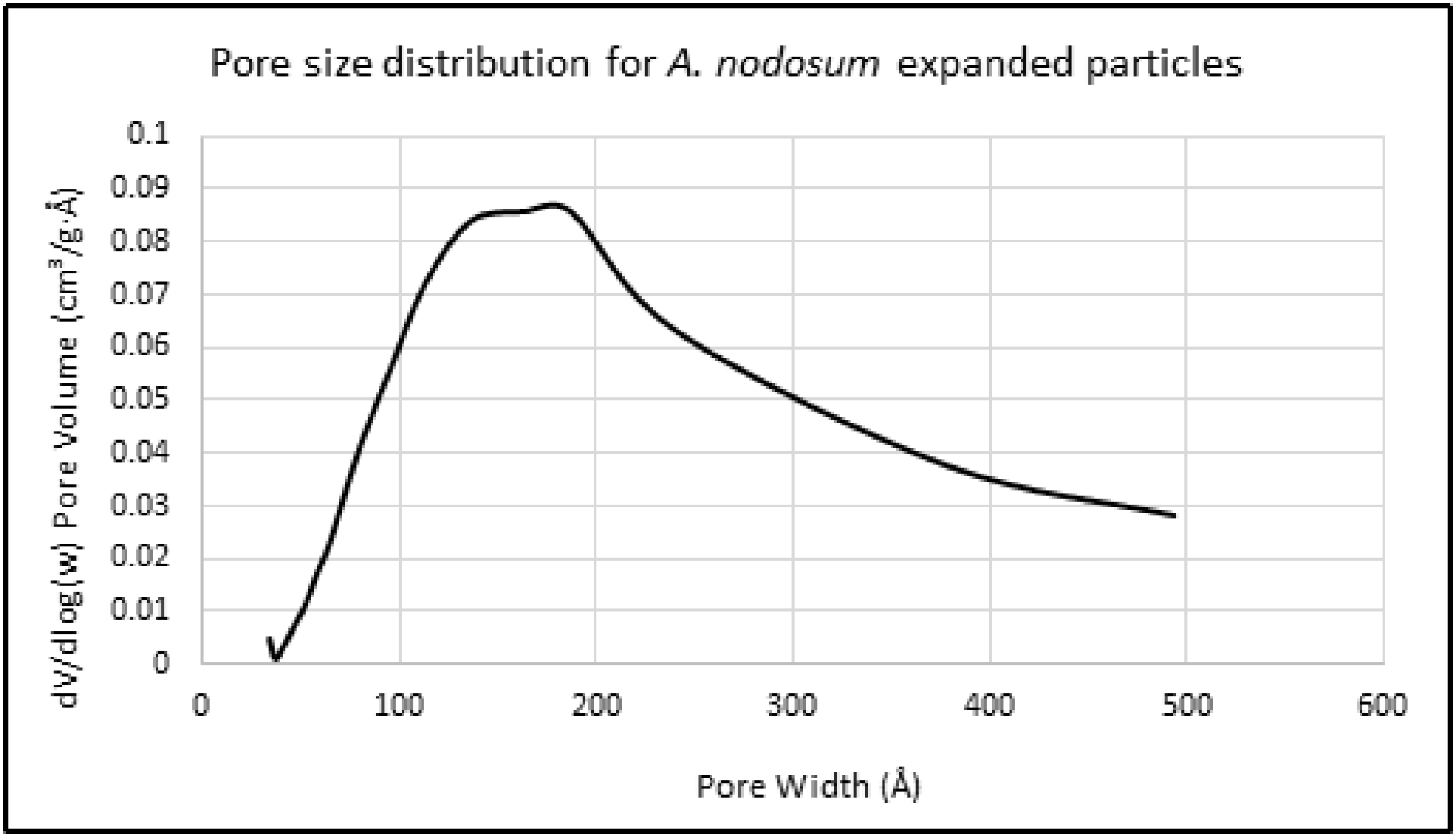


Figure 56 Pore size distribution graph for expanded A. nodosum particles

5.2.3 Discussion on adsorbent characteristics

To understand the behaviour of the biopolymer adsorbent produced, and its potential effectiveness as an adsorbent in an atmospheric CO_2 capture, the adsorptive properties of the material must be examined. In section 5.2.2, fig 55, the N_2 adsorption isotherm for the expanded A. nodosum particles is shown. The initial section of the isotherm follows that of a type II isotherm, increasing at first as monolayer adsorption occurs (fig. 57, Image 1) [91] [92]. Following this, multilayer adsorption begins to occur in the pores at a P/P_o of roughly 1.5 and is shown continuing, consistent with a type II isotherm (fig. 57, Image 1). The defining feature of the adsorption Isotherm, and the reason it can be assessed as type IV, is the hysteresis loop (fig. 57, Image 3). Hysteresis occurs due to capillary condensation, a phenomenon that occurs when residual pore space, which remains after monolayer and multilayer adsorption, is filled by liquid condensate from the vapour phase. This condensation occurs at pressures lower than the saturation pressure for the vapour in small pores or "capillaries" because the confined nature of the pore increases interaction between vapour molecules. Capilliary condensation is characteristic of a mesoporous substance which is how we identify the isotherm as being type IV and the material as mesoporous [91][92].

The hysteresis loop can be categorised as either H2 or H3, which indicates a broader range of pore size distribution, which is to be expected from an adsorbent material derived from a naturally occurring biopolymer [91]

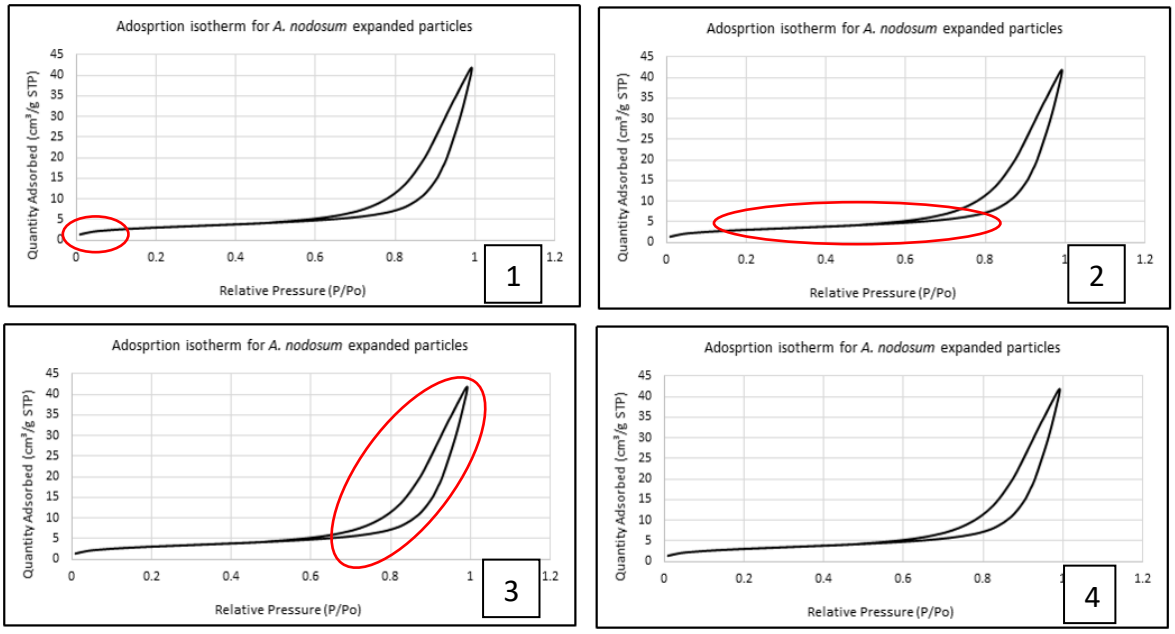


Figure 57 Features of A. nodosum N2 adsorption isotherm

Fig. 58 shows the different types of adsorption isotherms and hysteresis loops, confirming the assessment of the isotherm as type IV. Fig 59 confirms it with literature values.

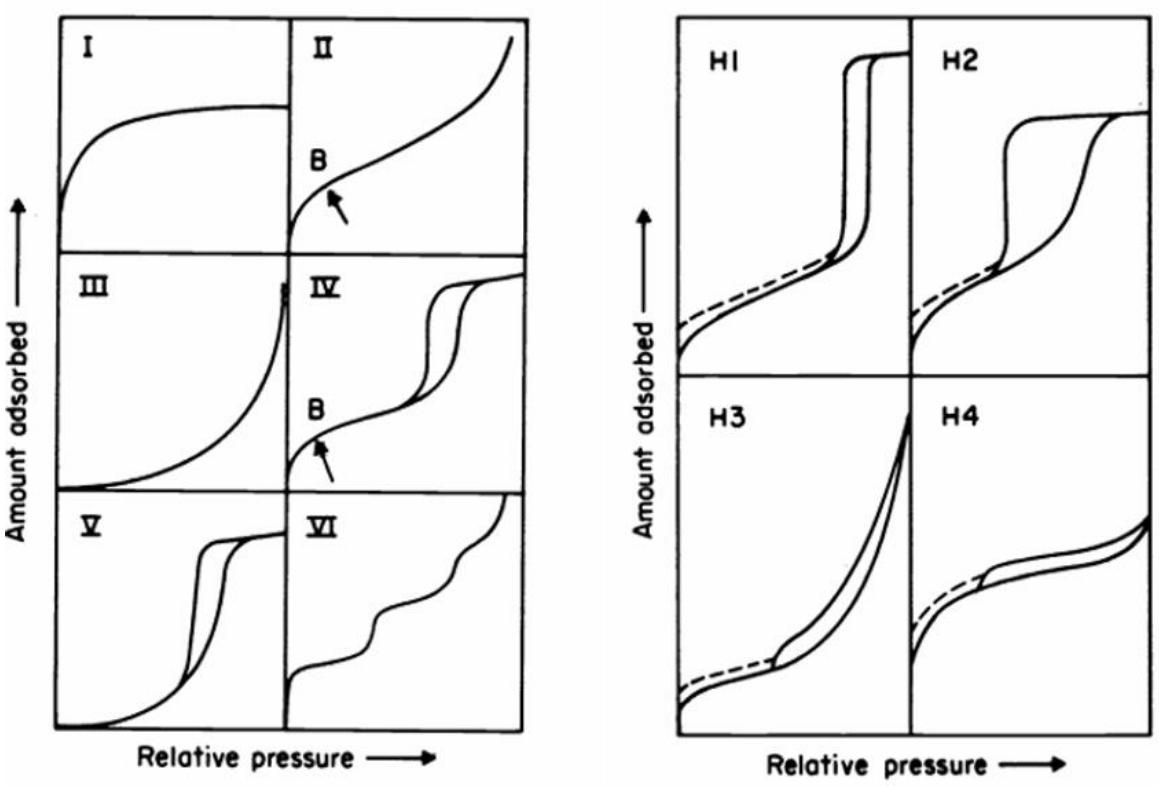


Figure 58 Types of adsorption isotherm and hysteresis loops [90]

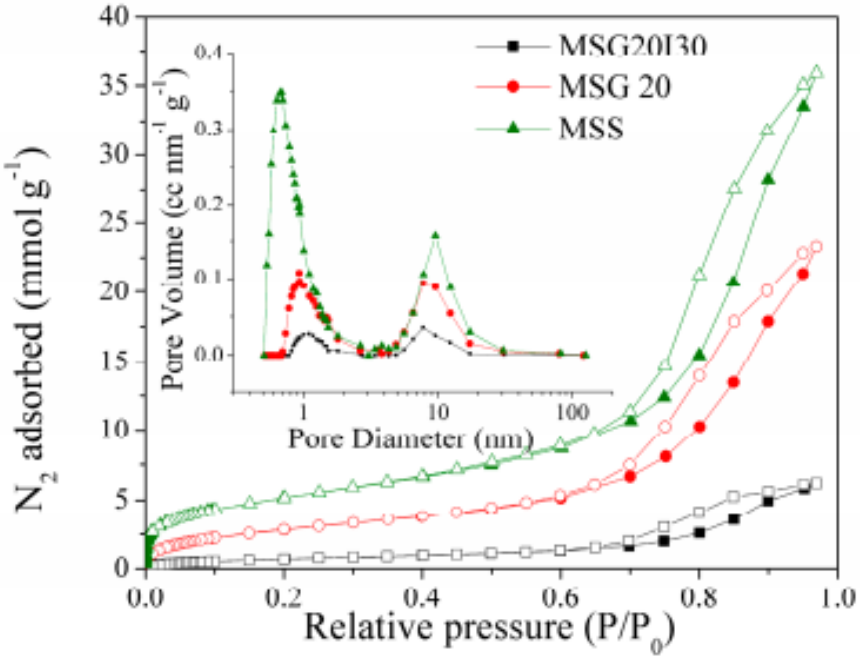


Figure 59 Type IV isotherms of three mesoporous silica-based CO_2 adsorbents [93]

To understand the potential of the material for use in atmospheric CO_2 capture systems, it's properties must be compared to literature values for similar, existing atmospheric CO_2 adsorbent materials. Table 29 compares the adsorbent produced in this research to similar adsorbent materials.

Adsorbent	Material Family	A_{BET} ($m^2.g^{-1}$)	Pore Vol ($cm^3.g^{-1}$)	Pore Size (nm)	Micropore Vol ($cm^3.g^{-1}$)	Source
Expanded A. nodosum	Mesoporous Biopolymer	103	0.420	11.3	Unknown	This research
MSS	Mesoporous Silica	392	1.43	9.6	0.125	[93]
MSG20	Mesoporous Silica	211	0.96	7.8	0.056	[93]
MSG20I30	Mesoporous Silica	52	0.06	7.7	0.014	[93]
SS-biochar	Biochar	10	N/A	Unreported	0.022	[94]
PM-biochar	Biochar	32	N/A	Unreported	0.044	[94]
WS-biochar	Biochar	20	N/A	Unreported	0.041	[94]
ACF	Activated Carbon Fibre	862	0.3472	Unreported	0.0427	[95]
aACF	Activated Carbon Fibre	1224	0.528	Unreported	0.1135	[95]
nACF	Activated Carbon Fibre	599	0.2610	Unreported	0.0612	[95]

Table 29 – Comparison of novel biopolymer adsorbent to literature values.

From table 29, we see that the adsorbent material has a below average surface area for mesoporous silica adsorbents (MSS, MSG20, MSG20I30), with the surface area of mesoporous silicas falling in the range of 52-393 $m^2.g^{-1}$ [93]. The pore volume is also slightly below compared to that of a mesoporous silica. When comparing the surface area to non-activated carbonaceous materials (Sewage Sludge-biochar, Pig manure-biochar, Wheat Straw biochar) the A. nodosum adsorbent performs more favourably with a comparatively high surface area. Finally, comparing the substance to activated carbon fibres (ACF, aACF, nACF), we can see that the surface area is comparatively low.

Mesoporous silicas are used in several industrial DAC processes and thus can be used as a benchmark, although the majority of these molecules are functionalized with amine groups to increase the affinity capacity for CO_2. MOFs, which can have surface area in excess of 4,000 $m^2.g^{-1}$ and are being researched in the context of atmospheric CO_2 capture. By comparing the structural properties, it is deemed unlikely that the biopolymer produced in this research would be an effective CO_2 molecule. While the adsorbent produced has a vastly expanded surface area compared to the original biopolymer, the surface area (a key indicator of adsorbent performance) is unremarkable. It is also considered likely that the adsorbent material would degrade more rapidly than other adsorbents due to the interaction between impurities in atmospheric air naturally occurring polysaccharides, particularly water, and reduce the adsorptive capacity and useful lifespan of the material.

Future research should revolve around experimentally enhancing the surface properties of the adsorbent and testing CO_2 capacity in atmospheric air to assess degradation of the molecule.

5.2.4 Pelletisation & Agglomeration

Pelletisation was achieved using the extrusion method. As suitable equipment was not available for spheronisation, cylindrical pellets of approximately 0.5-0.8 cm in length were produced for input into the PSA system. Several batches of pellets were produced, using bentonite and methylcellulose as binding and plasticising agents respectively. After the powder blend was created in a dry, clean 100ml beaker, deionised water was added dropwise until the texture resembled that of a putty, dough or firm paste. The quantities of each material used in each batch are outlined in tables 29, 30 & 31. The quantity of bentonite and methylcellulose required for the pelletisation is 15% by weight of the quantity of A. nodosum adsorbent powder. The quantity of product used in each batch is an arbitrary quantity measured at the beginning of the batch.

The paste was transferred into an extruder in small quantities (Makin's Professional Ultimate Clay Extruder, Fig. 61) and packed in to endure no voids or air traps exist within extrusion paste. When all of the paste had been transferred, an extrusion plate was fixed in place at the top of the extruder. The handle of the extruder was turned slowly clockwise, which pushed the paste through the orifice, onto a tin-foil sheet, creating a line of extruded paste (approximately 20cm). When all of the paste was extruded into lines (5-20 lines), they were cut using a knife into small pellets (approximately 0.5-0.8 cm).

Two batches of pellets were created using an extrusion plate with a circular orifice, approximately 1.5 mm in diameter, to create small, cylindrical pellets. For the third batch, a different extrusion plate was utilised to create pellets with a different geometry, for the purpose of comparison. The extrusion plate in the third batch had a hexagonal orifice, approximately 3mm in diameter, creating thicker, hexagonal prism adsorbent pellets. Varied amounts of deionised water and slightly different ratios of components in the powder blend in each batch meant that very slight differences in the consistency of the paste were observed. The colour and texture of the pellets in each batch was largely indistinguishable.

The final solid adsorbent shapes were created accidentally, using an agglomerating agent in the vacuum drying process. This process involved the addition of glycerol to the A. nodosum and ethanol suspension. Glycerol acts as a cross-linking agent between two polysaccharides present in the seaweed particles, fucoidan, and alginate, which makes them less water-soluble and has the effect of binding. This created lumps or clumping of seaweed in the suspension, and upon vacuum drying, the seaweed formed irregular dry solid shapes approximately 1cm in diameter and 2-5mm in thickness, with the potential for direct input into a PSA system. This is an interesting, and unexpected method of powder shaping, as it is

a cheap and efficient means of producing shapes for use in a PSA system. The shapes were not uniform, which could have unpredictable effects on the performance of the adsorption powder. However, in a process with a large rate of adsorbent replacement (PSA system with a biopolymer adsorbent), the shaping of the material carries less importance.
The purpose of creating pellets and shapes of different geometry in this research is to assess the effect of pellet shape and size on process variables in the PVSA system designed. These variables include pressure drop across the column, the adsorption isotherm of the material, and the heat transfer properties of the material, all of which impact the effectiveness of the adsorbent material.

Material	Percentage (of Total)	Target Quantity (g)	Actual (g)
A. **Nodosum**	76.69	-	5.00
Bentonite	11.5	0.75	0.75
Methylcellulose	11.81	0.75	0.77

Table 30 Material composition of adsorbent pellet batch 1 (cylindrical)

Material	Percentage (of Total)	Target Quantity (g)	Actual (g)
A. **Nodosum**	76.82	-	4.15
Bentonite	11.58	0.625	0.626
Methylcellulose	11.60	0.625	0.627

Table 31 Material composition of adsorbent pellet batch 2 (cylindrical)

Material	Percentage (of Total)	Target Quantity (g)	Actual (g)
A. **Nodosum**	76.73	-	6.10
Bentonite	11.57	0.915	0.92
Methylcellulose	11.70	0.915	0.93

Table 32 Material composition of adsorbent pellet batch 3 (hexagonal prism)

The material composition of the agglomerate batch is not included as it is not known precisely. The agglomerates comprise almost exclusively of A. nodosum particles, with a very small amount of glycerol present (by weight) and thus have a greater overall ratio of adsorbent material to overall weight than the pellets produced in batches 1, 2 and 3. All of the pelletisation batches had similar composition, in which the adsorbent material comprised of approximately 75% (by weight) of the overall weight of the pellet.

Fig. 60-64 show images of the pelletisation process and the final pellet and agglomerate samples produced in the research.

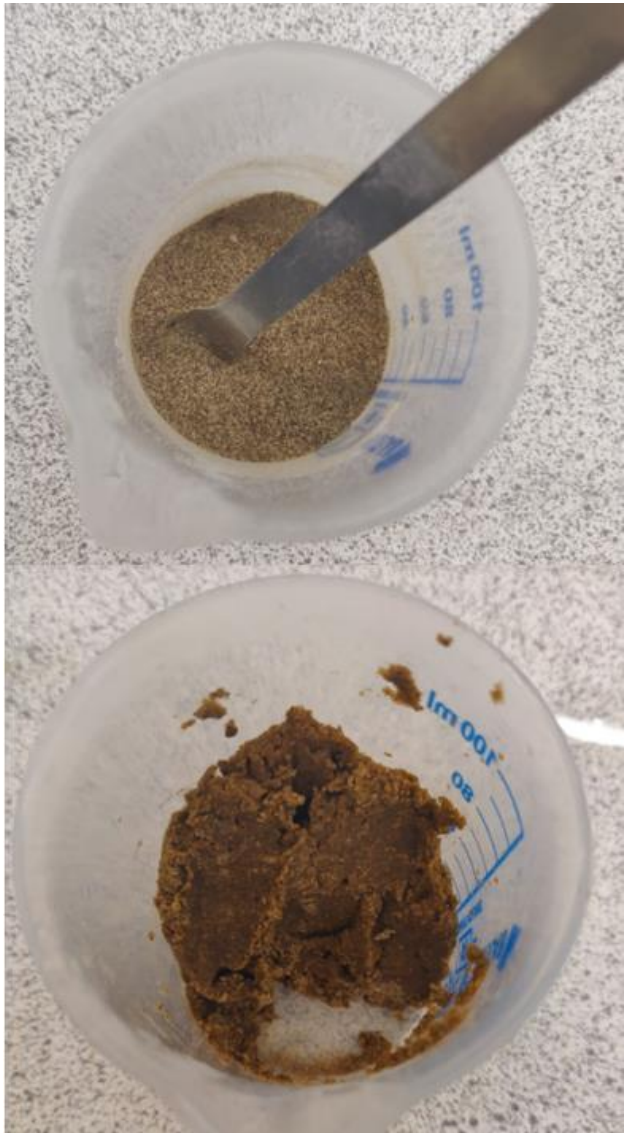


Figure 60 Powder blend (top) and adsorbent paste (bottom)



Figure 61 Clay extruder and hexagonal and circular extrusion plates



Figure 63 Extruded adsorbent paste



Figure 62 Wet adsorbent pellets

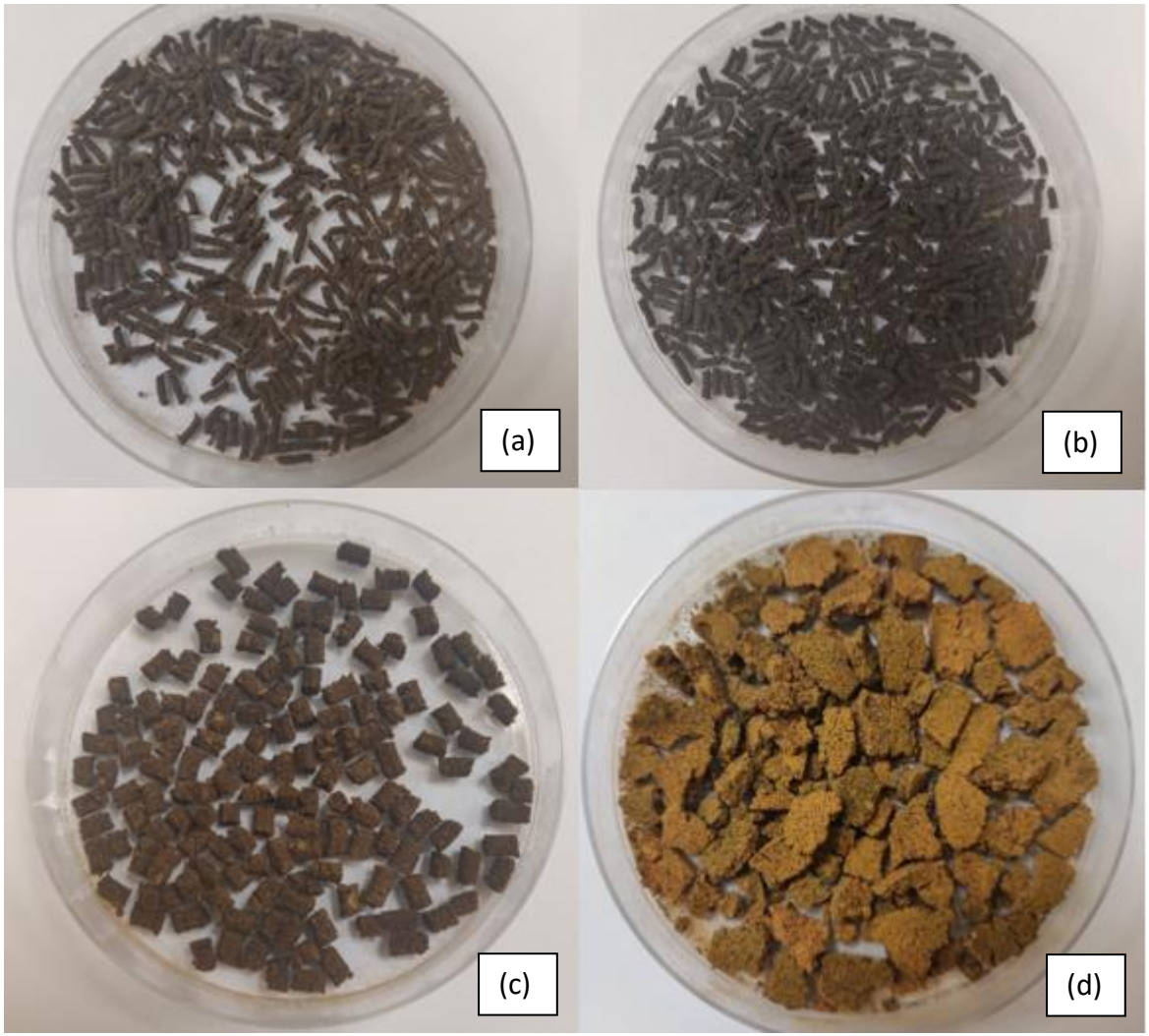


Figure 64 Dry cylindrical adsorbent pellets (a); Dry cylindrical adsorbent pellets (b); Dry hexagonal prism adsorbent pellets (c); Dry agglomerated adsorbent (bd)

5.2.4.1 Compression Analysis

After the powder shaping steps, testing was carried out to determine the compressive strength of the pellets. This analysis can be used to assess their physical characteristics, and determine if they would be robust enough to retain their shape in a PVSA rig system. The testing was carried out using a texture analyser (Fig. 65) owned by the UCC Process & Chemical Engineering department.

Testing consisted of placing a sample pellet on a load plate (Fig 66) and slowly lowering a load cell, capable of measuring the resistive force, onto the pellet. The texture analyser works in conjunction with an accompanying software package, which allows the user to manipulate the testing variables in order to accurately examine the sample. When the sample is loaded onto the load plate, the load cell is lowered at a pre-set rate (mm/s) and slowly makes contact with the pellet or sample. The load cell continues to lower until it reaches the pre-set target for the distance moved (mm) which cannot exceed the starting distance between the load cell and load plate. The load cell transmits data to the computer about the force applied to the sample, producing a data set. The analyser is capable of logging hundreds of data points per second, allowing for a comprehensive overview of force applied to the sample, even in the case of a very small sample such as the pellets produced in this research.

Compression analysis was carried out on ten individual pellets from each batch, and ten individual pieces of agglomerate, and the results were graphed by the software. The results of this analysis are shown in Fig. 67-70. The graphs show the force applied to the sample pellet against the distance travelled by the load cell, which represents the compressive strength of the material. Compressive strength is an effective representation of the magnitude of the force that would be required to break or destroy the pellets. While this is not of significant importance in a lab-scale PVSA system, it indicates potential suitability of the pellets for a commercial scale PSA system, where compressive force due to the weight of the bed itself, as well as forces due to higher rates of airflow or fluidisation of the bed could compromise the structural integrity of the pellets.

Each graph consists of ten data sets, each described by a line in a unique colour, representing an individual pellet from the batch. To understand the graphs they should be analysed with respect to Hooke's Law for continuous media, which states that the strain in a solid is proportional to the applied stress within the elastic limit of that media.

$$\sigma = E\epsilon = \frac{F}{A} \tag{5.1}$$

The graphs show a linear deformation first, where the pellets behave elastically, for this region, the uniaxial compressive stress in the material (σ) is proportional to Youngs Modulus for the material (E) and the proportional strain is ϵ.

Graphs 1 and 2 (Fig. 67, 68) show the results of compression testing in two consecutive batches of cylindrical adsorbent pellets. The results for batches 1 and 2 are similar, with the compressive force resisted by the pellets in the range of 175-350 N. The datasets are largely linear, this means that the pellets are behaving elastically, according to Hooke's Law, which sees strain in the pellets increasing in direct proportion with the stress applied by the load plate. From the graphs, there is no exact point at which yielding occurs, and the elastic limits of the pellets are exceeded. The variation in compressive strength between pellets of the same batch can be attributed to slight natural variations in the composition of the powder blend, which could be avoided with more comprehensive blending.

Graph 3 (Fig. 69) shows the results of compression testing in the hexagonal prism pellets. These results show a different compression profile to the cylindrical pellets, at a compressive stress of approximately 75N, the pellets reach their yield point, and elastic deformation appears to occur, causing the strain in the pellets to rise exponentially in the range of 75-300N. These results indicate that after compressive force reaches 75N the pellets begin to behave plastically, resulting in irreversible changes to the structure and properties of the pellet. Plastic deformation of the pellet structures could carry unknown implications for the CO_2 adsorption performance of the pellets in a PVSA system, however, it is difficult to predict the operational significance of this without testing. A possible explanation for the difference in behaviour between the hexagonal prism and cylindrical pellets is that the larger pellet size allowed the load plate to travel further in the former. The increased distance travelled by the load plate means that the elastic limits of the pellet material are more likely to be exceeded and the material deformed. As seen in the cylindrical pellets, the slight variation between pellets of in the batch is attributed to slight natural variations in the material composition of the powder blend.

Graph 4 (Fig. 70) shows the results of the compression testing in the agglomerates. As expected these results are drastically different to both the cylindrical and hexagonal prism pellets. The graph shows significant variation from unit to unit in the agglomerate shapes, both the compressive strength, and the elastic profile. The majority of agglomerates fracture or break in the range of 40-100N, indicated by inflection points in the graph, and the data sets bear no consistency. The significant differences in the properties of each unit of the agglomerate are attributed to the fact that they were created through the addition of a cross-linking agent, and formed spontaneously upon drying, rather than being the product of a shaping process, which ensures a degree of uniformity in shape and composition of the units. The compressive strength of the agglomerate units is significantly lower than that of the pellets, meaning that they break far more easily, potentially making them unsuitable for commercial-scale PVSA processes. The degree of variation in their compressive strength indicates a potential variation in the CO_2 adsorption performance, which could make them unsuitable for industrial processes.



Figure 65 Texture Analyser



Figure 66 Load cell and base plate of Texture analyser

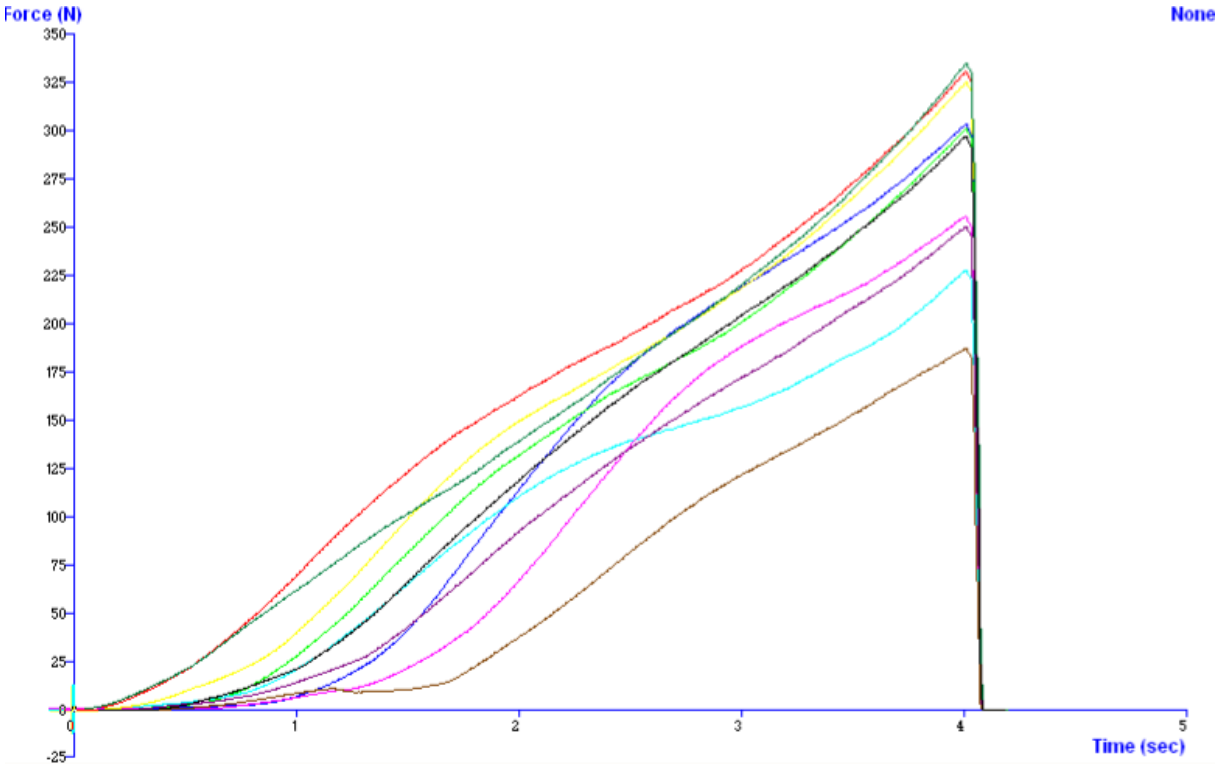


Figure 67 Force v Time graph (compressive strength) for 1mm diameter cylindrical pellets (10 units, Batch 1)

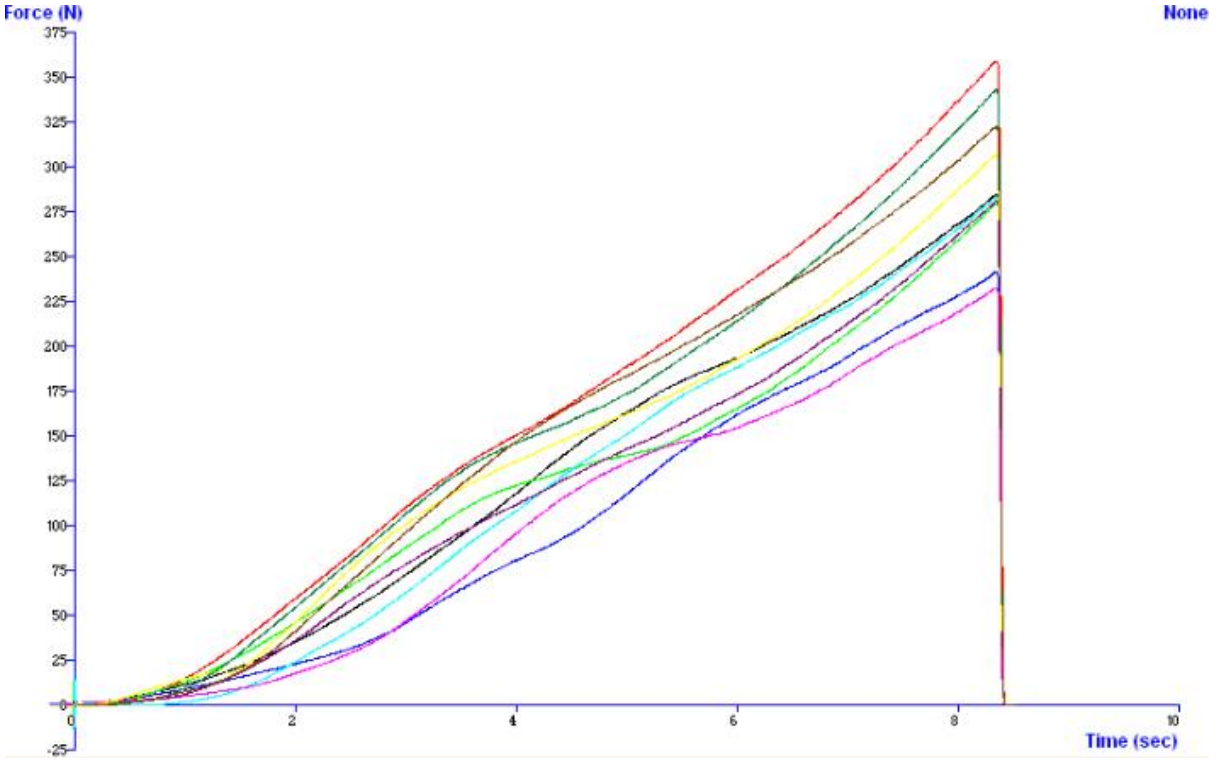


Figure 68 Force v Time graph (compressive strength) for 1mm diameter cylindrical pellets (10 units, Batch 2)

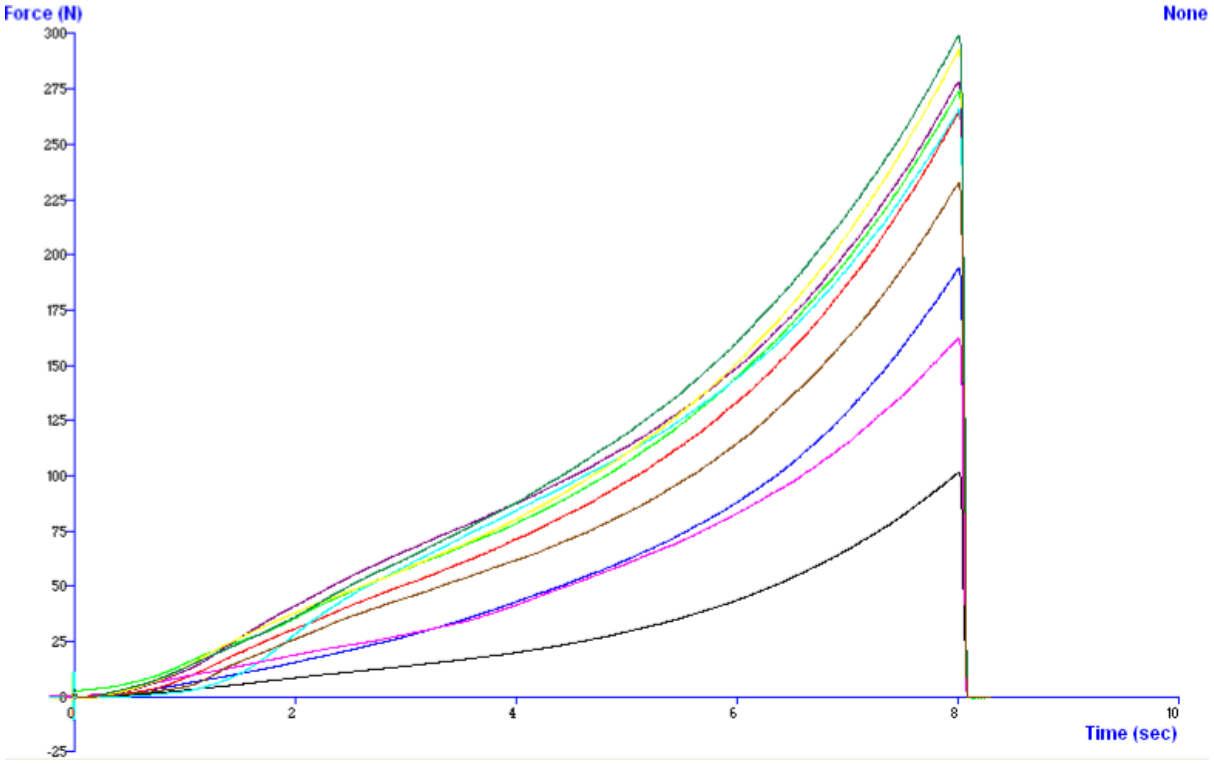


Figure 69 Force v Time graph (compressive strength) for 3mm diameter Hexagonal Prism pellets (10 units, Batch 1)

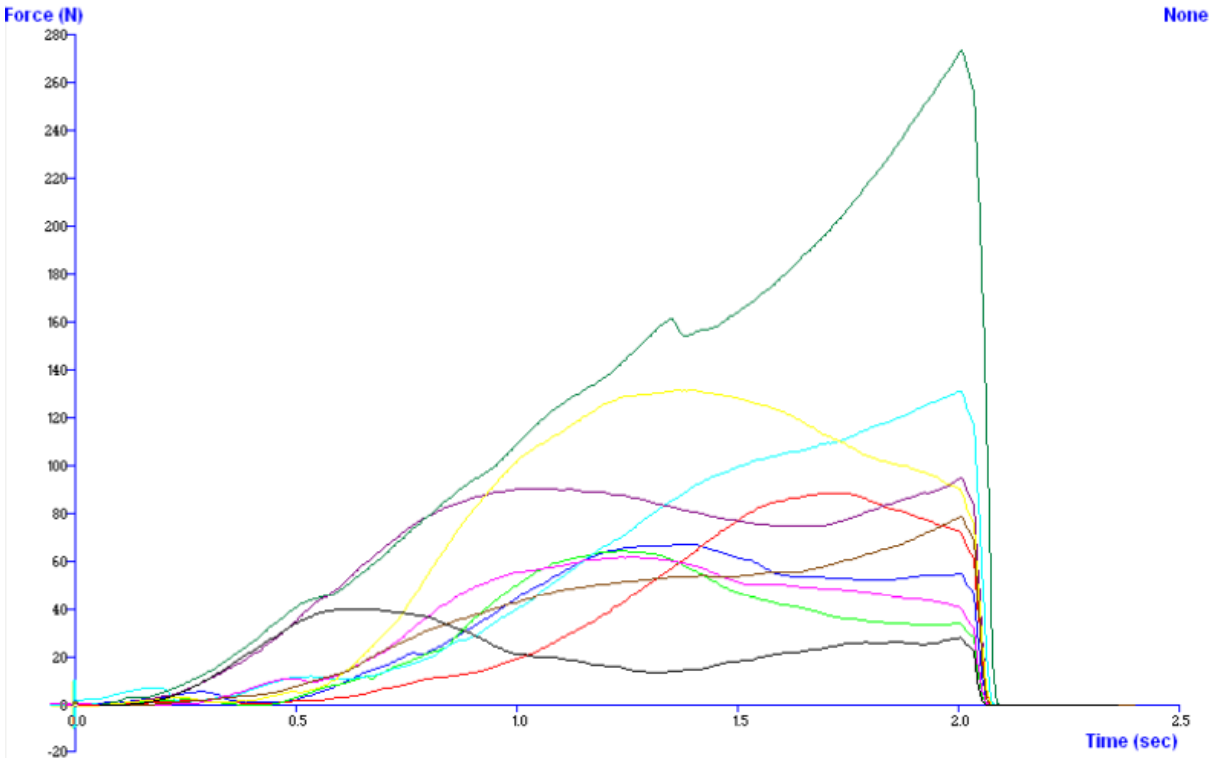


Figure 70 Force v Time graph (compressive strength) for varied agglomerates (10 units, Batch 1)

5.2.4.2 Determining Young's Modulus for the Adsorbent Pellets

Based on the results of the compression analysis Young's modulus was calculated for each of the pellets. Young's modulus describes the relationship between stress and strain for a material under uniaxial deformation. Youngs modulus is an important parameter in solid-gas adsorbent materials as it is a proxy for the overall mechanical robustness of the pellet. This is particularly important for an adsorbent material undergoing rapid cycling within a PSA system. A higher Young's Modulus means that as the adsorbent pellet is exposed to a large number of high-pressure gas-flow cycles it is less likely to degrade, with pellet degradation leading to operational efficiency losses due to dust emissions from the pellets. Adsorbent dust emissions drastically reduce the efficiency of a solid-gas PSA system by having the duel effect of adsorbent loss, which reduces system capacity and system blockages, which affect gas flow through the system over time. Young's modulus, among other mechanical properties, has a direct relationship with the operational lifespan of a solid adsorbent in a PSA system which is a key process parameter and directly impacts operational cost.

Calculating Young's Modulus:

Young's Modulus (the Modulus of Elasticity) can be found by applying Hooke's Law:

$$\sigma = E\epsilon$$

Where
σ = Compressive stress
E = Young's Modulus
ε = Normal strain

Rearranging:

$$E = \frac{\sigma}{\epsilon} = \frac{Fn/A}{\Delta L/L_0} = \frac{Fn/A}{\Delta L/L_0}$$

Where:
Fn = Force acting perpendicular to the area (N)
A = Area (m^2)
dL = Length
L_0 = Initial length

The data from the compression test (5.2.3.1) was exported to excel, which provided sequential values for displacement (dL) against force for 10 individual pellets from each batch. These values were used to calculate Young's Modulus for the pellet type, which is taken as the average value of E from the 10 measured pellets in each batch.

Cylindrical Batch 1:

Variable		Unit	Pellet 1	Pellet 2	Pellet 3	Pellet 4	Pellet 5	Pellet 6	Pellet 7	Pellet 8	Pellet 9	Pellet 10
Initial Length	L_0	m	0.003	0.003	0.003	0.003	0.003	0.003	0.003	0.003	0.003	0.003
Diameter	D	m	0.0015	0.0015	0.0015	0.0015	0.0015	0.0015	0.0015	0.0015	0.0015	0.0015
Area	A	m2	1.76715E-06	1.76715E-06	1.76715E-06	1.76715E-06	1.7671E-06	1.76715E-06	1.7671E-06	1.76715E-06	1.76715E-06	1.76715E-06
Force	Fn	N	297.7502	303.5327	330.8532	301.3973	228.056	256.1106	250.5952	325.286	335.2179	187.7588
Displacement	dL	mm	0.001	0.001	0.001	0.001	0.001	0.001	0.001	0.001	0.001	0.001
Youngs Modulus	E	MPa	505.48	515.29	561.67	511.67	387.16	434.79	425.42	552.22	569.08	318.75

Table 33 Calculation of Youngs Modulus for 10 pellets from Cylindrical Batch 1s

Cylindrical Batch 2:

Variable		Unit	Pellet 1	Pellet 2	Pellet 3	Pellet 4	Pellet 5	Pellet 6	Pellet 7	Pellet 8	Pellet 9	Pellet 10
Initial Length	L_0	m	0.003	0.003	0.003	0.003	0.003	0.003	0.003	0.003	0.003	0.003
Diameter	D	m	0.0015	0.0015	0.0015	0.0015	0.0015	0.0015	0.0015	0.0015	0.0015	0.0015
Area	A	m2	1.76715E-06	1.76715E-06	1.76715E-06	1.76715E-06	1.7671E-06	1.76715E-06	1.7671E-06	1.76715E-06	1.76715E-06	1.76715E-06
Force	Fn	N	284.2958	241.4597	358.7819	279.271	283.1029	232.7384	280.8934	306.628	342.7746	322.1365
Displacement	dL	mm	0.001	0.001	0.001	0.001	0.001	0.001	0.001	0.001	0.001	0.001
Youngs Modulus	E	MPa	482.64	409.91	609.09	474.11	480.61	395.11	476.86	520.55	581.91	546.88

Table 34 Calculation of Youngs Modulus for 10 pellets from Cylindrical Batch 2

Hexagonal Batch 1:

Variable		Unit	Pellet 1	Pellet 2	Pellet 3	Pellet 4	Pellet 5	Pellet 6	Pellet 7	Pellet 8	Pellet 9	Pellet 10
Initial Length	L_0	m	0.003	0.003	0.003	0.003	0.003	0.003	0.003	0.003	0.003	0.003
Diameter	D	m	0.003	0.003	0.003	0.003	0.003	0.003	0.003	0.003	0.003	0.003
Area	A	m2	7.06858E-06	7.06858E-06	7.06858E-06	7.06858E-06	7.0686E-06	7.06858E-06	7.0686E-06	7.06858E-06	7.06858E-06	7.06858E-06
Force	Fn	N	20.5357	43.6067	71.8684	78.9344	84.8074	41.9902	87.9275	80.7074	88.3216	62.267
Displacement	dL	mm	0.001	0.001	0.001	0.001	0.001	0.001	0.001	0.001	0.001	0.001
Youngs Modulus	E	MPa	8.72	18.51	30.50	33.50	35.99	17.82	37.32	34.25	37.48	26.43

Table 35 Calculation of Youngs Modulus for 10 pellets from Hexagonal Batch 1

Agglomerate Batch 1:

Variable		Unit	Pellet 1	Pellet 2	Pellet 3	Pellet 4	Pellet 5	Pellet 6	Pellet 7	Pellet 8	Pellet 9	Pellet 10
Initial Length	L_0	m	0.003	0.003	0.003	0.003	0.003	0.003	0.003	0.003	0.003	0.003
Diameter	D	m	0.0015	0.0015	0.0015	0.0015	0.0015	0.0015	0.0015	0.0015	0.0015	0.0015
Area	A	m2	1.76715E-06	1.76715E-06	1.76715E-06	1.76715E-06	1.7671E-06	1.76715E-06	1.7671E-06	1.76715E-06	1.76715E-06	1.76715E-06
Force	Fn	N	297.7502	303.5327	330.8532	301.3973	228.056	256.1106	250.5952	325.286	335.2179	187.7588
Displacement	dL	mm	0.001	0.001	0.001	0.001	0.001	0.001	0.001	0.001	0.001	0.001
Youngs Modulus	E	MPa	2.45	0.85	0.31	0.75	0.74	1.13	3.61	1.33	3.42	1.14

Table 36 Calculation of Youngs Modulus for 10 pellets from Agglomerate Batch 1

5.2.4.3 Analysis of results of mechanical stress testing

The average Young's Modulus for 10 discrete units of each of the pellet types created is summarised in table 37, using data calculated in the compression test and shown in tables 33-36. For the length of the cylindrical and hexagonal prism pellets, length was taken as the target length. In actuality, the length from particle to particle should vary based on human error in the pellet cutting process, which was done using a ruler and scalpel, with variation expected to be ±1mm. For calculating Young's Modulus, this uncertainty did not significantly alter results as an average E was taken over 10 pellets, with varying length partially explaining the outliers in the data set. The diameter was taken as the diameter of the extrusion plate orifice, measured using Vernier callipers.

For the agglomerates, a different approach was taken due to their irregular shape. The agglomerates were broken manually using the scalpel into irregular, cylindrical particles, roughly 8mm in diameter, L_o was taken as 1mm for calculation as this represented the average thickness of the agglomerates.

Variable		Unit	Cylindrical Pellets 1	Cylindrical Pellets 2	Hexagonal Pellets 1	Agglomerate Pellets 1
Young's Modulus	E	MPa	478.15	497.77	28.05	1.57

Table 37 Experimental calculation of Young's Modulus for different Biopolymer Adsorbent particles

As shown in table 37, Youngs Modulus for the pellets varies significantly depending on the shape and composition of the material. The cylindrical pellets had the highest Young's Modulus – roughly agreeing with literature values for biopolymer-bentonite composites which fall in the range of 200-400 MPa [87]. Interestingly, E in the cylindrical pellets exceeded the literature values, this indicates that Young's Modulus of the biopolymer adsorbent material exceeds that of bentonite. The value of E for cylindrical batch 2 was approximately 5% greater than batch 1 which is an acceptable level of difference and can be explained by both limitations in the particle analysis (L_o) and natural variations in composition based on manual blending of the powder material.

Young's Modulus for the Hexagonal Prism pellets was significantly reduced when compared to the cylindrical value. This was expected based on the Force v Time graph produced in the compression test (fig. 70) which shows the hexagonal pellets yielding at approximately 75N, however, the magnitude of the difference was greater than expected (approximately 17 times smaller than E for the cylindrical pellets). The drastic reduction in mechanical strength of the hexagonal prism when compared to the cylindrical prism could have be caused by several things. Firstly, experimental error may be the reason for lower than expected mechanical strength. If the powder blend was made incorrectly, with a blend composition that did not match the target, the resultant pellet could have significantly altered mechanical properties. Another source of experimental error that could have affected the result is insufficient drying. Given that the hexagonal prism pellets were produced after the cylinder pellets, they were

dried for slightly less time. A higher water content is another potential explanation for the disparity. Finally, the shape of the pellet, and the ratio between L_o and D for the pellets [88]. The L_0 to D ratio of the hexagonal prism pellets was approximately 1, with the cylinder being 2, which is expected to reduces mechanical strength [88] although not at the magnitude expected.

Finally, Youngs Modulus for the agglomerate pellets was the lowest of the three produced, a result which was expected. The agglomerates were formed in the drying process, aided by the addition of glycerol and were processed in the absence of specific powder binding agents (bentonite). The agglomerates had a very low yield force, and as expected, a low Young's Modulus, indicating that the pellets had low mechanical strength.

5.2.4.4 Results in the context of a PSA system

In the context of suitability for a carbon PSA system, the results must be interpreted on predicted performance according to two criteria:

Mechanical Strength:

Mechanical strength, assessed based on the E value for the material, is indicative of how well the adsorbent material will withstand high-pressure rapid PSA cycles, as well as the effective lifespan of the adsorbent material. The mechanical strength of a granule made of an adsorbent powder should be viewed as a proxy for likelihood of mechanical degradation. A low Value for Young's Modulus means that the pellet or granule has a higher likelihood of being broken down by gas flow [88] [92].

For the reasons specified, the cylindrical pellets would likely perform best out of the three adsorbent structured produced. Their comparatively high mechanical strength results in less pellet degradation and system blockages which reduces operational efficiency in the PSA system. The agglomerates, which exhibited very low mechanical strength in the compression test, would likely degrade into powder and cause system blockages. While this has not been experimentally confirmed, based on the value for Young's Modulus, it is very likely.

Shape and Size:

The shape and size of the adsorbent pellets directly influence the pressure drop across the packed bed. For CO_2 adsorption in a dilute stream, vast quantities of air must be processed if the technology is to succeed, meaning that an adsorbent which creates a large pressure drop can significantly increase the operational costs of the system. The size of and sphericity of the particles are key parameters in determining pressure drop [92]. Larger, more spherical particles invoke a smaller pressure drop than smaller particles. However, low mechanical strength can cause larger particles to deform or break into smaller particles in packed beds, a phenomenon which must also be considered.

Overcoming pressure drop across the bed is a key process parameter in determining the energy penalty for air contact in DAC systems. A higher pressure drop requires higher pumping capacity to supply the same gaseous flow, a consideration which is critical in DAC systems, which due to the dilute nature of the adsorbate in the gas stream, require extraordinarily large volumetric throughput. For the reasons specified, and literature analysis [92] it is deemed likely that the hexagonal prism pellets would invoke the smallest pressure drop. The cylindrical pellets, due to their smaller size (approximately half the diameter of the hexagonal prism), would invoke a larger pressure, though this should be confirmed experimentally.

Considering the mechanical strength and particle shape of the three adsorbent structures produced, it is predicted that the cylindrical pellets would perform best in an industrial scale PVSA CO_2 capture system.

6. Conclusions & Future Perspectives

6.1 Conclusion

This work was carried out in two major sections. The first involved the design and commissioning of a lab-scale PVSA system, suitable for the testing of the CO_2 adsorption capacity (cm^3/g) of CO_2 adsorbents atmospheric air. The second section involved the development of a biopolymer adsorbent material, derived from a sample of Ascophyllum Nodosum, a common Irish brown seaweed. The two sections of the project were carried out concurrently over the duration of the research (1 year).

The PVSA system designed operates an adsorption-desorption scheme called the "Skarstrom Cycle", named after its inventor Charles Skarstrom. The process is designed to supply compressed atmospheric air, at a maximum of 6 bar, to one of two $25cm^3$ columns containing an adsorbent material. The system is designed to measure the CO_2 concentration in both the inlet and vent streams, as well as the flow rate of air within the system to calculate the quantity of CO_2 adsorbed, and therefore the loading capacity of any solid CO_2 adsorbent material. Based on the results of the preliminary and detailed process design phases of this research, suitable equipment was evaluated and purchased from lab equipment suppliers. The PVSA system was built by hand in the UCC Process & Chemical Engineering Mechanical Work Shop. Safety analysis of the PVSA system was carried out, in the form of a Hazards and Operability study, and a full operational manual for the system was written. At the time of submission, no adsorbent testing has yet been carried out on using the system. This is due to supplier issues, particularly in the sourcing of suitable CO_2 sensors. Upon acquisition, the sensors can be integrated into the system and future research involving the testing of CO_2 adsorption capacity can be carried out using the system.

The second part of this research involved the development of a biopolymer adsorbent material with potential applications in CO_2 adsorption from atmospheric air. A dried sample of A. nodosum, a native Irish brown seaweed was harvested in West Cork and processed in the lab to create an adsorbent material. The adsorbent produced was a solid powder, derived from A. nodosum. The surface area of A. nodosum was expanded by a factor of 4490 times the initial value by the experimental procedure. After the surface expansion procedure, the powder samples were shaped using different experimental methods. Adsorbent powder shaping was a necessary step to prior experimental testing of the material using the PVSA rig, to overcome the significant pressure drop associated with airflow through a powder. The mechanical properties of the adsorbent pellets were tested and evaluated for suitability in a PVSA system using compressive strength testing.

More work is required to complete this research, specifically the integration of the CO_2 sensors into the rig and the testing of the CO_2 loading capacity of the adsorbent produced. At the time of writing this work has not been carried out, due to sourcing issues with the CO_2 sensors for the PVSA system.

6.2 Discussion & Suggestions for Future Work

The research frontier for DAC has reached the bid to reduce the overall cost of CO_2 removal from the atmosphere and make it competitive with other decarbonisation strategies. A significant reduction in cost would have the compounding effect of encouraging large scale investment from governments and private investors and driving further innovation. Achieving a significant reduction in capture cost will likely be a result of the marriage of new developments in multiple social and scientific disciplines, including chemical engineering (upstream and downstream process optimisation), chemistry and material science (sorbent developments) and economic policy (introduction of carbon taxes etc.) [14], [77].

6.1.1 Chemical and Material Sciences

The development of better and more effective sorbent materials (both absorbents and adsorbents) is central to the development of DAC as a feasible climate technology. Sorbent development should be pursued in a number of separate areas:

6.1.1.1 New Sorbent Identification & Improved Sorbent Regeneration:

A key aspect of improving sorbent materials is improving energy efficiency in the regeneration process. The most important development to be made in this regard is the reduction of the binding strength between CO_2 and the sorbent material, which reduces the energy required for the regeneration of the sorbent (heat or mechanical energy input). The key problem with the development of sorbents with reduced binding strength is maintaining an adequate level of CO_2 capture efficiency, which is very important in DAC (as opposed to CCS) due to the small partial pressures of CO_2 in the inlet stream (atmospheric air) [11], [14]. The development of new, better sorbents in the future has three key areas:

- Synthesis of entirely new tailor-made materials for CO_2 capture.
- Development and adjustment of existing sorbents.
- Testing of extant materials that have desirable physical characteristics required for CO_2 capture (i.e. testing of NH_x containing bio-polymers) [1]

Research in each of these three areas needs to be undertaken concurrently to maximise the likelihood of establishing the optimal sorbent (or sorbent group) for DAC which, once established, would allow for accelerated development in the field. Central to new sorbent identification should be the development of a new comparative framework for aggregating sorbent effectiveness under all of the relevant criteria. This framework should compare new and existing sorbents on a variety of key performance parameters (availability, capture capacity, the energy requirement for regeneration etc.) and be able to ascertain how likely a sorbent material, or family of sorbents, is likely to perform in commercial DAC operations. The development of an effective framework would negate the need for costly and time-consuming testing of new materials, and further accelerate the optimisation of DAC systems.

6.1.1.2 Specific Areas for Carbon-Based Adsorbents

An area of particular interest to this research, but not prevalent in commercial or academic research in the field of DAC technologies is the development of CBA. Numerous naturally occurring, carbon-based substances have been shown to exhibit high selectivity for CO_2 at atmospheric concentrations. Due to the inherent sustainability of naturally occurring polymers and the reduced in environmental risk when compared to chemical solvents (i.e. the entrainment of corrosive chemicals in liquid hydroxide systems, or degradation in solid adsorbent systems [14]), CBA is a promising branch of sorbents. They can be viewed as a "green" and inexpensive alternative to other available sorbents for DAC technologies.

The biopolymers in question are usually obtained directly from cultivated biomass or waste biomasses from agricultural or industrial processes. Substances of interest to this research include alginates and chitosan, which exhibit good potential due to the combination of high N content for CO_2 selectivity as well as high porosity (which can be enhanced through simple preparation procedures) [78]. Chitosan is a chitin derivative abundantly available as a waste product from the shellfish harvesting industry, found in the shells of crab, lobster and shrimp. Due to its relative abundance as a waste product and its wide array of applications (agricultural, biomedical, material sciences), there is a lot of information regarding the nature of its surface and how the surface can be functionalised. Recent research has begun to examine the potential of activated chitosan. Alginates, chitosan and their derivatives have a high percentage of nitrogen (approximately 5-8% by mass) and NH groups, which boost performance in CO_2 adsorption. Aside from being low-cost, non-toxic and sustainable alternatives to chemical systems for DAC, natural biopolymers such as alginates and chitosan can be processed in various ways to maximise air contact and surface area. Shaping methods for biopolymers include beads, membranes, aerogels, scaffolds and nanoparticles [79].

Further research needs to be conducted into the utilisation of biopolymers for DAC, and specifically, the regeneration of the sorbent following adsorption. It is not yet fully understood whether these naturally occurring substances possess the ability to retain usefulness over hundreds and thousands of adsorption-desorption cycles, and this a crucial factor in establishing their usefulness in DAC processes. Another gap in the research is establishing further data on the energy cost of regenerating biopolymer adsorbents, it remains unknown whether they are compatible with conventional PSA/VSA/TSA systems and the energy requirement might be for the regeneration of these biopolymers. The physical properties of the polymers such as composition, density and shape are all encouraging for sorbent regeneration but not enough research has been conducted [78], [80]. A particularly interesting property of natural biopolymers is their electrical conductivity. It has been suggested that high electrical conductivity offers a new potential regeneration strategy. It is theorized that application of electrical current to the sorbent system could precipitate desorption, and result in a far smaller energy requirement than conventional systems[78], which provides further justification for research into these naturally occurring biopolymers.

6.1.1.3 Specific research areas for MOF development

To reduce the binding strength of CO_2 in MOFs, and the overall energy penalty for regeneration, material scientists are focusing on a better understanding of surface interactions. By understanding surface interactions between the MOF and the CO_2 molecules, it is also possible to create a higher CO_2 selectivity in atmospheric conditions (high moisture content). MOFs have a unique advantage over conventional adsorbent materials which exists due to the near-infinite possibilities for the tailoring and manipulation of their surface characteristics. Newly created MOFs, which have been shown to exhibit tremendous CO_2 selectivity and capacity in DAC applications generally exhibit these characteristics due to the tailoring of the pore size[29], [81]. The synthesis of next-generation MOFs, which is underway globally, could solve the issues associated with the energy penalties in DAC processes. It is hoped that new MOFs with optimised characteristics such as pore size and the addition of amine group-containing CO_2 selective organic ligands can be created. These developments could result in new adsorbent materials with a high degree of selectivity for CO_2 over other components in atmospheric air, while also retaining the low regeneration energy requirement afforded by weak Van der Waals interactions [29]. Future research in the area of MOF development should attempt to integrate DAC process considerations in the design philosophy, taking an interdisciplinary approach that optimises the new MOFs from a materials science perspective as well as a process engineering perspective.

6.1.1.3 Specific research areas for Solid Amine Adsorbent development

Over the course of the last decade, solid-amine adsorbent materials for CO_2 adsorption have been the focus of a significant amount of research. Significant advances have been made in the development and deployment of more robust, solid-amine CO_2 adsorbents. Two of the companies operating pilot DAC plants utilise solid adsorbents, and these commercial operations have shown promise. However, there are a number of areas in which development is required to make these adsorbents commercially and chemically competitive with other sorbent systems. Thermal stability is an issue that has become prevalent. When subjected to high temperatures, as is necessary for TSA systems, it has been found that a significant loss of adsorbent material can occur[82], [83]. This loss stems from irreversible chemical reactions that invoke degradation, evaporation and leaching of the amine molecules, and occurs upon exposure to elevated temperatures. This drastically reduces the operational lifespan, and efficacy of the CO_2 adsorbent materials, which manifests as a manifold increase in operational expenditure. Further research needs to be carried out to increase the thermal and chemically stability of solid amine adsorbents. Another area of research, particularly relevant to the DAC field, is the structuring of solid-amine adsorbents within capture systems. Structuring is currently done by impregnating, tethering or coating the amines on specially designed solid supports. Maldistribution of the amine at the surface of the support is commonplace and gives rise to unpredictable operational phenomena during the capture process[83]. Research needs to be conducted on how to best produce adsorbent structures with a more uniform distribution of amine groups at the surface.

6.1.2 Engineering and Process Design:

Developments in the engineering and process design of atmospheric CO_2 capture devices and commercial plants must also be made to optimise energy efficiency and reduce the cost of the technology. The key aspects of process design that should be the focus of engineers are energy-intensive unit operations such as regeneration, which can be optimised through the implementation of novel heat integration approaches, and optimised air contactor design.

6.1.2.1 Process Integration:

Another obstacle to the development of DAC technologies is the large energy requirements of the process. Reducing the energy penalty for commercial-scale DAC processes is difficult. Firstly, there are large operational expenses associated with regeneration of sorbent which is achieved through the application of mechanical energy, heat energy, or a combination of the two. Secondly, unless the DAC process energy requirements are met by a fully renewable source, the CO_2 emissions stemming from the large energy input into the process must also be captured, further increasing the energy requirement of the process.

Heat integration is crucial to the development of efficient and cheaper DAC processes. The literature surrounding DAC processes offers vastly different costs ($/t$CO_2$) for DAC technologies, which is almost entirely based on the energy requirements of the regeneration stage. In the case of liquid hydroxide systems, the calcination step requires large energy input (heating of $CaCO_3$ from approximately 298K to 1200K). The APS study, while providing thermodynamic analysis based on the chemical reaction scheme for a liquid hydroxide regeneration process [14], did not provide any optimisation and assumed that all energy was provided by paying market rate, resulting in a capture cost of approximately 430-660 $/t$CO_2$. This does not represent a real commercial DAC process, which uses typical process engineering principles to recover and make use of waste energy throughout the process A Royal Society of Chemistry (RSC) study in 2018 provided insight into the energy savings possible[80]. In the RSC study, it was proposed that waste heat from the calcination step can be used to preheat the $CaCO_3$ for calcination. Waste heat from the hydration step can also be recovered in the form of stream production, which drives a turbine and provides electricity for the process. A similar process is described in the Carbon Engineering (CE) pilot process, which provides the best end-to-end analysis on how energy can be recovered throughout a liquid hydroxide DAC process[12]. They claim that the thermal energy demand of their calciner is reduced by 2.85 GJ/tCO_2 (approximately 35%) by employing simple heat recovery principles to pre-heat the calciner inlet. Coupled with the electricity provided from steam generation (utilising a Heat Recovery Steam Generator (HRSG) as part of their power system), and the energy-saving exhibited by the use of steam slaking over conventional slaking, the process requires significantly less energy and shows a drastic reduction in capital costs when compared to the APS study [12], [14].

6.1.2.2 Air Contactor Design:

An air contactor is the only uniform requirement of any DAC process and is independent of the sorbent material. The air contactor is the equipment or unit operation that brings atmospheric air in contact with the sorbent material, enabling CO_2 sorption to occur. Air contactor design plays an important role in DAC processes due to the large volumetric throughput of air required for substantial CO_2 capture in DAC processes. The physical size of the air contactor is an important process parameter and is dictated by the desired CO_2 removal (t/year) of the facility.

The APS review conducted in 2011[14] describes the physical requirements for the air contactor. If CO_2 concentration in atmospheric air is taken to be 400ppm, then the mass of CO_2 per unit volume of air is (6.1):

$$C_{co2} \approx 0.72 \frac{gCO_2}{m^3\ air} \tag{6.1}$$

To find the rate of CO_2 removal per unit area of air contactor we can use equation (2) which describes the mass flowrate of CO_2 being removed from the inlet stream:

$$M = \alpha C_{co2} Q \tag{6.2}$$

Where *M* is the mass flow rate of CO_2 removal, α is the capture fraction of CO_2 that passes through the contactor, C is the mass of CO_2 per unit volume of air (1), and *Q* is the volumetric flow rate of air in the inlet stream. Q can be described by equation (3):

$$Q = UA \tag{6.3}$$

Where *U* is the velocity of airflow through the contactor and *A* is the inlet area. The base case for DAC technology analysis is taken as a 1 Mt/year facility, which is the generalised scale of a fully commercial DAC plant described throughout the literature and used for comparison of DAC technologies. There are various estimations of air contact area requirement for a 1Mt facility throughout the literature, with CO_2 capture fraction (α) being the disputed variable. The APS study assigns a value of 0.50 [14] (this means that 50% of the CO_2 that passes through the process is captured), and Holmes & Keith assigning a value of 0.75 [84] (75% of CO_2). Optimal airflow velocity through the system is accepted as 1-3m/s in both studies. For the purpose of this examination, we take 2m/s to be the airflow velocity of our idealised system.

Subbing equation (6.2) into (6.3) we get the following equation:

$$M = \alpha C_{co2} UA \tag{6.4}$$

Rearranging (6.4) to find A (the area requirement):

$$A = \frac{M}{\alpha C_{co2} U} \tag{6.5}$$

Equation (6.5) now contains all of the information required to calculate the area required for the air contactor (A) as it relates to the desired mass flow rate of CO_2 removal (M) in the DAC system

Subbing in the literature values we can now estimate the capture flux:

So for the APS facility [14]:

$$Capture\ flux = \alpha C_{co2} U = (0.50)(0.72)(2) = 0.72 \frac{g}{m^2 s} = 22705.92 \frac{kg}{m^2 - year}$$

Subbing this value into (6.5) along with M (1Mt CO_2 facility) to get the area requirement:

$$A = \frac{1 \times 10^9}{22705.92} = 44{,}041\ m^2$$

Holmes & Keith facility[12]:

$$Capture\ flux = \alpha C_{co2} U = (0.75)(0.72)(2) = 0.72 \frac{g}{m^{2-} s} = 34058.88 \frac{kg}{m^2 - year}$$

Subbing this value into (6.5) along with M (1Mt CO_2 facility) to get the area requirement:

$$A = \frac{1 \times 10^9}{34058.88} = 29{,}361\ m^2$$

So the range of required air contactor area for a facility designed to capture 1 Mt-CO_2/y is approximately 30,000 – 44,000 m^2/ Mt-CO_2/y. This represents a very large physical scale, largely due to the dilute nature of CO_2 in atmospheric air, and results in large capital cost requirements. To frame the problem, these results can be used to assess the overall area requirement of air contact to capture the entire yearly global CO_2 emissions. Global CO_2 emissions are approximately 37 GtCO_2/year [85]. Based on this figure, we can assume that capturing all of the global CO_2 emissions would require the construction of 37,000 1 Mt CO_2/year DAC processing facilities, which roughly corresponds to the number of operational power plants globally (34,700) [86]. By this estimation, the required air contactor area is in the range of 1110-1628 km^2 for the capture of all global CO_2 emissions. For perspective, that roughly corresponds to the land area of London, UK, or approximately 250,000 football pitches.

As seen from the example stated above, the physical scale of DAC air contactors would be very large if they are to be deployed in any significant manner as a feasible climate technology, resulting in enormous capital expenditure. This is before the capital and operational costs of the fan systems required to ensure a 2 m/s airflow through the contactors which would have to be large in order to overcome internal pressure drops within the system.

Based on the findings, the task is not impossible considering that it roughly corresponds to the scale of the global power system, which has largely been built in the last 50 years. It also roughly corresponds to the timeframe we have to produce net negative emissions and avoid catastrophic climate change according to the IPCC (this assumption based on the predicted decline in CO_2 emissions for the next 50 years coupled with net negative CO_2 technologies).

6.1.3 Final Remarks

Over the course of the coming decade, humanity will face its greatest ever challenge. The deferral period for addressing the scientific root causes of our changing climate has now concluded. The accelerating changes in the global climate are already manifesting themselves as natural disasters. Hurricanes, flash floods, water shortages, and events of such nature, have already resulted in death and suffering in particularly exposed global regions. Unless climate change is addressed with utmost urgency, such events, and their social and political consequences, will compound over the remainder of the century. By 2100, without a drastic shift in our GHG emissions trajectory, our planet and our societies will no longer resemble the same entities that gave rise to the period of relative prosperity for humanity that has been witnessed since the beginning of the industrial revolution or Anthropocene.

The current global political landscape lacks the required mechanisms to enact unilateral global action on GHG emissions. The political discord between different countries and, at a more fundamental level, between the different political ideologies that exist within countries, is too great. The varying effects of climate change based on different geographic locations further clouds the issue and amplifies the discord between nations. For these reasons, it is the opinion of the author that the environmental policies that would be required to curb emissions at the rate required to avoid the most catastrophic effects of climate change (as outlined by the IPCC SR15[1]) are all but impossible to achieve. As a result of this fundamental obstacle that exists, the only logical solution to our shared problem that can be inferred is the removal of atmospheric GHG by technological means.

DAC is one of a number of possible technological solutions to our warming climate that have emerged as our most promising weapons in our fight against climate change. All of these technologies must be examined, without sparing resource or expense, if we are to avoid the most devastating consequences of change, including the suffering and loss of life of many millions of members a new generation who will play no part in their own fate.

7. Bibliography

[1] IPCC, "Special Report on 1.5 degrees: Summary for Policymakers," 2018.

[2] J. Rogelj *et al.*, "IPCC Special Report 2018 - Chapter 2 - Mitigation Pathways Compatible With 1.5°C in the Context of Sustainable Development," *IPCC Spec. Rep. Glob. Warm. 1.5 °C*, p. 82pp, 2018.

[3] S. Fuss *et al.*, "Negative emissions — Part 1 : Research landscape and synthesis," *Environ. Res. Lett.*, vol. 13, 2018.

[4] Y. G. Zhang, M. Pagani, Z. Liu, S. M. Bohaty, and R. Deconto, "A 40-million-year history of atmospheric CO2," 2013.

[5] D. L. Sanchez, G. Amador, J. Funk, and K. J. MacH, "Federal research, development, and demonstration priorities for carbon dioxide removal in the United States," *Environ. Res. Lett.*, vol. 13, no. 1, 2018.

[6] N. Spector and D. Barnett, "Removal of Carbon Dioxide from Atmospheric Air," *Trans. Am. Inst. Chem. Eng.*, vol. XLII, pp. 827–848, 1947.

[7] M. Ranjan and H. J. Herzog, "Feasibility of air capture," in *Energy Procedia*, 2011.

[8] J. Isobe, P. Henson, A. MacKnight, S. Yates, D. Schuck, and D. Winton, "Carbon Dioxide Removal Technologies for U.S. Space Vehicles: Past, Present, and Future," *46th Int. Conf. Environ. Syst.*, no. July, pp. 10–14, 2016.

[9] R. Carey, A. Gomezplata, and A. Sarich, "An overview into submarine CO2 scrubber development," *Ocean Eng.*, vol. 10, no. 4, pp. 227–233, 1983.

[10] K. S. Lackner, P. Grimes, and H. J. Ziock, "Carbon dioxide extraction from air: Is it an option?," 1999.

[11] E. S. Sanz-Pérez, C. R. Murdock, S. A. Didas, and C. W. Jones, "Direct Capture of CO2 from Ambient Air," *Chem. Rev.*, vol. 116, no. 19, pp. 11840–11876, 2016.

[12] D. W. Keith, G. Holmes, D. St. Angelo, and K. Heidel, "A Process for Capturing CO2 from the Atmosphere," *Joule*, 2018.

[13] M. Mahmoudkhani and D. W. Keith, "Low-energy sodium hydroxide recovery for CO2 capture from atmospheric air-Thermodynamic analysis," *Int. J. Greenh. Gas Control*, 2009.

[14] R. Socolow *et al.*, "Direct Air Capture of CO2 with Chemicals A Technology Assessment for the APS Panel on Public Affairs," *Technology*, pp. 1–119, 2011.

[15] D. W. Keith, K. Heidel, and R. Cherry, "Capturing CO2 from the atmosphere: Rationale and Process Design Considerations," in *Geo-Engineering Climate Change Environmental Necessity or Pandora's Box?*, 2010, pp. 107–125.

[16] A. Wurzbacher, Jan, "Development of a temperature-vacuum swing process for CO2 capture from ambient air," 2015.

[17] C. Gebald, "Development of amine-functionalized adsorbent for carbon dioxide capture from atmospheric air," 2015.

[18] J. A. Wurzbacher, C. Gebald, and A. Steinfeld, "Separation of CO 2 from air by temperature-vacuum swing adsorption using diamine-functionalized silica gel," *Energy Environ. Sci.*, vol. 4, no. 9, pp. 3584–3592, 2011.

[19] C. Gebald, J. A. Wurzbacher, P. Tingaut, T. Zimmermann, and A. Steinfeld, "Amine-based nanofibrillated cellulose as adsorbent for CO 2 capture from air," *Environ. Sci. Technol.*, vol. 45, no. 20, pp. 9101–9108, 2011.

[20] Climeworks, "Climeworks raises CHF 30.5M (USD 30.8M) to commercialize carbon dioxide removal technology," 2012. [Online]. Available: http://www.climeworks.com/wp-content/uploads/2018/08/Press-

Release_FinancingRound_final.pdf.
[21] Y. Ishimoto, M. Sugiyama, E. Kato, R. Moriyama, K. Tsuzuki, and A. Kurosawa, "Putting Costs of Direct Air Capture in Context," *SSRN Electron. J.*, 2017.
[22] L. Beaumont, Maximus and C. Thirkettle, Anthony, "Method and Device for the Reversible Adsorption of Carbon Dioxide," 2017.
[23] D. Li *et al.*, "Experiment and simulation for separating CO2/N2 by dual-reflux pressure swing adsorption process," *Chem. Eng. J.*, vol. 297, pp. 315–324, 2016.
[24] S. Brunauer, P. H. Emmett, and E. Teller, "Adsorption of Gases in Multimolecular Layers," *J. Am. Chem. Soc.*, vol. 60, no. 2, pp. 309–319, 1938.
[25] S. Sircar, "Pressure swing adsorption," *Appl. Catal.*, vol. 46, no. 1, p. 180, 1989.
[26] C. W. Skarstrom, "By Ou-Ouay . i . Attorney Attorney," 1960.
[27] C. A. Grande, "Advances in Pressure Swing Adsorption for Gas Separation," *ISRN Chem. Eng.*, vol. 2012, pp. 1–13, 2012.
[28] A. Goeppert, M. Czaun, G. K. Surya Prakash, and G. A. Olah, "Air as the renewable carbon source of the future: An overview of CO 2 capture from the atmosphere," *Energy Environ. Sci.*, vol. 5, no. 7, pp. 7833–7853, 2012.
[29] K. Sumida *et al.*, "Carbon Dioxide Capture in Metal–Organic Frameworks," *Chem. Rev.*, vol. 112, no. 2, pp. 724–781, Feb. 2012.
[30] J. A. Mason, K. Sumida, Z. R. Herm, R. Krishna, and J. R. Long, "Evaluating metal-organic frameworks for post-combustion carbon dioxide capture via temperature swing adsorption," *Energy Environ. Sci.*, vol. 4, no. 8, pp. 3030–3040, 2011.
[31] V. Mulgundmath and F. H. Tezel, "Optimisation of carbon dioxide recovery from flue gas in a TPSA system," *Adsorption*, vol. 16, no. 6, pp. 587–598, 2010.
[32] A. Demessence, D. M. D'Alessandro, M. L. Foo, and J. R. Long, "Strong CO2 binding in a water-stable, triazolate-bridged metal-organic framework functionalized with ethylenediamine," *J. Am. Chem. Soc.*, vol. 131, no. 25, pp. 8784–8786, 2009.
[33] M. Clausse, J. Merel, and F. Meunier, "Numerical parametric study on CO2 capture by indirect thermal swing adsorption," *Int. J. Greenh. Gas Control*, 2011.
[34] X. Shi, H. Xiao, X. Liao, M. Armstrong, X. Chen, and K. S. Lackner, "Humidity effect on ion behaviors of moisture-driven CO 2 sorbents," *J. Chem. Phys.*, vol. 149, no. 16, 2018.
[35] T. Wang, J. Liu, M. Fang, and Z. Luo, "A moisture swing sorbent for direct air capture of carbon dioxide: Thermodynamic and kinetic analysis," *Energy Procedia*, vol. 37, pp. 6096–6104, 2013.
[36] T. Wang, K. S. Lackner, and A. Wright, "Moisture swing sorbent for carbon dioxide capture from ambient air," *Environ. Sci. Technol.*, vol. 45, no. 15, pp. 6670–6675, 2011.
[37] R. M. Siqueira *et al.*, "Carbon Dioxide Capture by Pressure Swing Adsorption," in *Energy Procedia*, 2017.
[38] D. Ko, R. Siriwardane, and L. T. Biegler, " Optimization of a Pressure-Swing Adsorption Process Using Zeolite 13X for CO 2 Sequestration ," *Ind. Eng. Chem. Res.*, vol. 42, no. 2, pp. 339–348, 2003.
[39] B. J. Maring and P. A. Webley, "A new simplified pressure/vacuum swing adsorption model for rapid adsorbent screening for CO2 capture applications," *Int. J. Greenh. Gas Control*, 2013.
[40] B. Sreenivasulu, D. V. Gayatri, I. Sreedhar, and K. V. Raghavan, "A journey into the process and engineering aspects of carbon capture technologies," *Renewable and*

Sustainable Energy Reviews. 2015.
[41] M. Kacem, M. Pellerano, and A. Delebarre, “Pressure swing adsorption for CO2/N2 and CO2/CH4 separation: Comparison between activated carbons and zeolites performances,” *Fuel Process. Technol.*, 2015.
[42] M. Younas, M. Sohail, L. L. Kong, M. J. K. Bashir, and S. Sethupathi, “Feasibility of CO2adsorption by solid adsorbents: a review on low-temperature systems,” *Int. J. Environ. Sci. Technol.*, vol. 13, no. 7, pp. 1839–1860, 2016.
[43] N. Querejeta, M. G. Plaza, F. Rubiera, C. Pevida, T. Avery, and S. R. Tennisson, “Carbon Monoliths in Adsorption-based Post-combustion CO2 Capture,” *Energy Procedia*, vol. 114, no. November 2016, pp. 2341–2352, 2017.
[44] Swagelok, “Sample Cylinders , Accessories, and Outage Tubes Features,” vol. 3. pp. 1–8, 2017.
[45] Swagelok, “Swagelok Medium-Pressure, Gaugeable Tube Fittings and Adapter Fittings.” pp. 1–10, 2017.
[46] SMC, “Normal Close High Vacuum Solenoid Valve,” 2018.
[47] Swagelok, “Check Valves.” pp. 1–17, 2017.
[48] Swagelok, “Bleed Valves and Purge Valves.” pp. 506–517, 2017.
[49] Swagelok, “General Utility Service Needle Valves.” pp. 6–7, 2017.
[50] Vacuubrand, “Technology for Vacuum Systems: Diaphragm Pumps,” *Health (San Francisco)*. pp. 1–17, 2018.
[51] Swagelok, “Pressure Gauges: Industrial and Process.” pp. 0–1, 2019.
[52] T. Kletz, *Hazop and Hazan*, 4th ed. IChemE, 1999.
[53] J. L. Woodward, *LNG Safety and Security Aspects*. 2013.
[54] A. Kumar *et al.*, “Direct Air Capture of CO2 by Physisorbent Materials,” *Angew. Chemie - Int. Ed.*, vol. 54, no. 48, pp. 14372–14377, 2015.
[55] D. G. Madden *et al.*, “Flue-gas and direct-air capture of CO 2 by porous metal – organic materials Subject Areas : Authors for correspondence :,” *Philos. Trans. R. Soc. A Math. Phys. Eng. Sci.*, vol. 375, pp. 2084–2094, 2017.
[56] Q. Wang, J. Luo, Z. Zhong, and A. Borgna, “CO2 capture by solid adsorbents and their applications: Current status and new trends,” *Energy Environ. Sci.*, vol. 4, no. 1, pp. 42–55, 2011.
[57] K. B. Lee, M. G. Beaver, H. S. Caram, and S. Sircar, “Reversible chemisorbents for carbon dioxide and their potential applications,” *Ind. Eng. Chem. Res.*, vol. 47, no. 21, pp. 8048–8062, 2008.
[58] K. S. Walton *et al.*, “Understanding inflections and steps in carbon dioxide adsorption isotherms in metal-organic frameworks,” *J. Am. Chem. Soc.*, vol. 130, no. 2, pp. 406–407, 2008.
[59] D. Saha and Z. Bao, “on MOF-5 , MOF-177 , and Zeolite 5A,” *Environ. Sci. Technol.*, vol. 44, no. 5, pp. 1820–1826, 2010.
[60] A. E. Creamer and B. Gao, “Carbon-based adsorbents for postcombustion CO2 capture: A critical review,” *Environ. Sci. Technol.*, vol. 50, no. 14, pp. 7276–7289, 2016.
[61] N. P. Wickramaratne and M. Jaroniec, “Activated carbon spheres for CO2 adsorption,” *ACS Appl. Mater. Interfaces*, vol. 5, no. 5, pp. 1849–1855, 2013.
[62] D. Bonenfant, M. Kharoune, P. Niquette, M. Mimeault, and R. Hausler, “Advances in principal factors influencing carbon dioxide adsorption on zeolites,” *Sci. Technol. Adv. Mater.*, vol. 9, no. 1, 2008.

[63] E. Baardseth, “Synopsis of Biological Data on Knobbed Wrack,” vol. 80, no. 38.
[64] A. Jensen, H. Nebb, and E. A. Sæter, *The Value of Norwegian Seaweed Meal as a Mineral Supplement for Dairy Cows*. 1968.
[65] A. Nanakoudis, “What is SEM? Scanning electron microscope technology explained,” *ThermoFisher Scientific*, 2018. [Online]. Available: https://blog.phenom-world.com/what-is-sem. [Accessed: 07-Aug-2019].
[66] A. Nanakoudis, “EDX analysis with a scanning electron microscope (SEM): how does it work?,” *ThermoFisher Scientific*, 2018. [Online]. Available: https://blog.phenom-world.com/edx-analysis-scanning-electron-microscope-sem.
[67] S. Jain, A. S. Moharir, P. Li, and G. Wozny, “Heuristic design of pressure swing adsorption: A preliminary study,” *Sep. Purif. Technol.*, vol. 33, no. 1, pp. 25–43, 2003.
[68] F. Rezaei and P. Webley, “Structured adsorbents in gas separation processes,” *Separation and Purification Technology*, vol. 70, no. 3. pp. 243–256, 2010.
[69] Y. Y. Li, S. P. Perera, and B. D. Crittenden, “Zeolite monoliths for air separation Part 2: Oxygen enrichment, pressure drop and pressurization,” *Chem. Eng. Res. Des.*, vol. 76, no. 8 A8, pp. 931–941, 1998.
[70] F. C. Patcas, G. I. Garrido, and B. Kraushaar-Czarnetzki, “CO oxidation over structured carriers: A comparison of ceramic foams, honeycombs and beads,” *Chem. Eng. Sci.*, vol. 62, no. 15, pp. 3984–3990, 2007.
[71] X. Mao, “Processing of Ceramic Foams,” in *Recent Advances in Porous Ceramics*, InTech, 2018.
[72] F. Akhtar, L. Andersson, S. Ogunwumi, N. Hedin, and L. Bergström, “Structuring adsorbents and catalysts by processing of porous powders,” *Journal of the European Ceramic Society*, vol. 34, no. 7. pp. 1643–1666, 2014.
[73] N. P. Jogad, “Pelletization techniques,” *J. Pharm. Res.*, vol. 3, no. 8, pp. 1793–1797, 2010.
[74] M. Koester and M. Thommes, “New Insights into the Pelletization Mechanism by Extrusion/Spheronization,” *Sci. Pharm.*, vol. 78, no. 3, pp. 640–640, 2010.
[75] C. Vervaet, L. Baert, and J. P. Remon, “Extrusion-spheronisation A literature review,” *International Journal of Pharmaceutics*. 1995.
[76] P. Schneider, “Adsorption isotherms of microporous-mesoporous solids revisited,” *Applied Catalysis A, General*. 1995.
[77] J. D. Figueroa, T. Fout, S. Plasynski, H. McIlvried, and R. D. Srivastava, “Advances in CO2 capture technology-The U.S. Department of Energy’s Carbon Sequestration Program,” *International Journal of Greenhouse Gas Control*. 2008.
[78] A. Primo, A. Forneli, A. Corma, and H. García, “From biomass wastes to highly efficient CO2 adsorbents: Graphitisation of chitosan and alginate biopolymers,” *ChemSusChem*, vol. 5, no. 11, pp. 2207–2214, 2012.
[79] R. S. Dassanayake, C. Gunathilake, N. Abidi, and M. Jaroniec, “Activated carbon derived from chitin aerogels: preparation and CO2 adsorption,” *Cellulose*, vol. 25, no. 3, pp. 1911–1920, 2018.
[80] H. A. Daggash *et al.*, “Closing the carbon cycle to maximise climate change mitigation: Power-to-methanol: vs. power-to-direct air capture,” *Sustain. Energy Fuels*, vol. 2, no. 6, pp. 1153–1169, 2018.
[81] Z. Hu, Y. Wang, B. B. Shah, and D. Zhao, “ CO 2 Capture in Metal-Organic Framework Adsorbents: An Engineering Perspective ,” *Adv. Sustain. Syst.*, vol. 3, no. 1, p. 1800080, 2019.

[82] M. Jahandar Lashaki, S. Khiavi, and A. Sayari, “Stability of amine-functionalized CO2 adsorbents: A multifaceted puzzle,” *Chem. Soc. Rev.*, vol. 48, no. 12, pp. 3320–3405, 2019.
[83] E. E. Ünveren, B. Ö. Monkul, Ş. Sarıoğlan, N. Karademir, and E. Alper, “Solid amine sorbents for CO2 capture by chemical adsorption: A review.” 2017.
[84] G. Holmes and D. W. Keith, “An air-liquid contactor for large-scale capture of CO2 from air,” *Philos. Trans. R. Soc. A Math. Phys. Eng. Sci.*, vol. 370, no. 1974, pp. 4380–4403, 2012.
[85] C. Le Quéré *et al.*, “Global Carbon Budget 2017,” *Earth Syst. Sci. Data Discuss.*, pp. 1–79, 2017.
[86] L. Byers *et al.*, “A Global Database of Power Plants,” no. x, pp. 1–18, 2019.
[87] N. Sarifuddin, H. Ismail, "Comparative Study on the Effect of Bentonite or Feldspar Filled Low-Density Polyethylene/Thermoplastic Sago Starch/Kenaf Core Fiber Composites" *Bioresources,* vol 8, pp. 4238-4257, 2013
[88] P. Yang, S. Ju, S. Huang, "Predicted structural and mechanical properties of activated carbon by molecular simulation" *Computational Materials Science,* vol 143, pp. 43-54, 2018
[89] C. Blaker, S. Heib, C. Pasel, B. Atakan, D. Bathen "Investigation of Mechanical, Chemical and Adsorptive Properties of Novel Silicon-Based Adsorbents with Activated Carbon Structure" *Journal of Carbon Research,* 2017
[90] K. S. W. Sing, D. H. Everett, R. A. W. Haul, L. Moscou, R. A. Pierotti, J. Rouquérol " Reporting physisorption data for gas/solid systems with Special Reference to the Determination of Surface Area and Porosity" *Pure and Applied Chemistry,* vol 54, No. 4, pp 603-619
[91] K. Zhang, "Adsorption and Desorption Isotherms", *The KE Research Group,* 2016
[92] A. Koekemoer, A. Luckos, "Effect of material type and particle size distribution on pressure drop in packed beds of large particles: Extending the Ergun equation", *Fuel,* vol 158, pp 232-238, 2015
[93] Sánchez-Zambrano *et al*, " CO2 Capture with Mesoporous Silicas Modified with Amines by Double Functionalization: Assessment of Adsorption/Desorption Cycles" *Materials (Basil), vol 11, pp 887*
[94] X. Xu, Y.Kan, L. Zhao, X. Cao, " Chemical transformation of CO2 during its capture by waste biomass derived biochars" *Environmental Pollution,* vol 213, pp 533-540
[95] Y. Chiang, C. Yeh, C. Weng, "Carbon Dioxide Adsorption on Porous and Functionalized Activated Carbon Fibers "*Applied Sciences,* vol 9, pp 1977